DOE/ER/60943--1

DE92 010027

FINAL TECHNICAL REPORT
FOR GRANT DE-FG02-90ER60943

submitted to

CARBON DIOXIDE RESEARCH PROGRAM
OFFICE OF HEALTH AND ENVIRONMENTAL RESEARCH
U. S. DEPARTMENT OF ENERGY
WASHINGTON, D. C. 20545

INVESTIGATION OF CARBON DIOXIDE IN THE SOUTH ATLANTIC AND NORTHERN WEDDELL SEA AREAS (WOCE SECTIONS A-12 AND A-21) DURING THE METEOR EXPEDITION 11/5, JANUARY-MARCH, 1990

by

David W. Chipman, Taro Takahashi, Dee Breger
and Stewart C. Sutherland

Lamont-Doherty Geological Observatory of Columbia University,
Palisades, N. Y. 10964

December, 1991

TABLE OF CONTENTS

ACKNOWLEDGMENTS

This investigation has been supported by a grant from the U. S. Department of Energy (No. DE-FGO2-90ER60943). We thank Drs. Michael Riches and John Downing (on leave from the Battelle Northwest Laboratories) of the Department of Energy for support and encouragement. The field work was conducted aboard the F/S METEOR of the Federal Republic of Germany. The concentrations of dissolved oxygen and nutrient salts were determined by Jim Costello and David Boss of the Oceanographic Data Facility, Scripps Institution of Oceanography; the salinity was determined mainly by Jose Arango of the Argentine Hydrographic Office; and the CTD was operated jointly by the Scripps' ODF staff and German scientists and technicians. We thank Dr. Wolfgang Roether of the University of Bremen, for scientific collaboration, and the captain and crew members of the METEOR for their effective assistance provided to us during the expedition.

ABSTRACT

This report summarizes the results of investigation the oceanographic expedition aboard the F/S METEOR in the South Atlantic Ocean including the Drake Passage (WOCE Section A-21), the northern Weddell Sea and the eastern South Atlantic (WOCE Section A-12) during the austral summer of January through March, 1990. The total CO_2 concen- tration in about 1300 seawater samples and CO_2 partial pressure (pCO_2) in about 870 seawater samples collected at 77 stations were determined aboard the ship using a coulometer and equilibrator/gas chromatograph system. The temperature, salinity, dissolved oxygen and nutrient salt data presented in this report were determined by other participants of the expedition including the members of the Oceanographic Data Facility of the Scripps Institution of Oceanography, Argentine Hydrographic Office and German institutions.

For each of the properties including temperature, salinity, potential density at 2000 db, total CO_2, pCO_2, oxygen and nutrient salts, the data are presented in five sets of contoured sections; a N-S section across the Drake Passage (56°S-63°S), a NW-SE section in the northern Weddell Sea (45°W-35°W), a E-W section along the 58°W parallel (25°W- prime meridian), and two segmented S-N sections between the northern Weddell Sea and Capetown. The atmospheric and surface water pCO_2 data show that the ocean was a weak to strong sink for atmospheric CO_2 virtually over the entire tracks of the expedition. Across the Drake Passage (WOCE Section A-21), the following water masses have been identified; the Circumpolar Deep Water (CPDW), Southeast Pacific Low Oxygen Water (SPLOW), Southeast Pacific Deep Water (SPDW) and Southeast Pacific Bottom Water (SPBW). In the northern Weddell Sea section, the Weddell Sea Deep Water (WSDW), Weddell Sea Bottom Water (WSBW) and Antarctic Bottom Water (AABW) have been identified. In the Capetown- Weddell section, the following four water masses have been observed; the Antarctic Intermediate Water (AAIW), Upper and Lower Circumpolar Deep Waters (UCPDW and LCPDW), North Atlantic Deep Water (NADW) and Cape Basin Bottom Water (CBBW). The chemical properties for these water masses are summarized and the total CO_2, pCO_2 and alkalinity data have been found to be helpful in identifying and assessing the extent of some of these water masses. On the basis of property-property relationships between various properties, some regulatory processes and their relationships with oceanographic environments have been identified. In the surface water of the Atlantic Southern Ocean including the northern Weddell Sea, the total CO_2 concentration normalized to 35 o/oo salinity has been found to be linearly related to water temperature. Assuming that the air-sea CO_2 flux is small, it has been estimated that about 80% of CO_2 removed from surface water is by organic carbon production by photosynthesis and 20% by biogenic $CaCO_3$ production. The surface water data show that the $CaCO_3$ production occurs mainly in the subantarctic and subtropical regions where water temperatures are above 3°C, whereas the production of siliceous organisms dominates in the Antarctic and Weddell Sea areas, where temperatures are less than 3°C.

I. INTRODUCTION

The deep interior of the oceans exchanges dissolved gases directly with the atmosphere when the deep water outcrops and becomes exposed to the atmosphere during winter in high latitude oceans. Thus, for our understanding of the CO_2 cycle in the global ocean-atmosphere system, it is important to know various physical, chemical and biological processes controlling such exchange as well as the resulting distribution of CO_2 in the high latitude oceans.

The high latitude South Atlantic Ocean occupies a unique place among the global oceans because of a number of major oceanographic features. Both the surface and deep waters enter into the Atlantic from the west through a topographically well defined channel, the Drake Passage located between the southern tip of the South America and the northern tip of the Palmer Peninsula of the Antarctic continent. The eastward flow in the sub-antarctic and antarctic areas constitutes the Atlantic sector of the Circumpolar Current. While these waters are in the Atlantic sector, they are modified via mixing with the more saline North Atlantic Deep Water, the outflow of the Weddell Sea and inflow (e.g. Agulhas Current) from the Indian Ocean. Furthermore, the deep waters outcrop during the winter and exchange gases and energy with the atmosphere in the sub-polar and polar regions. While some portion of these waters thus modified is transported to the north in the form of the Falkland (or Malvinas) Current in the sea surface regime, the Antarctic Intermediate Water in the mid-depth (~1000 meters) regime and the Antarctic Deep Water (below about 3000 meters deep), the remainder flows out of the Atlantic to the Indian Ocean through the broad area between the southern Africa and Antarctic continents. The major objective of the present investigation is to determine the depth and geographic distribution of the total CO_2 concen- tration and pCO_2 in seawater over high latitude areas of the South Atlantic Ocean including the Drake Passage (WOCE Section A-21), the northern Weddell Sea and the eastern South Atlantic (WOCE Section A-12) areas. In addition, the distribution of temperature, salinity and the concentrations of dissolved oxygen and three nutrient salts and their relationships with CO_2 are presented.

II. SAMPLING AND EXPERIMENTAL METHODS

II-1) Sampling Locations and Methods:

The Cruise No. 11/5 of the F/S METEOR of the Federal Republic of Germany started at Ushuaia, Argentina, on January 21, 1990, and ended at Capetown, South Africa, on March 7, 1990. During the 45-day expedition in the South Atlantic and the Atlantic sector of the Southern Ocean, 177 stations were occupied along the WOCE sections A-21 and A-12. The station locations are shown in Fig. 1.

The water samples were collected by means of a 24-bottle rosette unit equipped with CTD. Ten-liter capacity "Niskin" samplers made of PVC were used for water sampling. Four to six pairs of protected and unprotected reversing thermometers were used for each cast for the purpose of calibrating the temperature and pressure sensors of the CTD. Water samples for the determination of total CO_2 concentration and pCO_2 were drawn directly from the Niskin samplers to respective sampling bottles after the water samples for the determinations of CFC's, Helium-3, and dissolved oxygen were drawn from each sampler. A 500-ml Pyrex reagent bottle equipped with a standard-tapered ground glass stopper (vacuum silicone grease as sealant) was used for the total CO_2 samples and a 500-ml long-neck Pyrex bottle equipped with a plastic screw top with a plastic sealing cone was used for the samples for pCO_2 measurements. The sample bottles were rinsed three times with sample waters before the filling. About 5 ml of head space was left in each bottle to prevent damages of bottles by thermal expansion of water during the storage. About 200 microliters of 50%-saturated mercuric chloride solutions were added to each of these samples immediately after sample collection in order to prevent biological alteration of the samples during temporary storage. Most of the samples were analyzed within 24 hours, and all were done within 72 hours of collection, with the exception of surface water pCO_2 samples in the Drake Passage section. The determination of pCO_2 in the water samples collected in the Drake Passage were delayed several days after collection because of temporary malfunction of the gas chromatographic system.

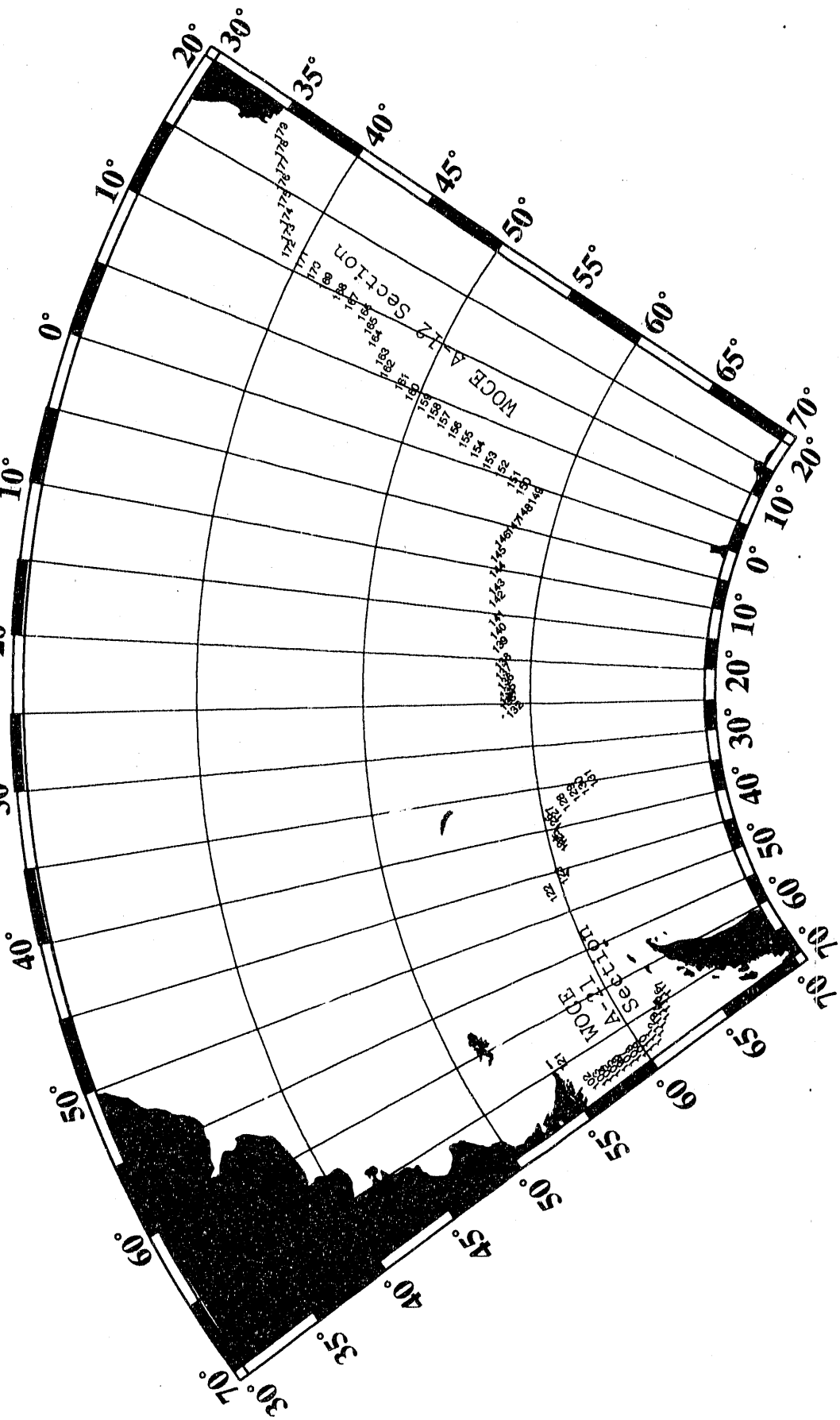

Fig. 1 - Map showing the station locations and station numbers occupied during the F/S Meteor, Cruise No. 11/5, January 25 through March 6, 1990, in the South Atlantic and Weddell Sea.

II-2) The Total CO_2 Concentration in Seawater:

The total CO_2 concentration (TCO_2) in seawater samples was determined using a coulometric system, which has been modified from the one described by Johnson et al. (1985).

For analysis, the seawater was introduced into the stripping chamber using fixed-volume syringes. The sample was acidified with 1 ml of 8.5% phosphoric acid while in the stripping chamber, where the evolved CO_2 gas was swept from the sample and transferred with a stream of CO_2-free air into the electrochemical cell of the CO_2 coulometer (UTC-Coulometrics Model-5011). In the coulometer cell, the CO_2 is quantitatively absorbed by a solution of ethanolamine in dimethylsulfoxide (DMSO). Reaction between the CO_2 and the ethanolamine forms the weak hydroxyethylcarbamic acid. The pH change of the solution associated with the formation of this acid results in a color change of thymophthalein pH indicator in the solution. The color change, from deep blue to colorless, is detected by a photodiode, which continually monitors the transmissivity of the solution. The electronic circuitry of the coulometer, on detecting the change in the color of the pH indicator, causes a current to be passed through the cell generating hydroxyl (OH^-) ions from a small amount of water in the solution. The OH^- generated titrates the acid, returning the solution to its original pH (and hence color), at which point the circuitry interrupts the current flow. The product of current passed through the cell and time is related by the Faraday constant to the number of moles of OH^- generated to titrate the acid and hence to the number of moles of CO_2 absorbed to form the acid.

The volumes delivered by the constant-volume syringes have been determined by repeatedly weighing distilled water dispensed in the same manner as a sample, and the volume calculated from the weight delivered, using the density of pure water at the temperature of the measurement and a buoyancy correction for the air displaced by the water (which amounts to about 0.1% of the weight of the water). The density of the seawater in the pipet was obtained at the temperature of injection using the International Equation of State (Millero et al., 1980).

The coulometer was calibrated using research grade CO_2 gas (99.998%) introduced into the carrier gas line upstream of the extraction tube, using a pair of fixed-volume sample loops on a gas sampling valve and measuring the pressure of the gas in the loops by venting it to the ambient atmosphere and determining the barometric pressure using the same electronic barometer used with the pCO_2 system; the loop temperature was measured to ± 0.05°C with a thermometer calibrated against one traceable to the NBS, and the non-ideality of CO_2 was incorporated in the computation of the loop contents. The volume of the calibration loop had previously been determined by weighing empty and filled with mercury. The volumes of these loops have additionally been checked by comparing the amount of CO_2 introduced by them with the amount derived from gravimetric samples of calcium car-

bonate and sodium carbonate, and found to be accurate to within 0.1%. During the expedition, the coulometer was calibrated several times daily using the calibrated loop and pure CO_2 gas.

In order to evaluate the long term reproducibility and precision of the coulometric determination of CO_2 in seawater, a number of sample bottles were filled with a homogeneous sample of surface water and deep water. Both Pyrex glass and PET plastic bottles (500 ml and 1000 ml respectively) were used. These bottled samples were poisoned with mercuric chloride solutions (200 microliters for each 500 ml water sample) and analyzed for total CO_2 during the expedition. The results are summarized in Fig. 2. Forty four determinations of the surface water samples conducted over 39 days at sea indicate a mean of 1965.2 uM/kg with a root mean square deviation of ±1.0 uM/kg (see Fig. 2-A). Sixteen determinations of the deep water samples conducted over 13 days show a mean of 2262.2 uM/kg with a root mean square deviation of ±1.0 uM/kg. Therefore, the precision for the total CO_2 concentration values reported in this report have been estimated to be ±1.0 uM/kg. However, as mentioned earlier, the water samples for total CO_2 analyses were collected from Niskin samplers after 1 to 2 liters of headspace was formed by the withdrawal of other water samples. Since marine air introduced into the headspace had lower pCO_2 values than those for the seawater in samplers, especially after several degrees of warming occurred during hoisting, it is likely that CO_2 was lost from the sample waters to the headspace. During the South Atlantic Ventilation Experiment (SAVE) program, the loss has been estimated by comparing the total CO_2 concentrations determined for those from the 10-liter Niskin samples with those from the 280-liter Gerard samplers. Because of its large mass, the water temperature in a Gerard sampler changed little during hoisting from the sampling depth. In addition, because of the height (about 1.5 meters), an water sample drawn from the base of the sampler was thought to be unaffected by the air introduced into the headspace. For these reasons, it was considered that little or no CO_2 had been lost from the water samples withdrawn from Gerard samples. The results of nearly 40 pairs of comparison indicate that the deep water samples collected from the Niskin samplers appear to have lost no more than 2 uM/kg of CO_2 before the seawater samples were transferred into the sample bottles.

II-3) Determination of pCO_2 in Seawater:

A fully automated equilibrator-gas chromatograph system was used during the expedition ... the determination of partial pressure of CO_2 exerted by the seawater samples. Its design and operation will be outlined below. Figure 3 gives a schematic diagram of this system.

The system consists of a pair of air circulation pumps (Spectrex Model AS-300-SS) plumbed to recirculate air through porous plastic gas dispersers which are immersed in two separate seawater sam-

Fig. 2 - The results of repeated measurements at sea of the total CO_2 concentration in surface (A) and deep (B) water samples. About 50 sample bottles were filled with a homogenized surface water sample and were analyzed over a 50-day period during the expedition. Only 20 bottles were filled with a homogenized deep water sample and analyzed subsequently over a period of 13 days. The analyses of these samples yield a mean value of 1965.2±1.0 for the surface wamples and 2262.2±1.0 for the deep water samples.

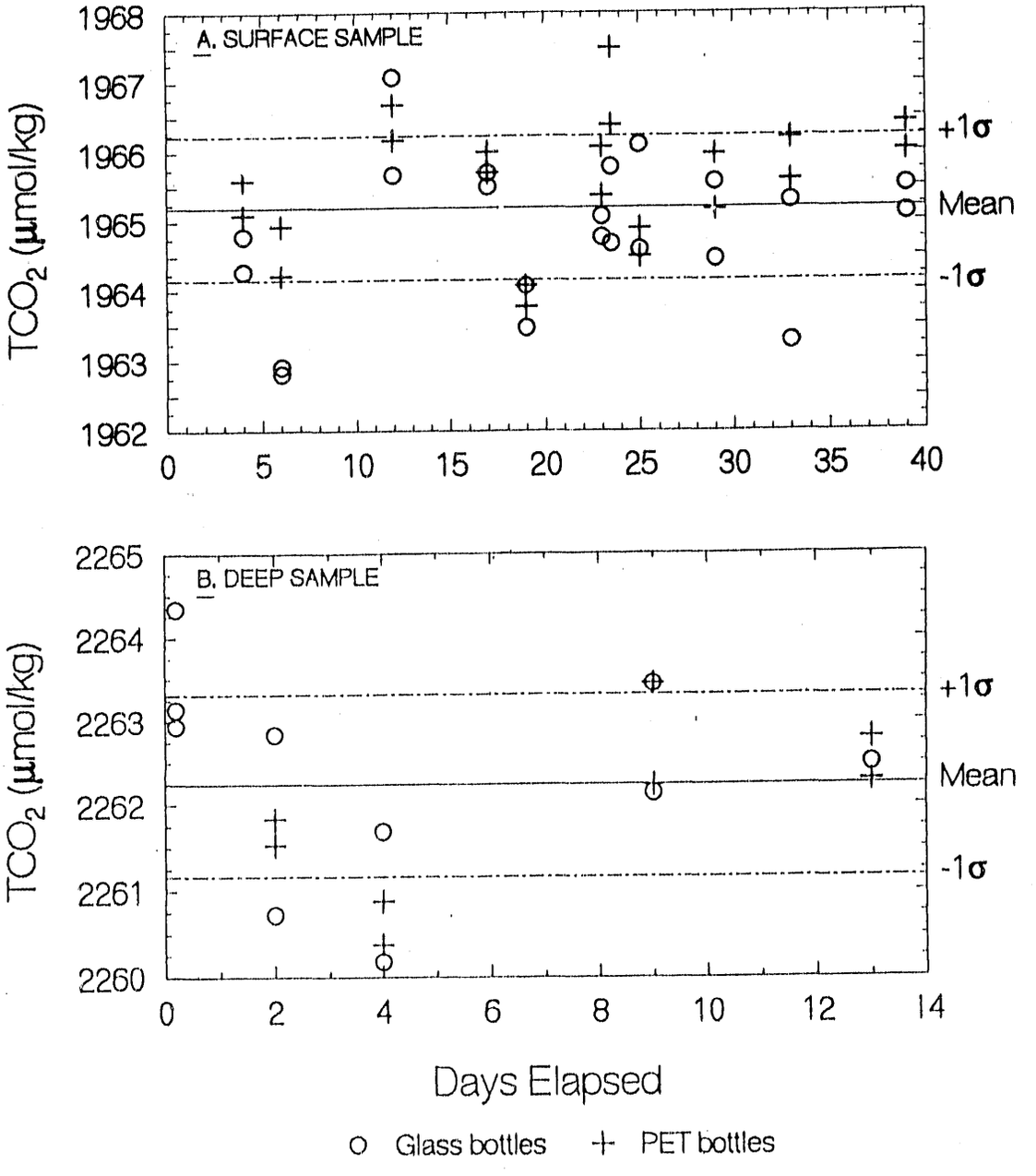

Fig. 3 - A schematic diagram showing the gas-water equilibrator and gas chromatographic system for the measurement of pCO_2 in discrete water samples. Two gas-water equilibration vessels are shown in this diagram. The electronic signals from the flame inoization detector are fed into and processed by an integrator (Shimadzu Chromatooac Model C-R6A) which is not shown.

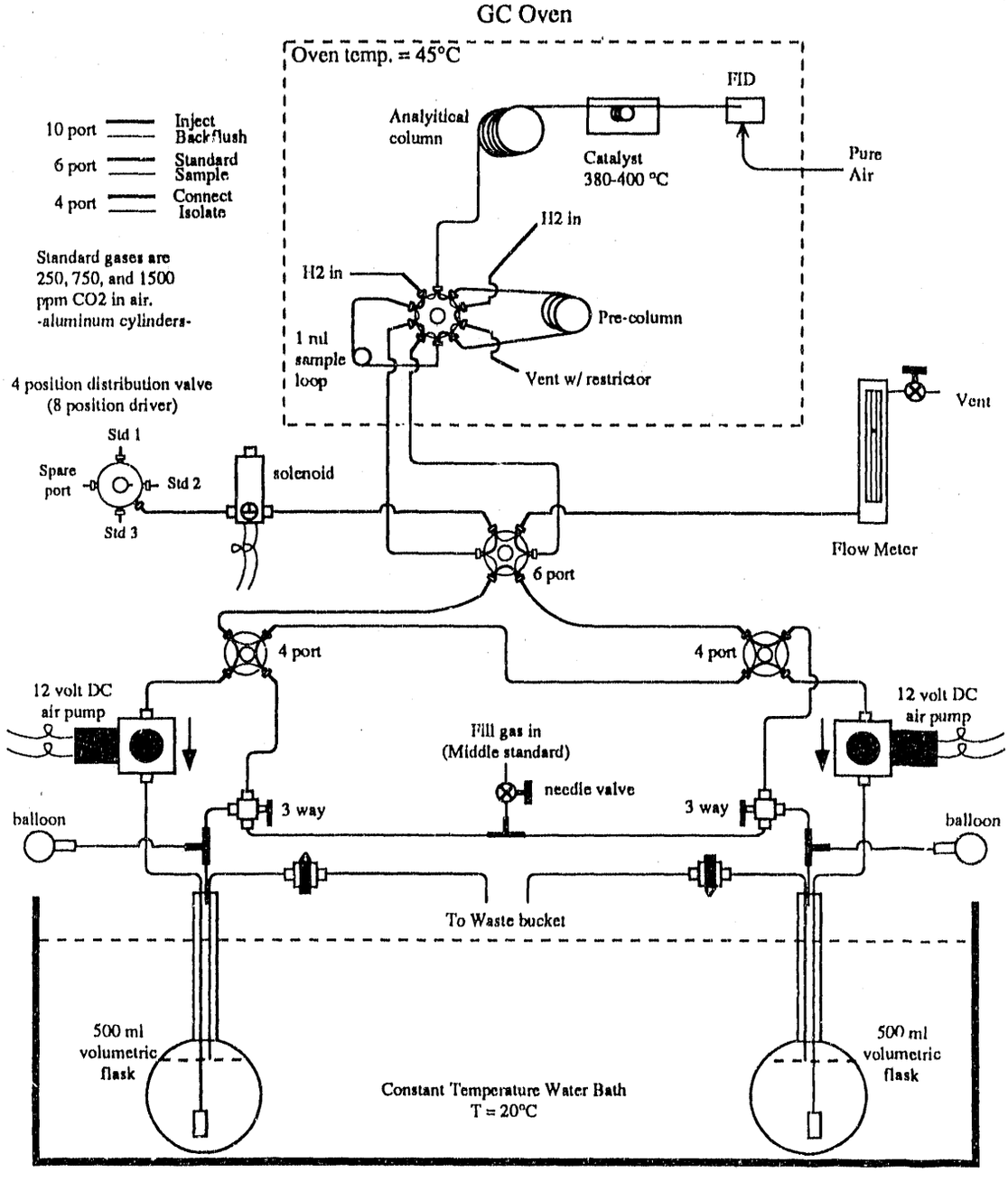

ples. Electrically driven Valco 4-port valves are used to isolate each of the equilibrators during the initial equilibration prior to analysis of the equilibrated air. Manually operated 2-way and 3-way Whitey valves allow part of the water in each equilibrator to be replaced with air of known initial CO_2 concentration, to create the necessary headspace for equilibration. A drain line in each equilibrator insures the ratio of water to air in each equilibrator will be constant, allowing accurate corrections to be made for the effect of the perturbation of the sample seawater by the headspace air. Diaphragms (thin rubber balloons) are plumbed to each equilibrator to provide "soft walls" to the system, so that the pressure in the equilibrators will be kept close to the ambient laboratory atmospheric pressure which is measured with a high precision electronic barometer. Since the partial pressure of CO_2 is strongly affected by temperature changes, the equilibration flasks are kept immersed in a constant temperature water bath, held at a temperature of 20.00°C. An electrically driven Valco 6-port valve allows the entire equilibration system to be isolated, simultaneously connecting a calibration gas selection valve (also electrically driven Valco, Model 4SD, with 4 input ports but with an eight-position driver, so that all gas flows will be blocked at the four intermediate positions). A 2-way normally-closed Skinner solenoid valve on the output of the calibration selection valve allows the gas flows to be controlled by the system controller, and provides a necessary second means of stopping the flow of the calibration gases to prevent the accidental loss of calibration gases in the event of control malfunction.

The analysis of the CO_2 in the equilibrated air or calibration gases is performed using a Shimadzu Mini-2 gas chromatograph, which is equipped with a flame ionization detector. A one-ml sample loop, a pre-column and an analytical column (both packed with Chromosorb 102 and 0.2 and 2.0 meters long respectively) are attached to an electrically driven Valco 10-port valve within the column oven of the gas chromatograph. Ultra-high purity hydrogen gas (electrolytically generated by an Aadco hydrogen generator and purified by means of diffusion through a palladium foil using an Aadco hydrogen purifier) serves as the carrier gas for the chromatographic separation of CO_2 from the other components of the air. The use of hydrogen for carrier gas also allows the CO_2 to be converted to methane in an attached catalytic converter prior to quantification by the flame ionization detector. Unlike the method described by Weiss (1981), our system uses a catalyst of ruthenium metal on Chromosorb W support and does not require a palladium pre-catalyst to remove oxygen from the carrier gas stream. Hydrocarbon-free air to support the combustion in the flame ionization detector is provided by means of a chromatographic air purifier (Aadco Model 737).

Integration of the output signal from the gas chromatograph and control of the entire equilibration and calibration procedure is provided by means of a Shimadzu Chromatopac (Model C-R6A) computing integrator.

The analytical procedure is as follows. Prior to analysis, the sample flasks are brought to 20.00°C in the thermostated water bath, and about 45 ml of water is displaced with air of known CO_2 concentration. The air in the flasks and in the tubing connecting the flasks to the gas chromatograph sample loop is recirculated continuously for approximately 20 minutes, with the gas disperser about 1 cm below the water surface providing large contact area between water and air bubbles. At the end of the equilibration period, the circulation pump is switched off and the air pressure throughout the system is allowed to equalize. A 1-ml aliquot of the equilibrated air is isolated from the equilibration subsystem and injected into the carrier gas stream of the gas chromatograph by cycling the gas sampling valve to which the sample loop is attached. After chromatographic separation, the CO_2 is converted into methane and water vapor by reaction with the hydrogen carrier in the catalytic converter. The methane produced by this reaction is then measured with a precision of ± 0.05 % (one standard deviation) by the flame ionization detector. The concentration of CO_2 in the sample is determined by comparison with the peak areas of known amounts of CO_2 from injections of three reference gas mixtures, which have been calibrated against the World Meteorological Organization standards of C. D. Keeling. The reference gas mixtures are injected into the gas chromatograph using the same sample loop as that used for the equilibrated air samples, and the pressure of the gas in the sample loop at the time of injection is determined by venting the loop to atmospheric pressure and measuring that pressure by means of a high-accuracy electronic barometer (Setra Systems, Inc., Model 270, accuracy ± 0.3 millibars, calibration traceable to the NBS provided by the manufacturer). The sample loop is located within the well-controlled temperature environment of the column oven of the gas chromatograph, and hence all injections are made at constant temperature.

In order to demonstrate that the equilibrator yields an equilibrium pCO_2 value and that use of gas bubbles does not affect the results, an experiment has been conducted. The equilibration vessel was first filled with a seawater sample which has a higher pCO_2 than the carrier gas. The temperature of water was kept at 20.0°C. While the water sample was gently stirred with a magnetic stirrer, the carrier gas was circulated through the equilibration vessel without bubbles (i.e. the gas disperser was pulled above the water). After 2 hours, a steady state value of 824.8 uatm was obtained. The water was then warmed by about a few degrees C, so that pCO_2 in the carrier gas was increased, while the amount of CO_2 within the system remained unaltered. The water was then cooled to 20.0°C within about 10 minutes, while the pCO_2 in the circulating carrier gas was monitored. As pCO_2 in the circulating gas decreased gradually over 2 to 4 hours of quiet stirring of water, a steady state value of 829.9 uatm was obtained, suggesting that the equilibrium value should lie between these two readings, 824.8 and 829.9 uatm or 827.4 ± 2.5 uatm. Next, the water was cooled by a few degrees C in order to lower the pCO_2 in the gas and then its temperature was restored to 20.0°C while circulating carrier gas was

Fig. 4 - Test for the CO_2 equilibration between air and seawater, and the effect of bubbles on equilibration. The equilibrium value is bracketed by the value of 824.8 and 829.9 uatm, which respectively represent steady state values approached from above and below after 2 hours of quiet stirring. The steady state value obtained after bubbling is 827.6 uatm, which agrees well with the mean of the quiet stirring values, 827.4 uatm.

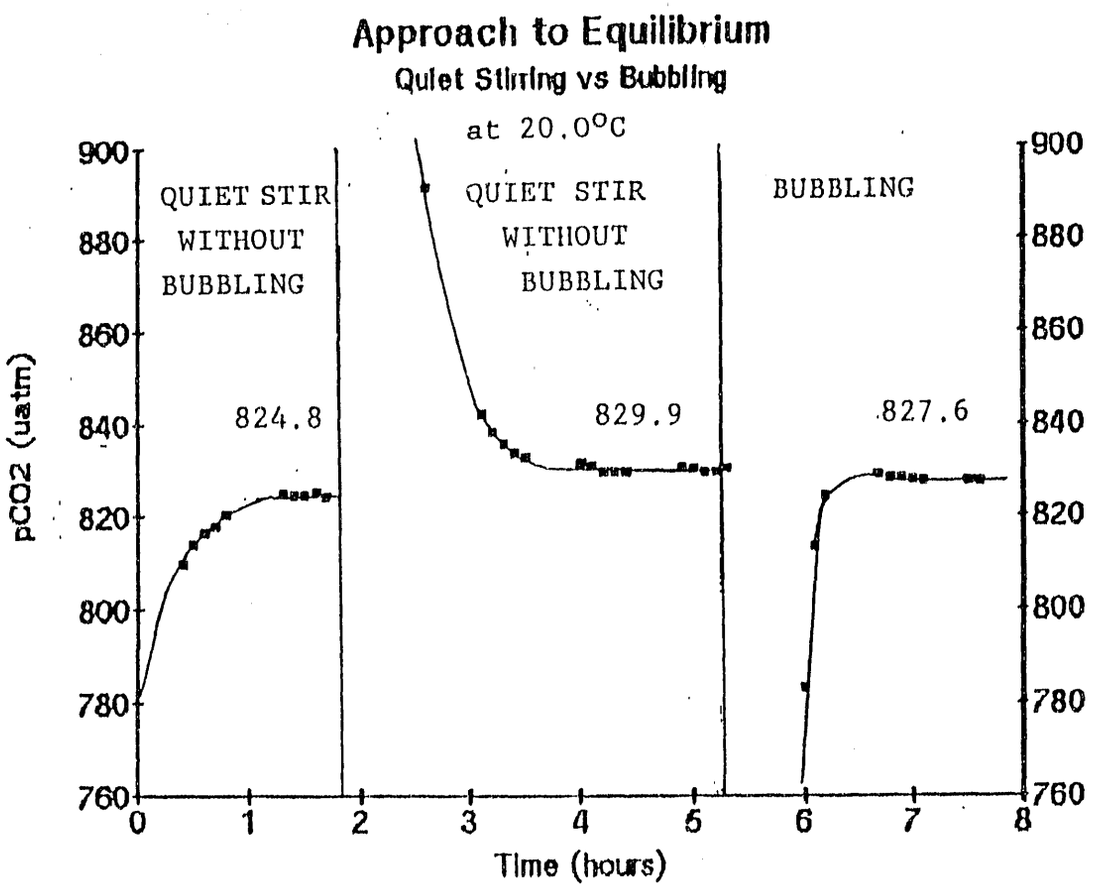

bubbled through the upper 1 cm of water column (i.e. by lowering the gas disperser head into the water). Fig. 4 shows that the bubbling process greatly enhances the rate of CO_2 gas exchange between the air and water and yields a steady state value of 827.6 uatm. This value is consistent with the mean value obtained for the quiet equilibration (i.e. no bubbles) approached from high and low pCO_2. Accordingly, the method used in this study appear to yield a thermodynamic equilibrium value without introducing systematic bias in the final composition of the equilibrated air.

The equilibrated air samples are saturated with water-vapor at the temperature of equilibration and have the same pCO_2 as the water sample. By injecting the air aliquot without removing the water vapor, the partial pressure of CO_2 is determined directly, without the need to know the water vapor pressure (Takahashi et al., 1982). It is necessary to know the pressure of equilibration, which is done by having the equilibrator flask always at atmospheric pressure. The atmospheric pressure is, in turn, measured with the electronic barometer at the time each equilibrated air sample is injected into the gas chromatograph. Corrections are required to account for the change in pCO_2 of the sample water due to the transfer of CO_2 to or from the water during equilibration with the recirculating air. The overall precision of the pCO_2 measurement is estimated to be about $\pm 0.10\%$ based on the reproducibility of replicate equilibrations.

II-4) Determination of pCO_2 in Air:

The air samples for pCO_2 analysis were collected in a 50 ml glass syringe equipped with a plastic shut-off valve. A small column of desiccant (P_2O_5) was attached at the air intake for the removal of water vapor. The syringe was flushed with several volumes of air from a point at the ship's rail facing into the wind, and the valve was closed to isolate the final volume of air. The syringe was then connected to the sampling loop (about 1 ml) of the gas chromatograph, and the loop was flushed with at least 40 ml of the sample air about 30 seconds before the loop contents were injected into the GC for analysis. The over-all precision for the atmospheric CO_2 measurements, including the effects of the sampling and analytical procedures, has been estimated to be about ± 0.2 ppm CO_2 mole fraction in dry air.

The pCO_2 values in air have been computed assuming that the air is saturated with water vapor at the seawater temperature. The following equation was used for this purpose:

$$(pCO_2)_{air} = (VCO_2)_{air} \cdot (Pb - Pw), \quad \text{.....(2)}$$

where $(VCO_2)_{air}$ is the mole fraction concentration of CO_2 in dry air, Pb is the barometric pressure measured at each station and Pw is the equilibrium water vapor pressure at sea surface temperature and salinity. The following empirical expression was used to compute the equilibrium water vapor pressure, Pw:

$$Pw\ (atm) = (1/760)[1 - 5.3684 \times 10^{-4}.(Sal - 0.03)].$$
$$EXP\{[0.0039476 - (1/TK)]/1.8752 \times 10^{-4}\} \quad .....(3)$$

where Sal is salinity in o/oo (PSU), and TK is the temperature in °K.

Since the variability of atmospheric CO_2 concentrations is expected to be small in the study area, only six determinations were made during the expedition. The measurements yield a mean atmospheric CO_2 concentration of 350.0±1.5 ppm (in mole fraction of CO_2 in dry air). This mean value has been used to compute the atmospheric pCO_2 and the sea-air pCO_2 difference at each station. The measured atmospheric concentrations and computed atmospheric pCO_2 values are listed in the Data Tables of this report.

II-7) Alkalinity:

The alkalinity of seawater has been computed using the observed values of pCO_2, total CO_2 concentration, phosphate concentration, temperature and salinity. For our computation, the total alkalinity (TALK) in seawater is defined by:

$$TALK = Ac + Ab + Asi + Ap + Aw \quad .....(4)$$

where Ac = Carbonate alkalinity = $[HCO_3^-] + 2[CO_3^=]$

Ab = Borate alkalinity = $[H_2BO_3^-]$,

Asi = Silicate alkalinity = $[H_3SiO_4^-]$,

Ap = Phosphate alkalinity = $[H_2PO_4^-] + 2[HPO_4^=] + 3[PO_4^{-3}]$,

Aw = Water alkalinity = $[OH^-] - [H^+]$.

The total concentration of borate (TB) has been assumed to be proportional to salinity: TB (uM/kg) = 410.6(Sal/35). The borate alkalinity ranges between about 40 ueq/kg for deep waters and 100 ueq/kg

for surface waters. Since the silicate concentration in surface waters may be as high as 150 uM/kg in deep waters, the silicate alkalinity is as high as 6 ueq/kg for deep water but it is negligibly small for surface waters. The phosphate alkalinity ranges from 0.5 ueq/kg for surface waters to about 5 ueq/kg in deep waters. The following apparent dissociation constants of acid in seawater were used; Merhbach et al. (1973) for carbonic acid; Lyman (1956) for boric acid; Kester and Pytkowicz (1967) for phosphoric acid; Ingri (1959) for silicic acid; and Millero (1979) and Culberson and Pytkowicz (1973) for water. The expressions used to compute these constants as a function of temperature and salinity and the computational scheme are described in Peng et al. (198?).

II-4) Measurements of Hydrographic Variables:

The following hydrographic variables were measured by the staff of the Oceanographic Data Facility of the Scripps Institution of Oceanography and by the members of the Hydrographic Group from the Alfred Wagner Institute, Bremerhaven; temperature, pressure (depth), salinity, the concentrations of dissolved oxygen, nitrate, nitrite, phosphate and silica. The temperature and pressure readings of the CTD unit were corrected using 4 to 6 pairs of reversing thermometers, and the electrical conductivity readings were corrected using the salinity values determined aboard the ship for all of the 24 Niskin samplers. A Guildline salinometer and the Wormley Salinity Standards were used for the determination of salinity in the discrete water samples. The precision of measurements has been estimated to be ± 0.002 °C for temperature and ± 0.002 o/oo for salinity. The potential temperature (θ) and potential density (σ_o, σ_2 and σ_4) values have been computed using the potential temperature algorithm of Fofonoff (1977), the International Equation of State of Seawater (Millero et al., 1980) and Bryden's (1973) formulation for the adiabatic temperature gradient.

The concentration of dissolved oxygen was determined using the Winkler titration method. For the conversion of volume to moles of oxygen, a molar volume at STP of 22.385 liter/mole (Kester, 1975) was used. The Apparent Oxygen Utilization (AOU) value was obtained by subtracting the measured value from the saturation value. The latter has been computed at the potential temperature of water and 1 atm total pressure using the following expression based on the data of Murray and Riley (1969):

$$\ln(O_2 \text{ in uM/kg}) = -173.9894 + 255.5907(100/TK) + 146.4813.\ln(TK/100) - 22.2040(TK/100) + Sal[-0.037362 + 0.016504(TK/100) - 0.0020564(TK/100)^2],$$

where TK is temperature in °K and Sal is salinity in o/oo.

The concentrations of nitrate, nitrite, phosphate and silicate dissolved in the seawater samples were determined using the standard colorimetric methods with an "Auto-Analyser" generally within 6 hours of collection. The water samples were kept in a refrigerator at about 4°C during the storage period.

All the concentration values are expressed in "per kg of seawater" units, although analytical samples were isolated by volumetric means. For the conversion from the volume to the mass of seawater sample, the density of each water sample was computed with the International Equation of Sate for seawater (Millero et al., 1980) using the measured salinity and the temperature at which the volumetric measurement was made.

III. DISTRIBUTION OF OCEANOGRAPHIC PROPERTIES

III-1) Distribution of Properties in Surface Waters:

The geographic distribution of temperature, salinity, pCO_2, sea-air pCO_2 difference (ΔpCO_2), AOU and the concentrations of dissolved oxygen, total CO_2, nitrate, phosphate and silicate in surface water is shown in Figs. 5, 6 and 7. Each of these properties is plotted along three sections: the Drake Passage (WOCE A-21), the northern Weddell Sea and the Capetown-Weddell (WOCE A-12) sections. The first and third sections are shown as a function of latitude and the second section is shown as a function of longitude.

Across the Drake Passage (Fig. 5), the surface water temperature increases northward from about 1.5°C at 63°S to about 10°C at 55.5°S, while the salinity remains nearly constant at about 33.9 o/oo. On the other hand, all other properties tend to decrease northward. The pCO_2 data show that the surface water is undersaturated with respect to atmospheric CO_2, with an exception of the southernmost area south of about 62.5°S, where the water is slightly supersaturated. The AOU values indicate that the surface water is supersaturated with respect to atmospheric oxygen by about 3 to 6 % (or 10 to 20 uM/kg) with an exception of the southernmost station (62.8°S), where it is undersaturated by about 20 uM/kg. A major feature observed is that the silicate concentration decreases rapidly northward from about 45 uM/kg at 63°S to about 1.5 uM/kg at about 61°S and remains at this low value in surface waters north of 61°S where the temperature exceeds 5°C. On the other hand, the concentrations of nitrate, phosphate, CO_2 and oxygen exhibit only a modest northward decrease across the Drake Passage.

The northern Weddell Sea section (Fig. 6) represents nearly a zonal section (58°S-60°S) along the northern margin of the Weddell Sea with an exception of 4 stations located between 35°W and 40°W (Stations 128 through 131) deviating southward into the Weddell Sea. Along this section, the surface water temperature and salinity are nearly constant at about 2°C and 33.6 o/oo respectively. The water along this section is undersaturated with respect to atmospheric CO_2 by 25 to 100 uatm or about 50 uatm on the average. It is supersaturated with respect to atmospheric oxygen by as much as 7 % (or 25 uM/kg) near 45°W and 61°S, and it becomes closer to saturation eastward becoming nearly saturated or slightly undersaturated east of about 25°W (and 58°S). A major change in the silicate concentration occurs near 58°S and 23°W. The waters west of this location show silicate concentrations as high as 70 uM/kg, whereas those east of 25°W contain less than 20 uM/kg. On the other hand, the nitrate and phosphate concentrations change little along this section and remain nearly constant at about 20 uM/kg and 1.3 uM/kg respectively.

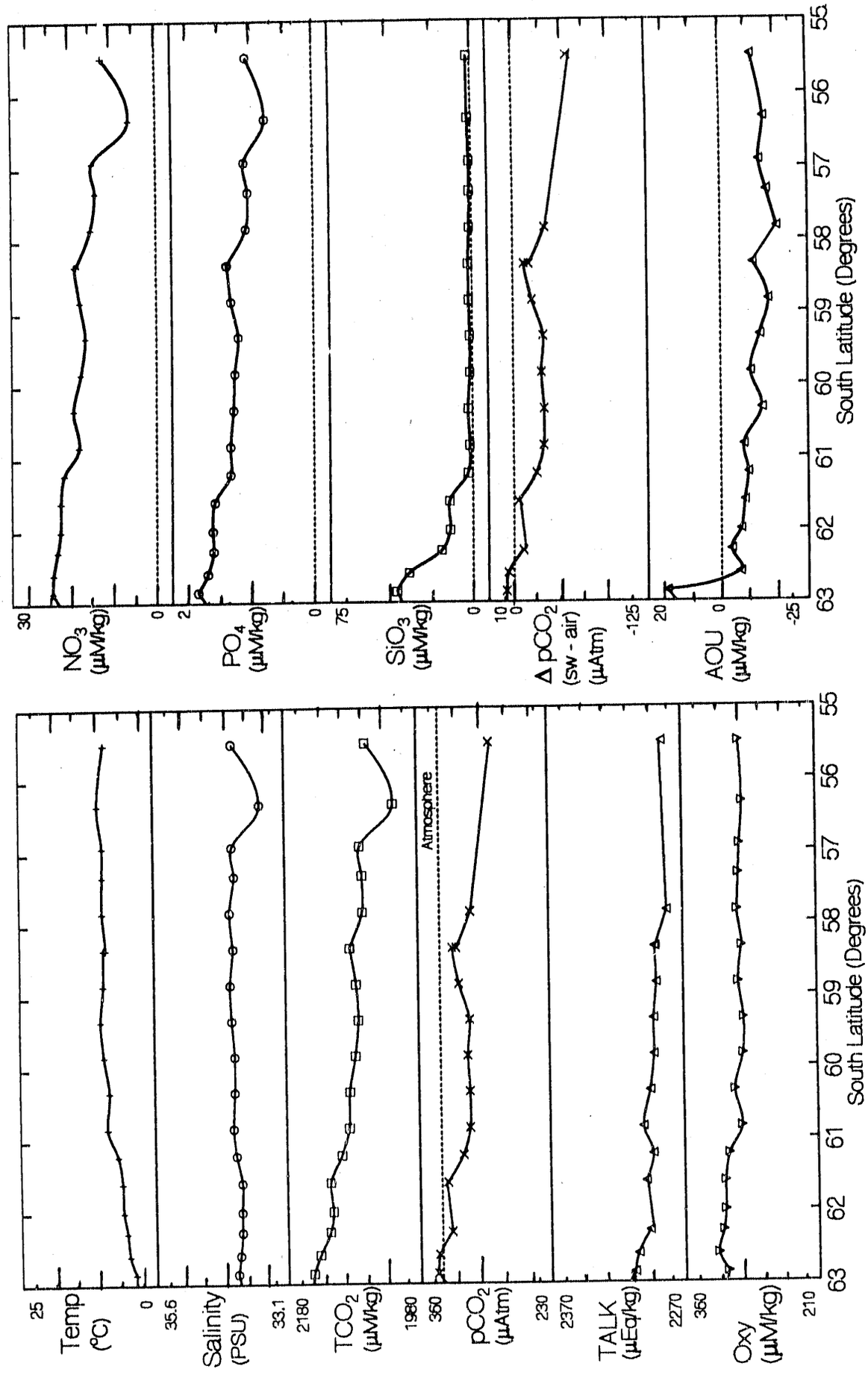

Fig. 5 - Distribution of surface water properties across the Drake Passage (Stations 102 through 121). Note that the vertical scales for the properties are same through Figs. 5, 6 and 7.

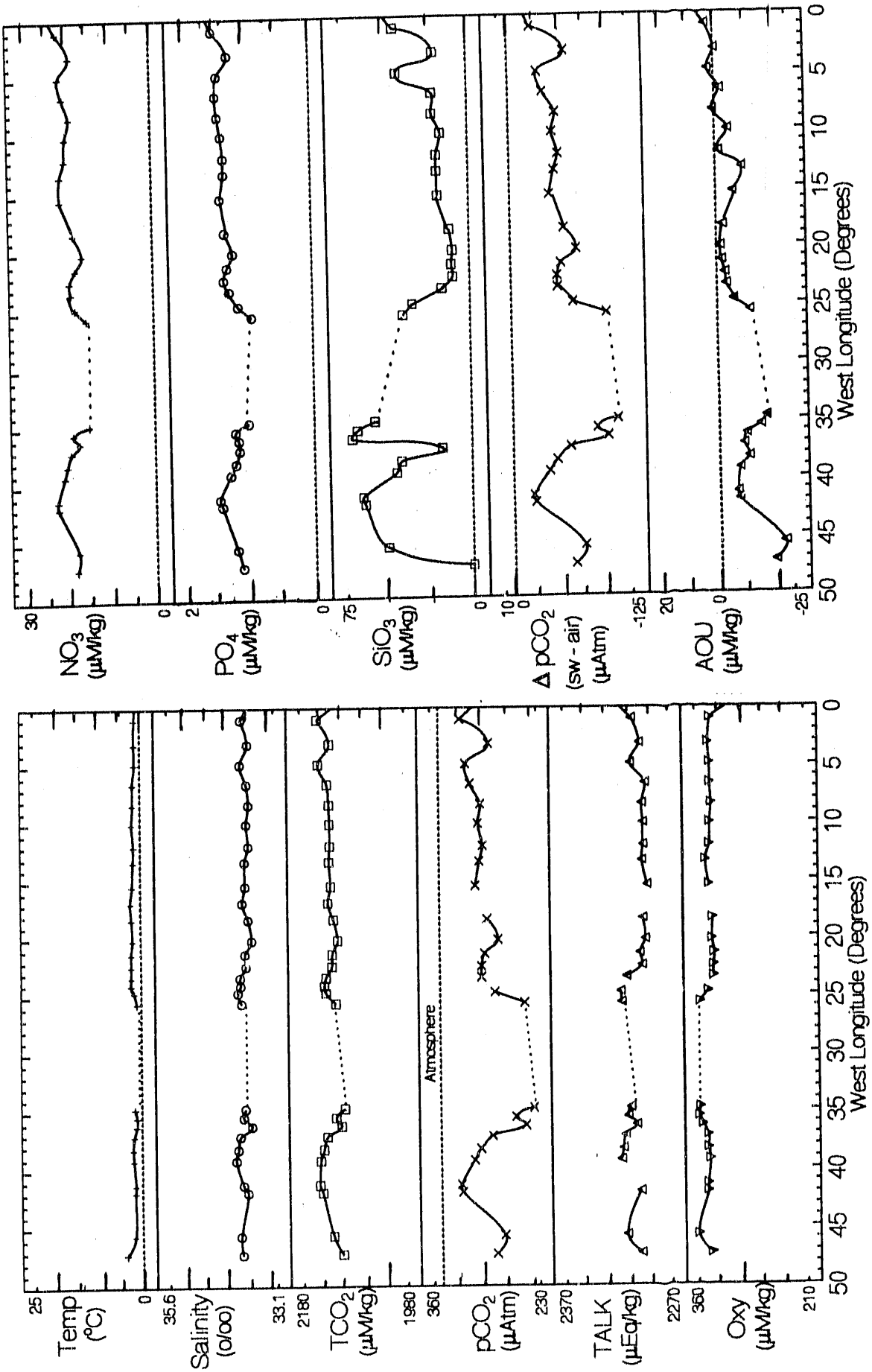

Fig. 6 - Distribution of surface water properties along the northern Weddell Sea section (Stations 122 through 149) in the southcentral South Atlantic Ocean.

Along the Capetown-Weddell section (Fig. 7), four types of waters marked by three major boundaries were traversed. South of about 53°S, the temperature and salinity are uniformly low at about 2 °C and 33.8 o/oo, whereas the concentrations of total CO_2, oxygen, nitrate, phosphate and silica are uniformly high. The surface water is slightly undersaturated with respect to both atmospheric oxygen (AOU ~ +3 uM/kg) and CO_2 (ΔpCO_2 ~ -10 uatm). From 53°S to 49°S, the temperature increases from 2 to 7°C, while all other properties decrease: total CO_2 concentration from 2160 to 2100 uM/kg, oxygen concentration from 340 to 315 uM/kg, nitrate concentration from 25 to 20 uM/kg, phosphate concentration from 1.7 to 1.5 uM/kg, silica concentration from 45 to 2 uM/kg and AOU from 0 to -5 uM/kg. North of 49°S, where the water temperature exceeds 7°C, the concentration of silica remains nearly zero. Between 49°S and 42°S, the temperature continues to increase from about 7 to 11°C, while other properties continue to decrease northward. North of 43°S, the temperature, salinity and alkalinity increase abruptly from about 11 to 17°C and from about 34.0 to 35.0 o/oo, indicating the Subtropical convergence. At the same time, the concentrations of nitrate and phosphate decrease respectively from about 10 to 0 uM/kg and from 1.0 to 0.1 uM/kg. South of the convergence, between 43°S and 35°S, the surface water is undersaturated with respect to atmospheric CO_2 by about 50 uatm whereas it is supersaturated with respect to oxygen by about 10 uM/kg.

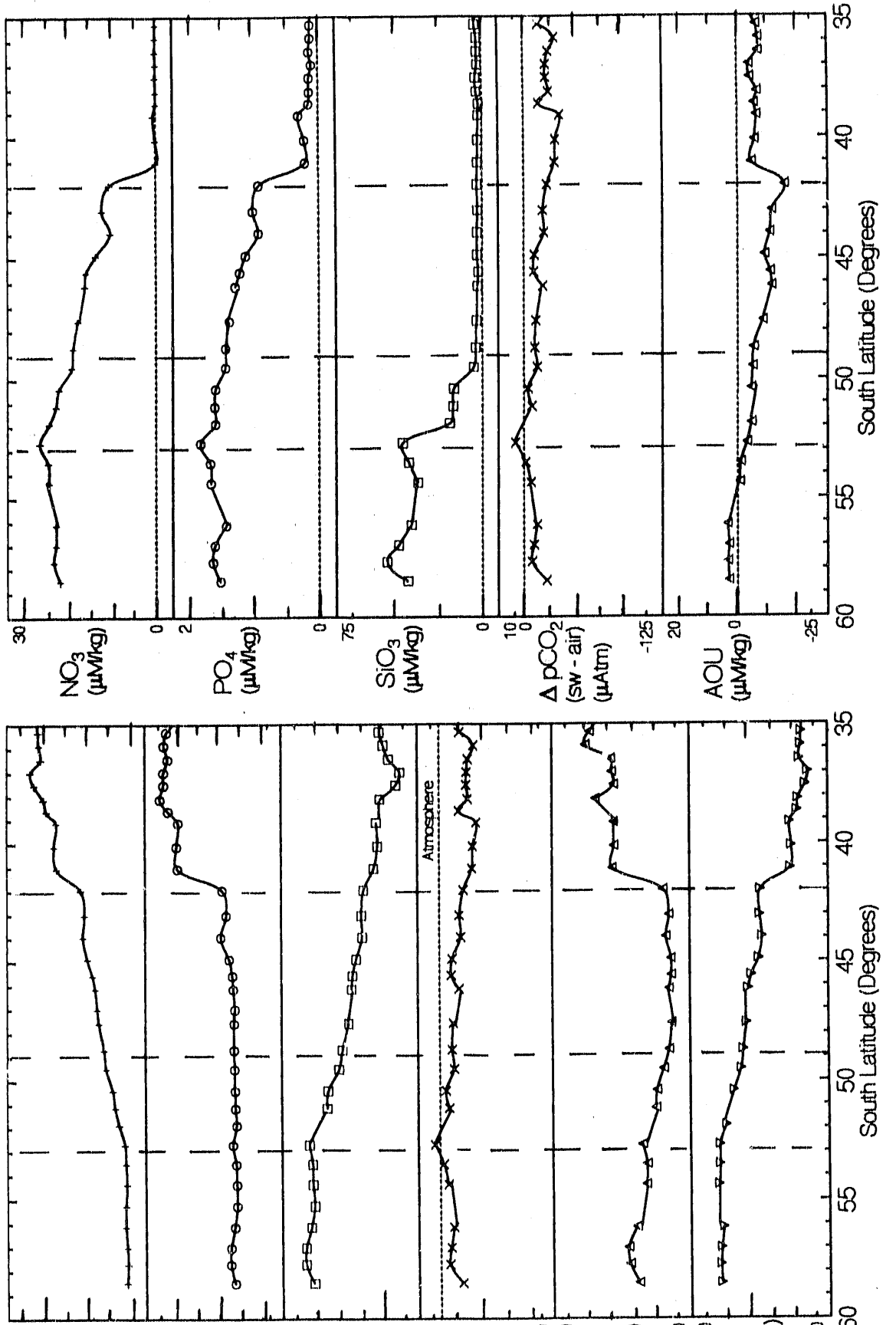

Fig. 7 - Distribution of surface water properties along the Capetown-Weddell section (Stations 149 through 179) in the southeastern South Atlantic Ocean. The dashed vertical lines indicate major changes in properties.

III-2) The Drake Passage (N-S) Section (Stations 102-121):

Contoured sections across the Drake Passage for the following properties are shown below; potential temperature, salinity, potential density at 2000 db, the apparent oxygen utilization (AOU) and the concen- trations of total CO_2, dissolved oxygen, nitrate, phosphate and silica. Since pCO_2 values were obtained at only one station, no section for pCO_2 is presented. All the sections shown in Fig. 8 through Fig. 61 are presented with the full X-axis span equaling to 800 nautical miles.

Fig. 8 shows potential temperature distribution across the passage. The temperature ranges from about 0.2°C at about 4000 meters deep in the southern extreme to about 8°C in surface waters near the coast of South America. Isotherms dip northward and show vertically coherent wavy pattern. This suggests that several bands of water flow zonally through the Drake Passage (i. e. right angles to the section).

Fig. 9 shows that the isohaline contours also are tilted to the north with vertically coherent wavy patterns above about 2000 meters deep. A salinity maximum which may be defined with the 34.73 o/oo contours coincides with the 1.0 and 1.5°C isotherms (Fig. 8) and 190 ~ 200 uM/kg contours for oxygen (Fig. 13). This salinity maximum represents the Circumpolar Deep Water which has temperatures of 0.9~1.4°C with salinities of 34.68 ~ 34.72 o/oo and is commonly found in a depth range of 300 ~ 950 meters in the Southern Ocean (Jacobs et al., 1985). The potential temperature-salinity relationships observed in this section are shown in Fig. 10. There is a minor salinity maximum which is centered around 3500 meters and outlined with the 34.70 o/oo isohalines in the southern extreme of this section. Below the Circumpolar Deep Water lies a colder water layer (0.2 ~ 1.0°C) with a salinity of about 34.70 o/oo. This has been identified as the Southeast Pacific Basin Deep Water (SPDW) (Gordon, 1971-a), and is clearly depicted as a kink point at about 2.0°C and 34.71 o/oo on the θ-S plot in Fig. 10. Below the depths exceeding about 3500 meters at the three southernmost stations, another colder and less saline water mass (34.70 ~ 34.685 o/oo) is present (see Figs. 8, 9 and 10). This represents the Bottom Water of the Southeast Pacific Basin (SPBW) (Gordon, 1971-a).

The distribution of the total CO_2 and oxygen concentrations (Figs. 12, 13 and 14) show additional features: a CO_2 maximum layer (outlined by the 2260 and 2270 uM/kg contours in Fig. 12) and an oxygen minimum layer (outlined by the 170 and 180 uM/kg contours in Fig. 12). Both of these features are located above the salinity maximum layer of the Circumpolar Deep Water and are centered around 2000 meters deep against the continental slope of the South America. They slope upward to the south and reach at a depth of about 500 meters near the Antarctic Peninsula. These features thus observed for the oxygen distribution (Fig. 13) are consistent with that obtained by Gordon and Moli-

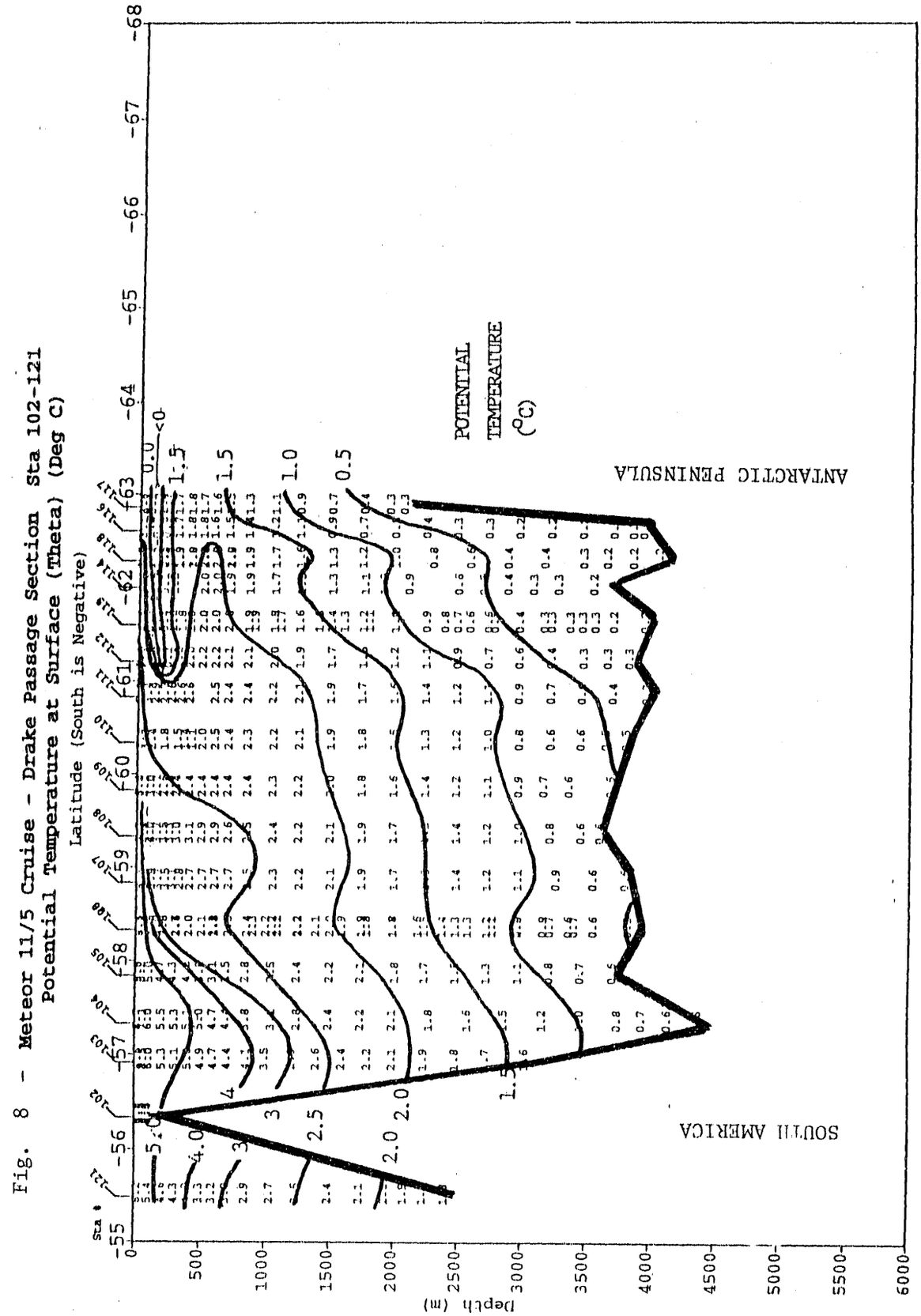

Fig. 8 - Meteor 11/5 Cruise - Drake Passage Section Sta 102-121
Potential Temperature at Surface (Theta) (Deg C)

Fig. 9 - Meteor 11/5 Cruise - Drake Passage Section Sta 102-121
Salinity (PSU)

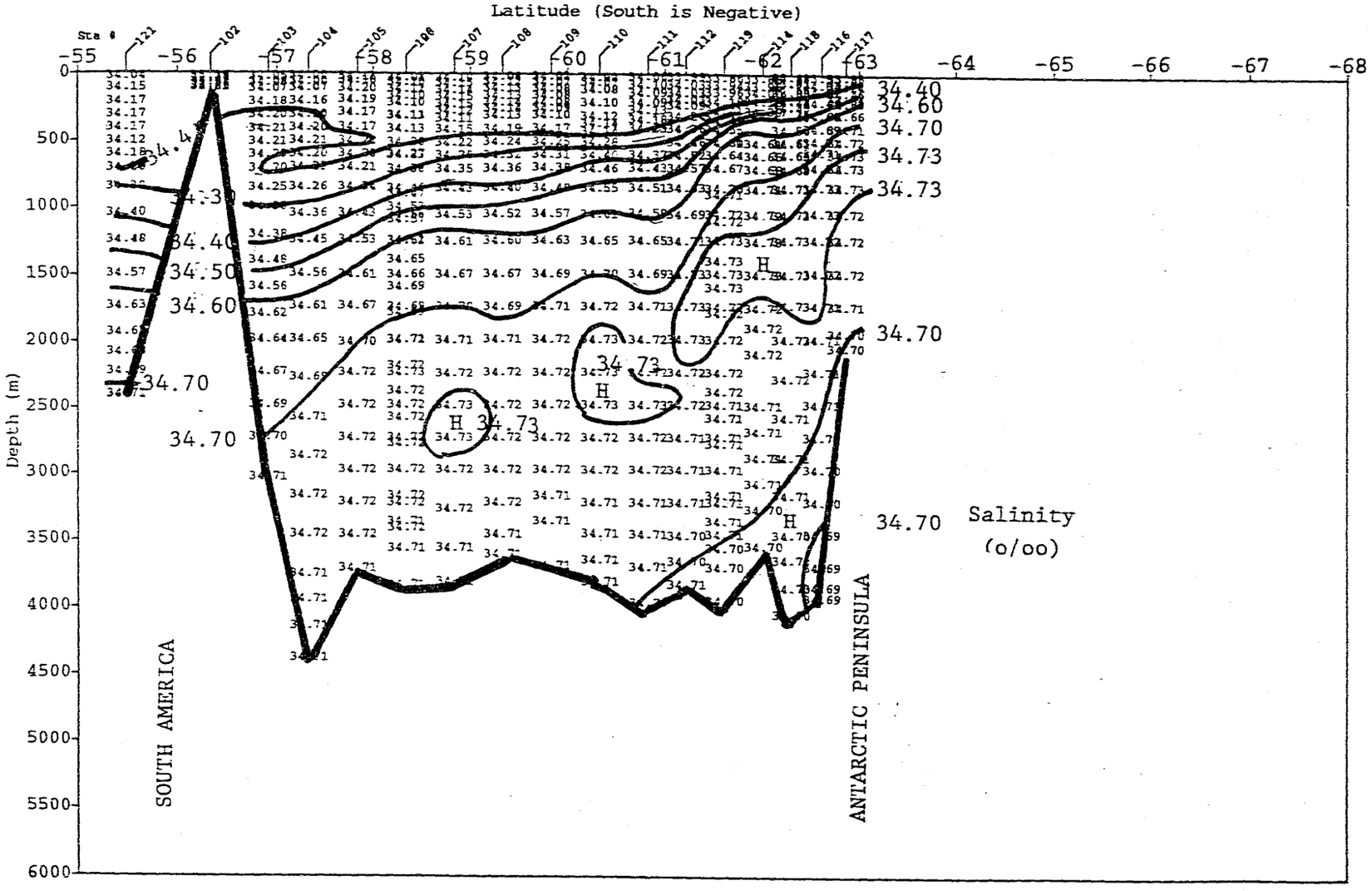

Fig. 10 - Potential temperature-salinity relationships observed in the Drake Passage section. CPDW = Circumpolar Deep Water.

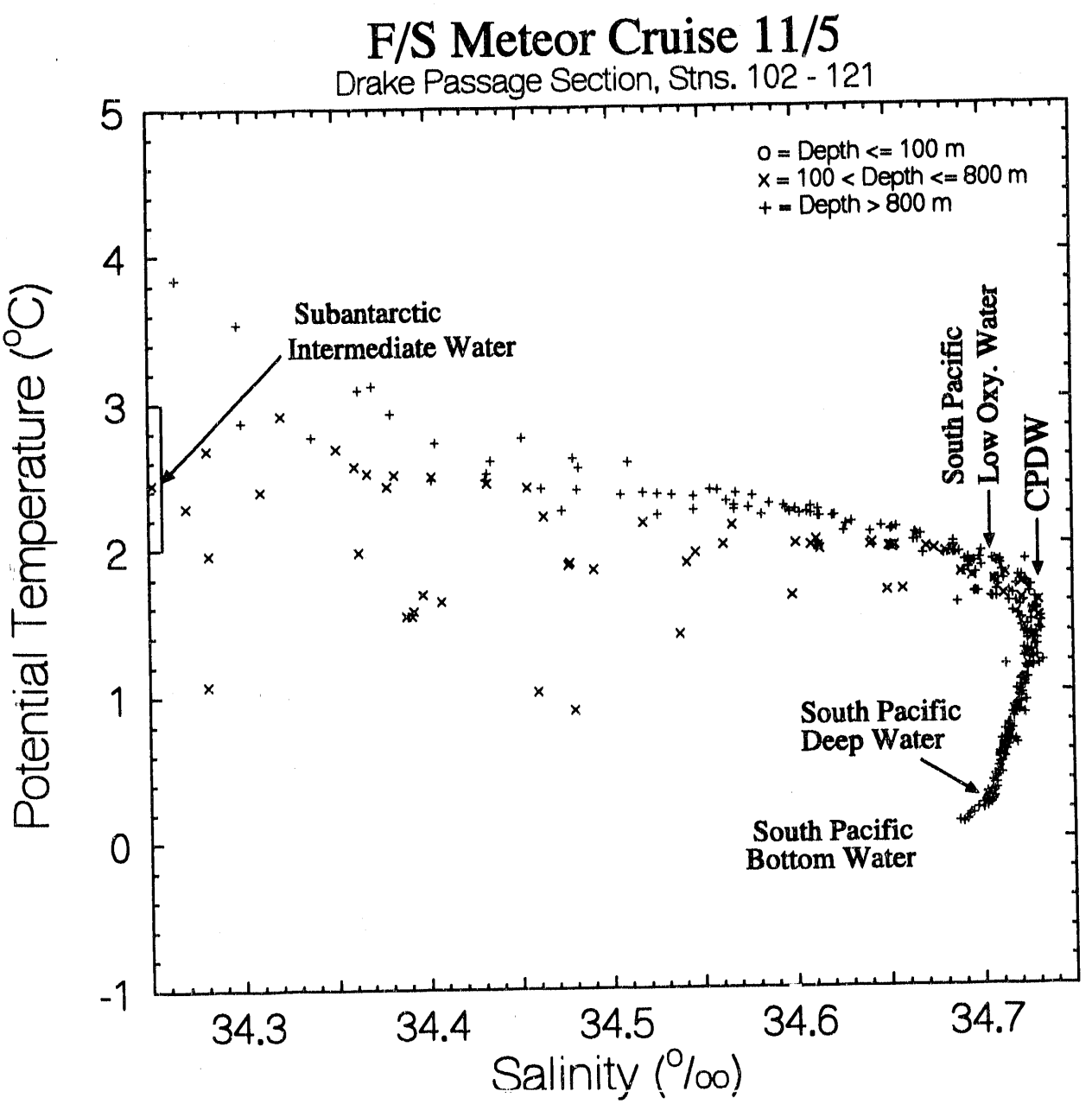

Fig. 11 - Meteor 11/5 Cruise - Drake Passage Section Sta 102-120
Potential Density at 2000 Meters (Sigma 2000) (Sigma Units)

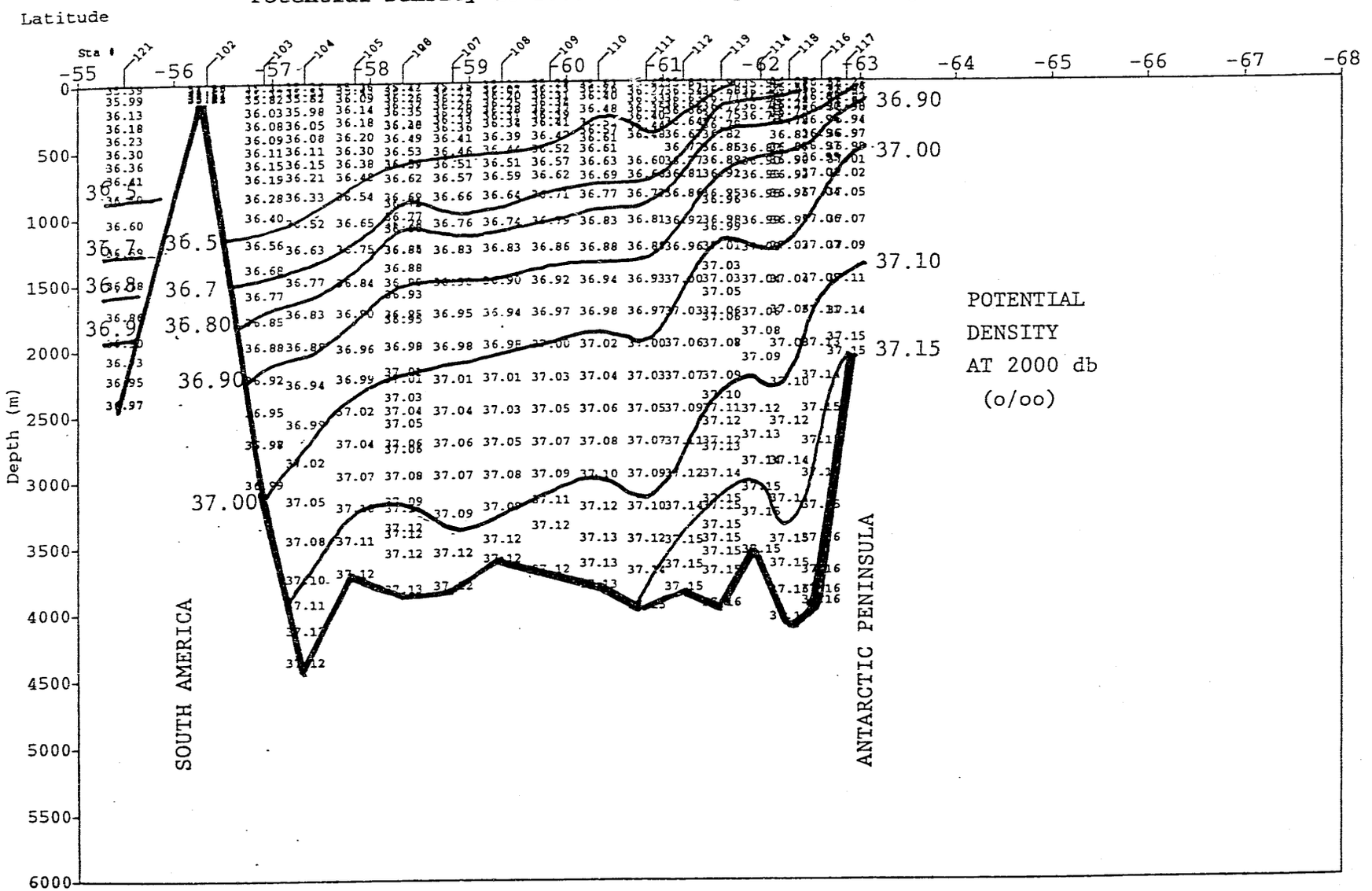

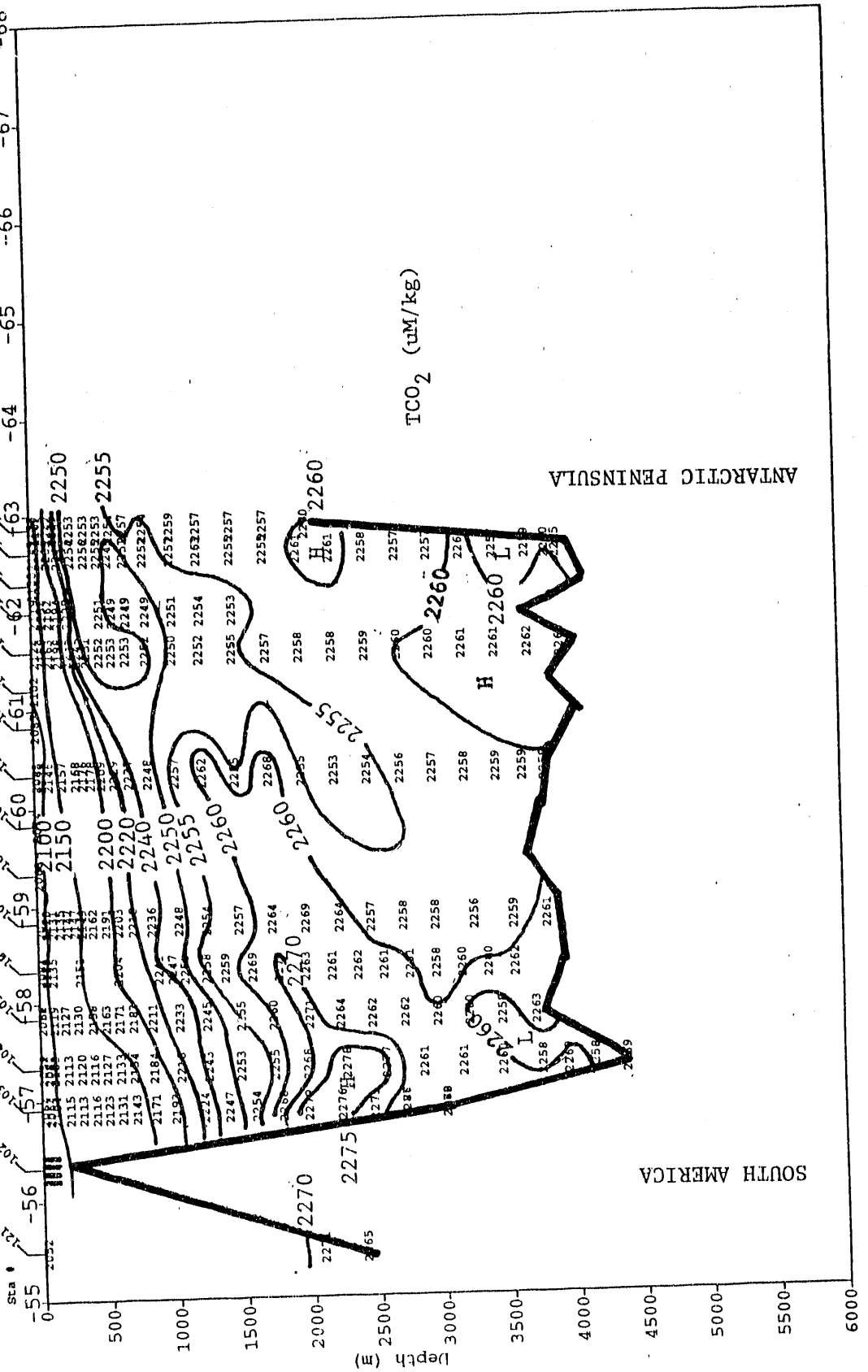
Fig. 12 - Meteor 11/5 Cruise - Drake Passage Section Sta 102-121
TCO2 (uM/kg)
Latitude (South is Negative)
Depth (m)
SOUTH AMERICA
ANTARCTIC PENINSULA
TCO_2 (uM/kg)

Fig. 13 - **Drake Passage - Meteor Cruise 11/5**
Oxygen (uM/kg)

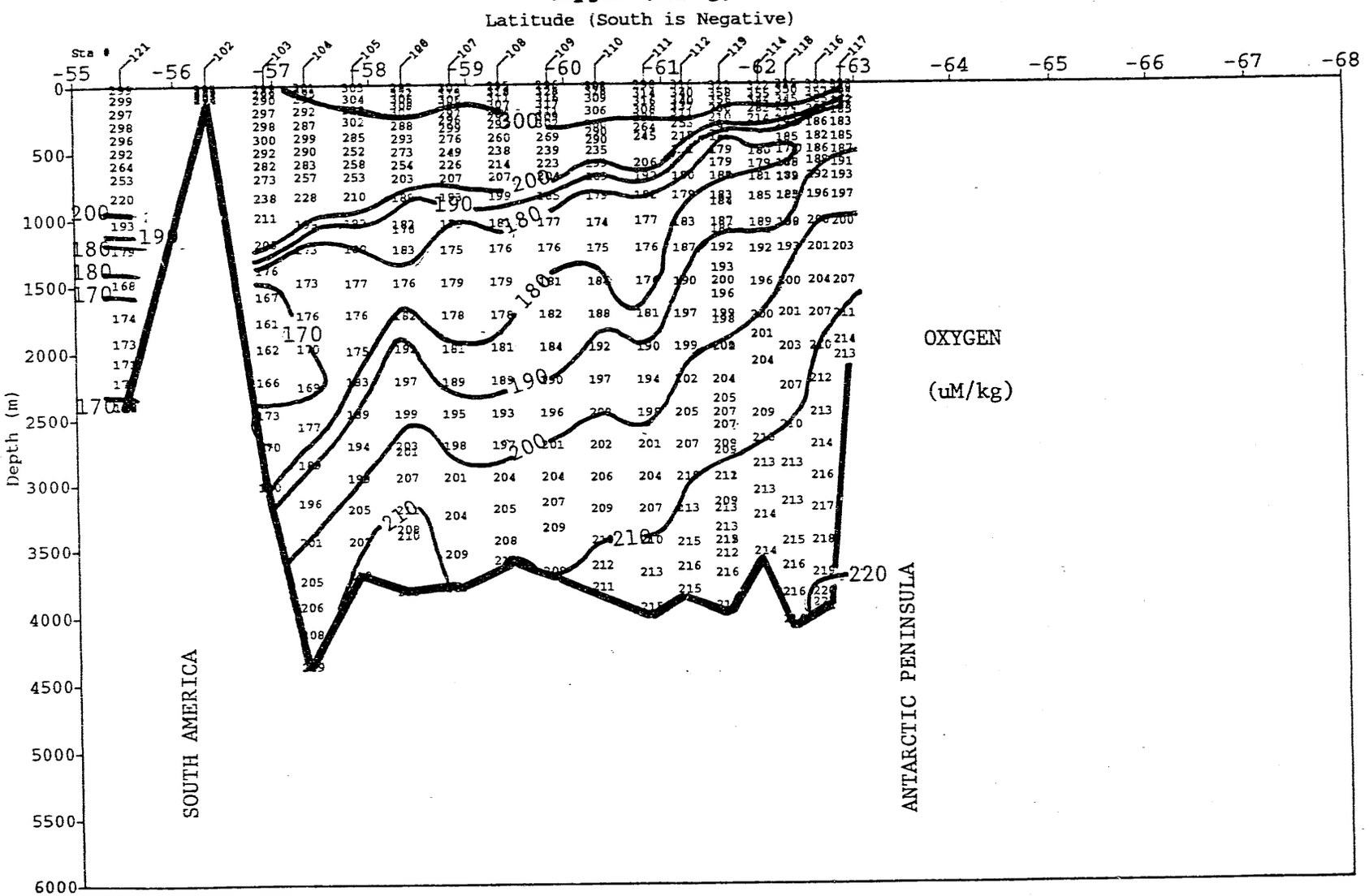

TABLE - 1 Summary of the physical and chemical characteristics of various water masses observed during the Meteor 11/5 expedition in the South Atlantic and northern Weddell Sea areas. The values represent extreme values observed during the expedition, but do not necessarily indicate the values for the "pure" end members of water mass. CPDW = Circumpolar Deep Water; SPLOW = South Pacific Low Oxygen Water; SPDW = South Pacific Deep Water; SPBW = South Pacific Bottom Water. (+) and (-) signs indicate that the values listed comprise a local maximum and minimum respecitvely.

Water Masses	CPDW	SPLOW	SPDW	SPBW
Sections	Drake Pass.	Drake Pass.	Drake Pass.	Drake Pass.
Stations	112-117	103-104	116-119	116
Depths (meters)	300-900	2000-2500	3000-3500	>3500
Pot. Temp. (°C)	0.9-1.4	1.8-2.1	0.2	0.1
Salinity (o/oo)	34.68-34.73(+)	34.64-34.69	34.705	34.685
Density (σ_θ)	27.78-27.82	27.55-27.71	27.85	27.85
Density (σ_2)	36.95-37.05	36.88-36.92	37.10-37.15	37.16
TCO_2 (uM/kg)	2255-2260	2270-2275(+)	2260	2255
pCO_2 @ 20°C (uatm)	1080-1100	1140-1190	No Data	No Data
O_2 (uM/kg)	190-200	160-170(-)	210	220
AOU (uM/kg)	140-150	165-170(+)	135	130
NO_3 (uM/kg)	31-33	34-35(+)	32.8	33.0
PO_4 (uM/kg)	2.2-2.3	2.4-2.5(+)	2.2	2.2
SiO_3 (uM/kg)	110-125	95-105	135-140	>140
TALK (uEq/kg)*	2365-2370	2365	No Data	No Data
Pot.ALK (uEq/kg)**	2418-2423	2418-2420	No Data	No Data

*/ Total alkalinity (TALK) values computed using the total CO_2 concentration and pCO_2 @ 20°C data at observed salinities.
**/ Potential alkalinity (Pot.ALK) computed as [(TALK) + (NO_3^-)] and normalized to a salinity of 35.00 o/oo.

nelli (1982) (see their Plate 185). Based upon the geometry of this oxygen minimum/CO_2 maximum zone, it appears that this water was originated in the southeastern Pacific by the oxidation of falling biogenic debris and advected southward along the South American continental slope into the Drake Passage.

In the southern half of the Passage, the oxygen concentration increases monotonically with depth reaching 220 uM/kg near the bottom (Fig. 13). The AOU value decreases to 130 uM/kg (Fig. 14) at the southern extreme indicating influx into the Drake Passage of a relatively young water mass present near the bottom of the Southeast Pacific Basin.

The sections for nitrate and phosphate (Figs. 15 and 16) do not add further information to those already discussed above. This is due mainly to much smaller dynamic ranges available for these two properties: the nitrate and phosphate concentrations change only from 30 to 33 uM/kg and from 2.2 to 2.4 uM/kg respectively, while the estimated precision of these measurements for the Drake Passage section is about $\pm$0.5 uM/kg for nitrate and $\pm$0.05 uM/kg for phosphate. Therefore, the small variations observed in deep waters below about 2000 meters do not appear to be significant, and the contour lines presented for the depths below about 2000 meters in Figs. 15 and 16 should not be reliable. On the other hand, the silica concentration (Fig. 17) varies from about 20 to 140 uM/kg. The lowest values are found in the shallow northernmost waters and the highest values located in the southernmost area near the sea floor. Its distribution parallels with that of potential temperature and exhibits the vertically coherent wavy patterns. The silica concentration ranges from about 80 to 100 uM/kg for the oxygen minimum layer and from about 105 to 120 uM/kg for the salinity maximum Circumpolar Deep Water. The characteristic chemical properties for the three water masses found in this section are summarized in Table 1.

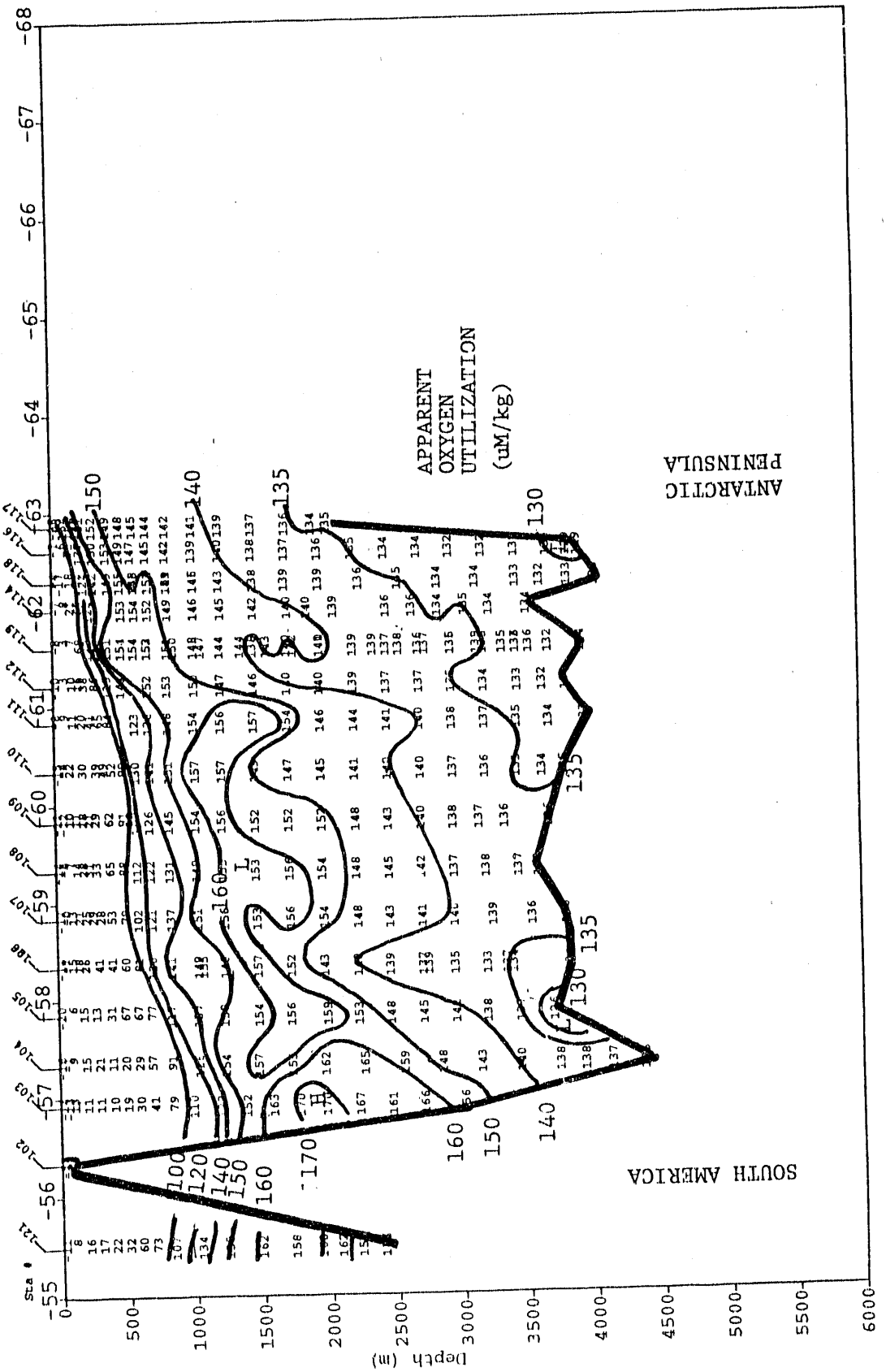
Meteor 11/5 Cruise - Drake Passage Section Sta 102-121
Apparent Oxygen Utilization (AOU) (uM/kg)
Latitude (South is Negative)
Depth (m)
SOUTH AMERICA
ANTARCTIC PENINSULA
APPARENT OXYGEN UTILIZATION (uM/kg)

Fig. 14 -

Fig. 15 - **Meteor 11/5 Cruise - Drake Passage Section Sta 102-121**
Nitrate Concentration (NO3) (uM/kg)

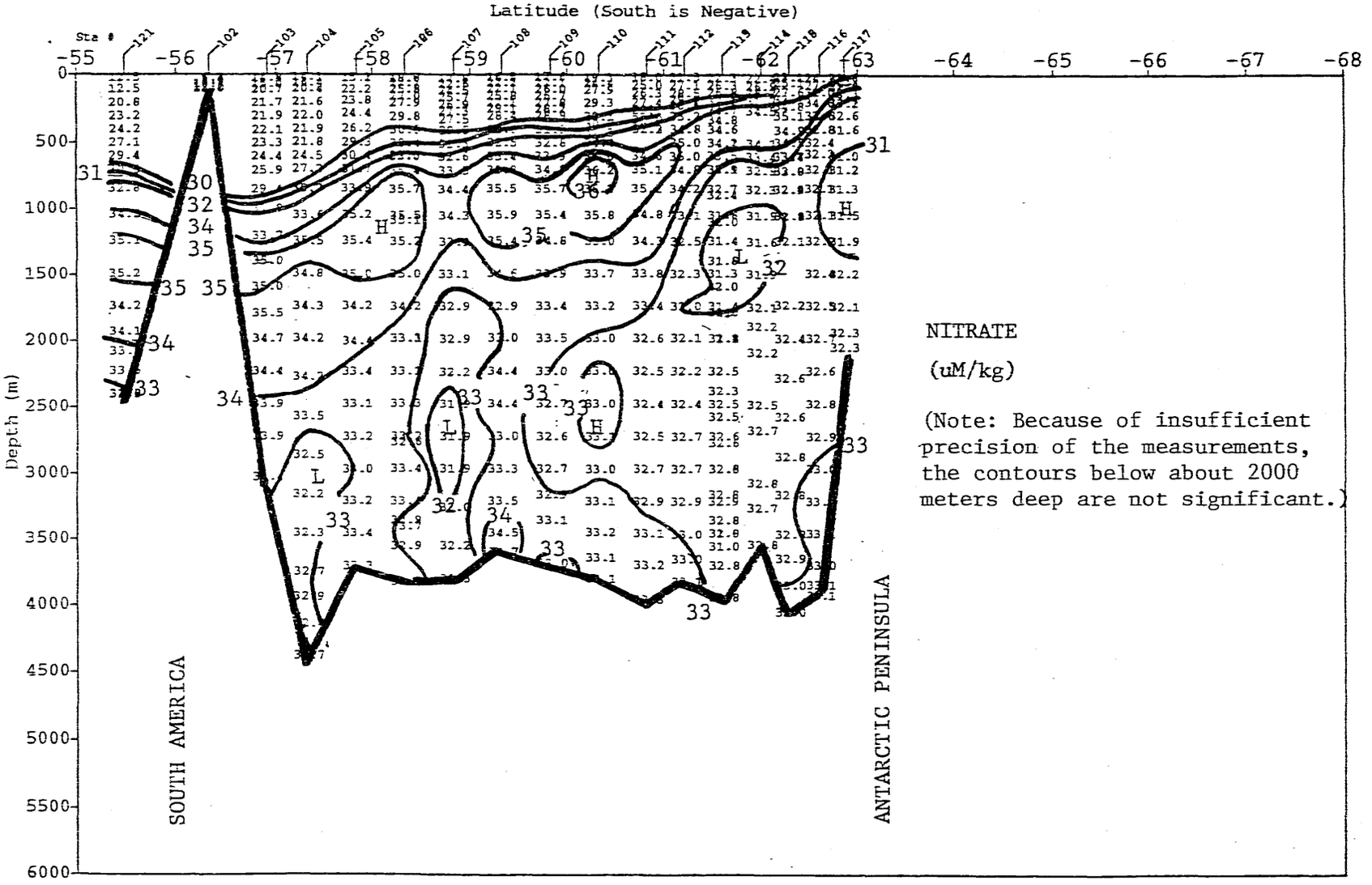

Fig. 16 - **Meteor 11/5 Cruise - Drake Passage Section Sta 102-121**
Phosphate Concentration (PO4) (uM/kg)

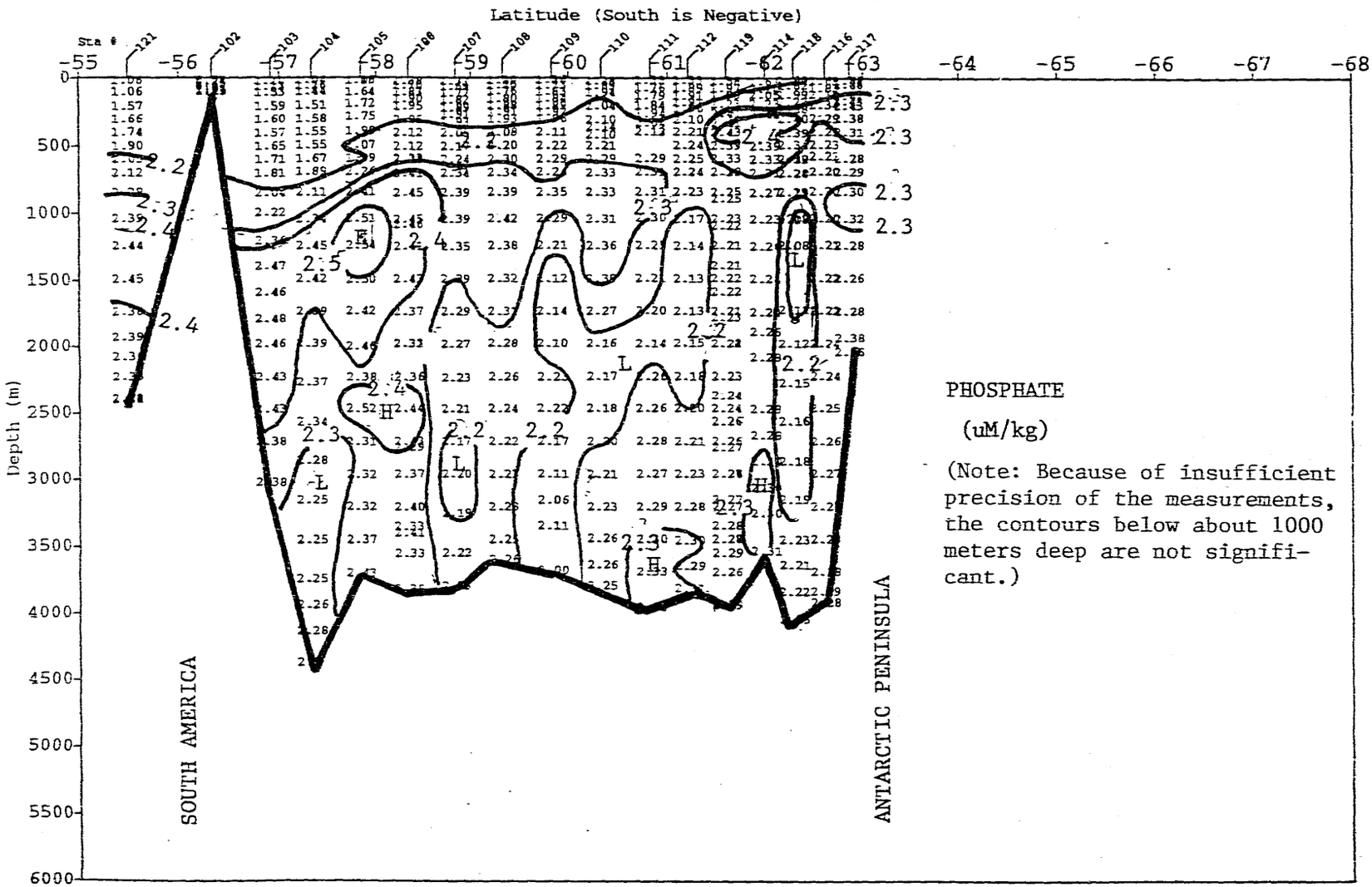

(Note: Because of insufficient precision of the measurements, the contours below about 1000 meters deep are not significant.)

Fig. 17 - **Meteor 11/5 Cruise - Drake Passage Section Sta 102-121**
Silicate Concentration (SiO3) (uM/kg)

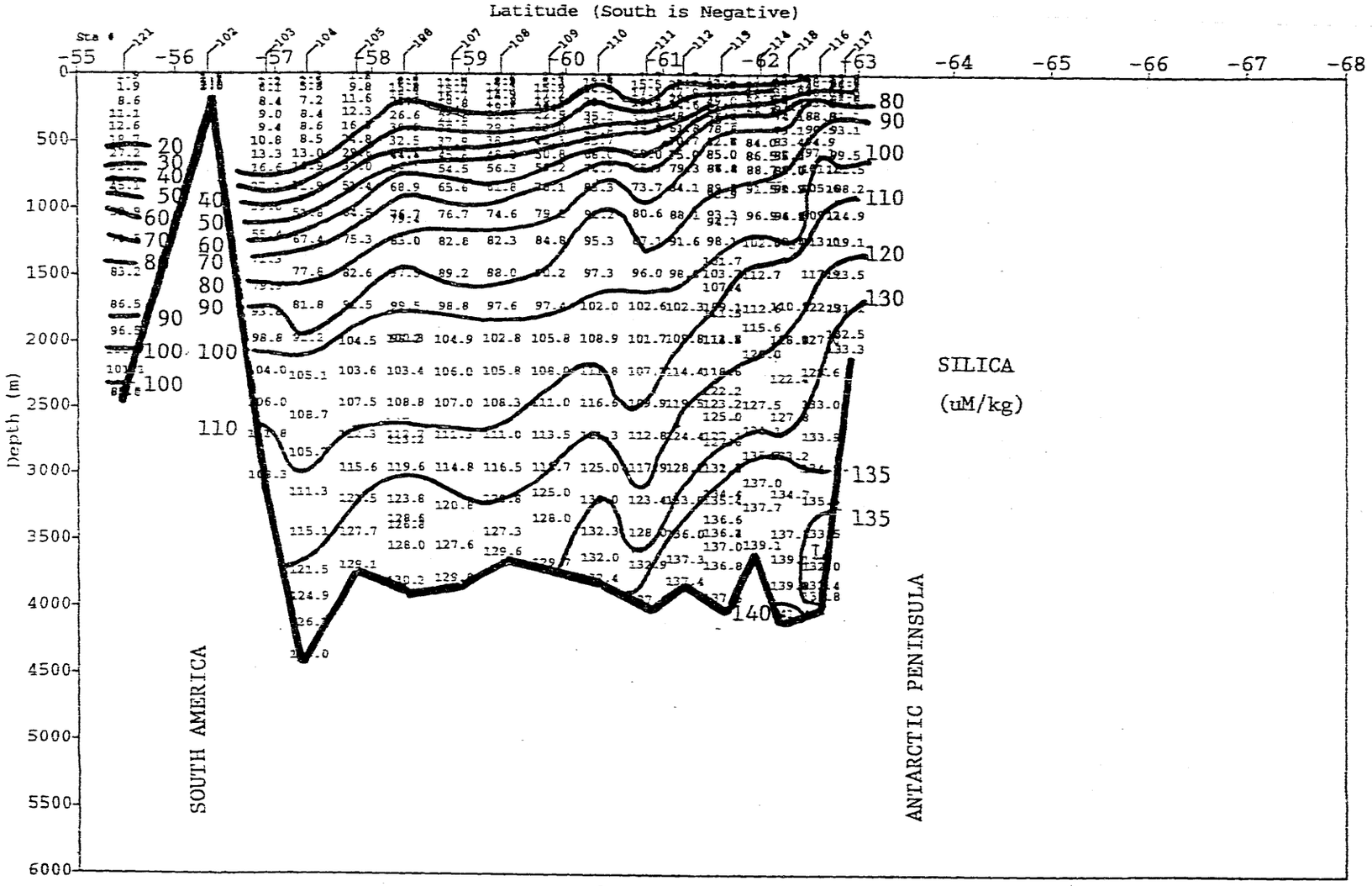

III-3) The Northern Weddell Sea Section (Stations 122-131):

This section runs more or less NW-SE direction cutting across the northern edge of the eastward out-flow of the cyclonic Weddell gyre. The X-axis scale has a full span of 800 nautical miles which is same as the Drake Passage section. Since the nitrate data at Stations 122 through 125 appear to be in error, no contour lines for nitrate are presented for the western half of this section (Fig. 26).

Fig. 18 shows the distribution of potential temperature. While the lowest temperature observed across the Drake Passage section is 0.2°C, temperatures as low as -0.88°C are observed in this section. The salinities in these cold waters below 0°C range between 34.66 and 34.64 o/oo (Fig. 19) and are much lower than those (34.70 ~ 34.73 o/oo) found in the deep waters in the Drake Passage section, indicating a dominating influence of the Weddell Sea Bottom Water (Carmack and Foster, 1975) in the sub-zero temperature regime. The potential temperature-salinity relationships observed in this section are shown in Fig. 20. At the southernmost station (Stn. 131, located at 63°10'S and 34°45'W)), both the temperature and salinity decrease to -0.88°C and 34.64 o/oo toward the sea floor about 5200 meters deep. At this station, the total CO_2 concentration and pCO_2 (at 20°C) decrease to 2240 uM/kg (Fig. 22) and 1025 uatm (Fig. 23) near the bottom, while the oxygen concentration increases to about 260 uM/kg (Fig. 24) and AOU decreases to about 100 uM/kg (Fig. 25). The concentrations of nitrate, phosphate and silica also decrease to about 32 uM/kg, 2.25 uM/kg and 113 uM/kg respectively (Figs. 26 and 27). All these values indicate the presence of recently ventilated water in the abyssal water in the Weddell Sea. The chemical properties of the Weddell Sea Bottom Water (WSBW) as observed in this section are listed in Table 2.

In the northern (or western) extreme of this section near Station 122, two layers of warmer (0.5 ~ 1.0°C) and more saline (34.67 ~ 34.70 o/oo) waters are found between about 300 and 2500 meters (Figs. 18 and 19). The salinity maxima are centered around about 700 and 1800 meters respectively and these appear to represent the upper and lower Circumpolar Deep Waters, which were observed by Reid et al. (1977) along the Scotia arc. These layers have σ_2 densities of about 36.95 and 37.10 respectively, but cannot be clearly resolved using other properties than salinity, although a weak maximum in AOU and a weak minimum in oxygen appear to be associated with the upper layer and a weak TCO_2 minimum appears in between these two layers.

In the southern half of this section (Stations 126 through 131), a layer of cooler (0 ~ 0.5°C) water with similar salinities is present in a depth range centered around 500 meters between 300 and 1500 meters. Although these northern and southern layers are found at similar depths, the southern layer has a greater σ_2 density of 37.13 at the salinity maximum than the σ_2 densities of 36.95 and 37.10

TABLE - 2 Summary of the physical and chemical characteristics of various water masses observed during the Meteor 11/5 expedition in the South Atlantic and northern Weddell Sea areas. The values represent extreme values observed during the expedition, but do not necessarily indicate the values for the "pure" end members of water mass. WSDW = Weddell Sea Deep Water; WSBW = Weddell Sea Bottom Water; AABW = Antarctic Bottom Water; AAIW = Antarctic Intermediate Water. (+) and (-) signs indicate that the values listed comprise a local maximum and minimum respectively.

Water Masses	WSDW	WSBW	AABW	AAIW
Sections Observed	N. Weddell	N. Weddell	58°S	Cape-Weddell
Stations	126-131	130-131	132-149	149-164
Depths (meters)	500-800	>4000	3000-4000	300-900
Pot. Temp. (°C)	0.2-0.5(+)	<-0.75	-0.25--0.50	2.5-3.0
Salinity (o/oo)	34.67-34.68(+)	34.64-34.69	34.65-34.68	34.0-34.3
Denisty (σ_θ)	27.82-27.84	>27.85	27.85	27.20-27.60
Density (σ_2)	37.10-37.13	>37.225	37.17-37.20	36.4-36.6
TCO_2 (uM/kg)	2260-2270(+)	<2245	2250-2255	2150-2200
pCO_2 @ 20°C (uatm)	1160-1120(+)	<1040	1075-1100	800-1000
O_2 (uM/kg)	200-210(-)	>260	230-240	210-250
AOU (uM/kg)	140-150(+)	<100	110-120	50-100
NO_3 (uM/kg)	33.5-34.5(+)	<32.0	33	28-34
PO_4 (uM/kg)	2.35-2.39(+)	<2.25	2.35	1.9-2.3
SiO_3 (uM/kg)	125-132(+)	<110	125-130	20-50
TALK (uEq/kg)*	2350-2360	2355	2360	2290-2310
Pot.ALK (uEq/kg)**	2410-2415	2410-2418	2415-2418	2375-2390

*/ Total alkalinity (TALK) values computed using the total CO_2 concentration and pCO_2 @ 20°C data at observed salinities.

**/ Potential alkalinity (Pot.ALK) computed as [(TALK) + (NO_3^-)] and normalized to a salinity of 35.00 o/oo.

Fig. 18 – Meteor 11/5 Cruise - Northern Weddell Sea - Sta 122-131
Potential Temperature at the Surface

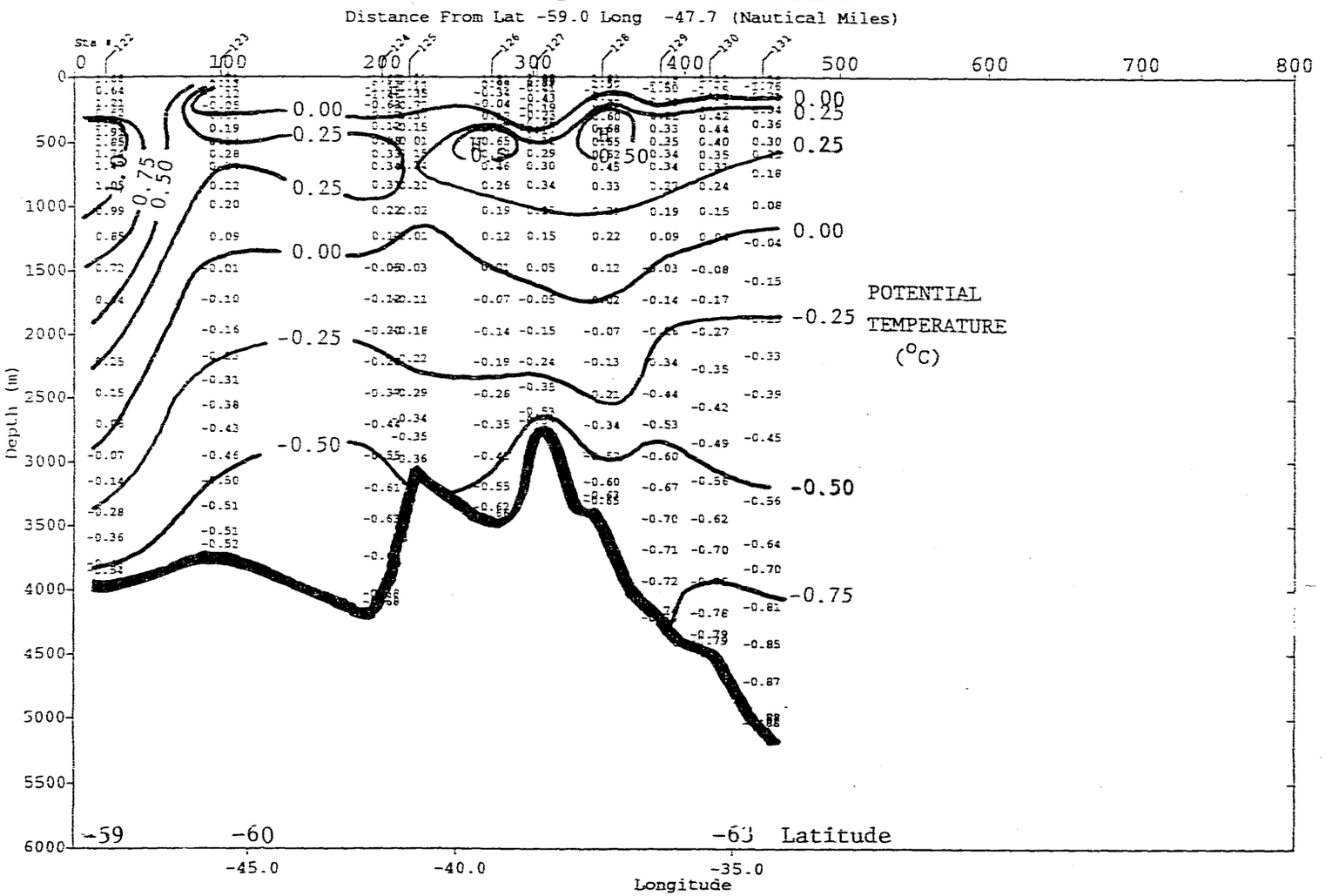

Fig. 19 - Meteor Cruise 11/5 - Northern Weddell Sea - Stn 122-131
Salinity (o/oo)

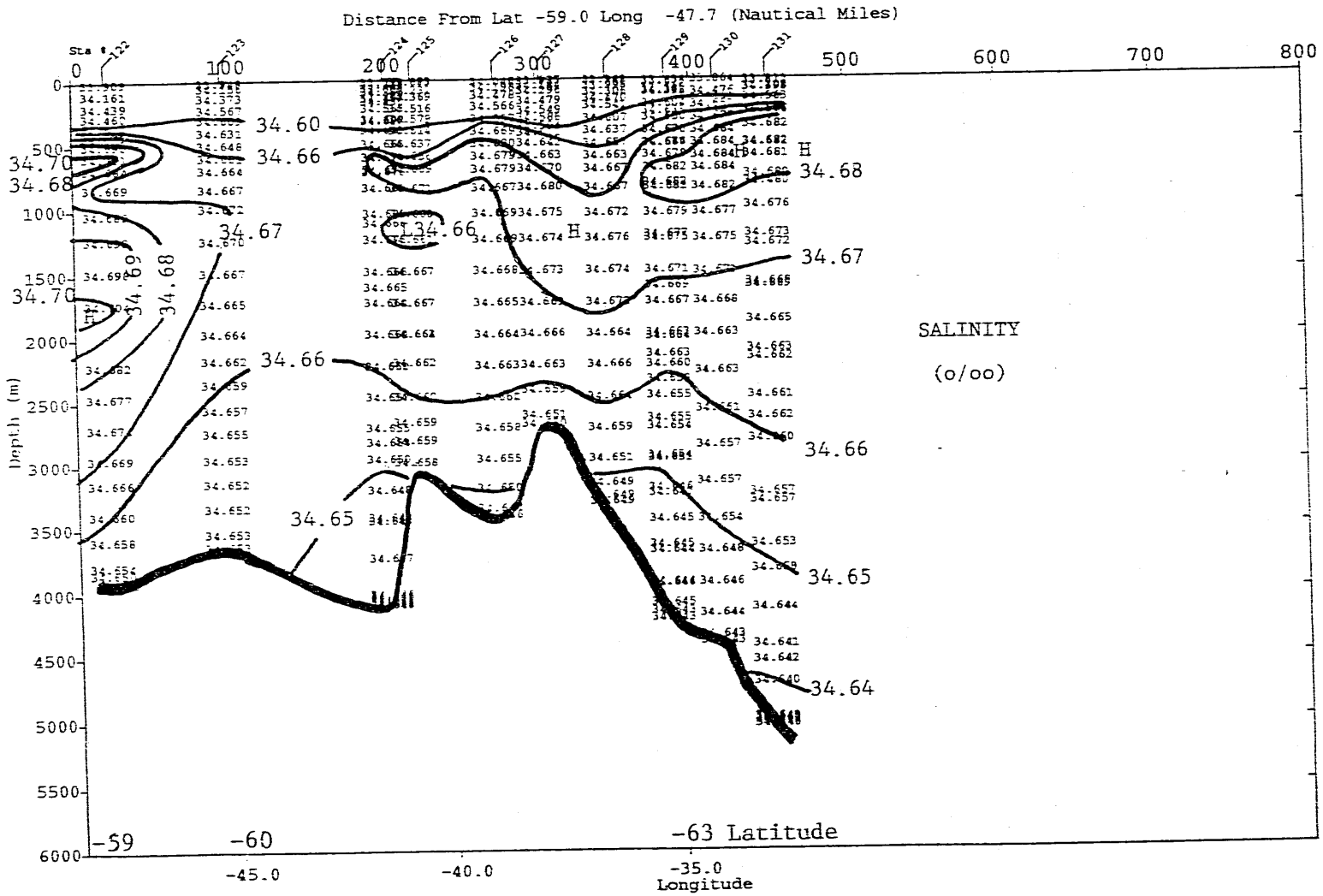

Fig. 20 - Potential temperature-salinity relationships observed in the northern Weddell Sea section. WSDW = Weddell Sea Deep Water; WSBW = Weddell Sea Bottom Water.

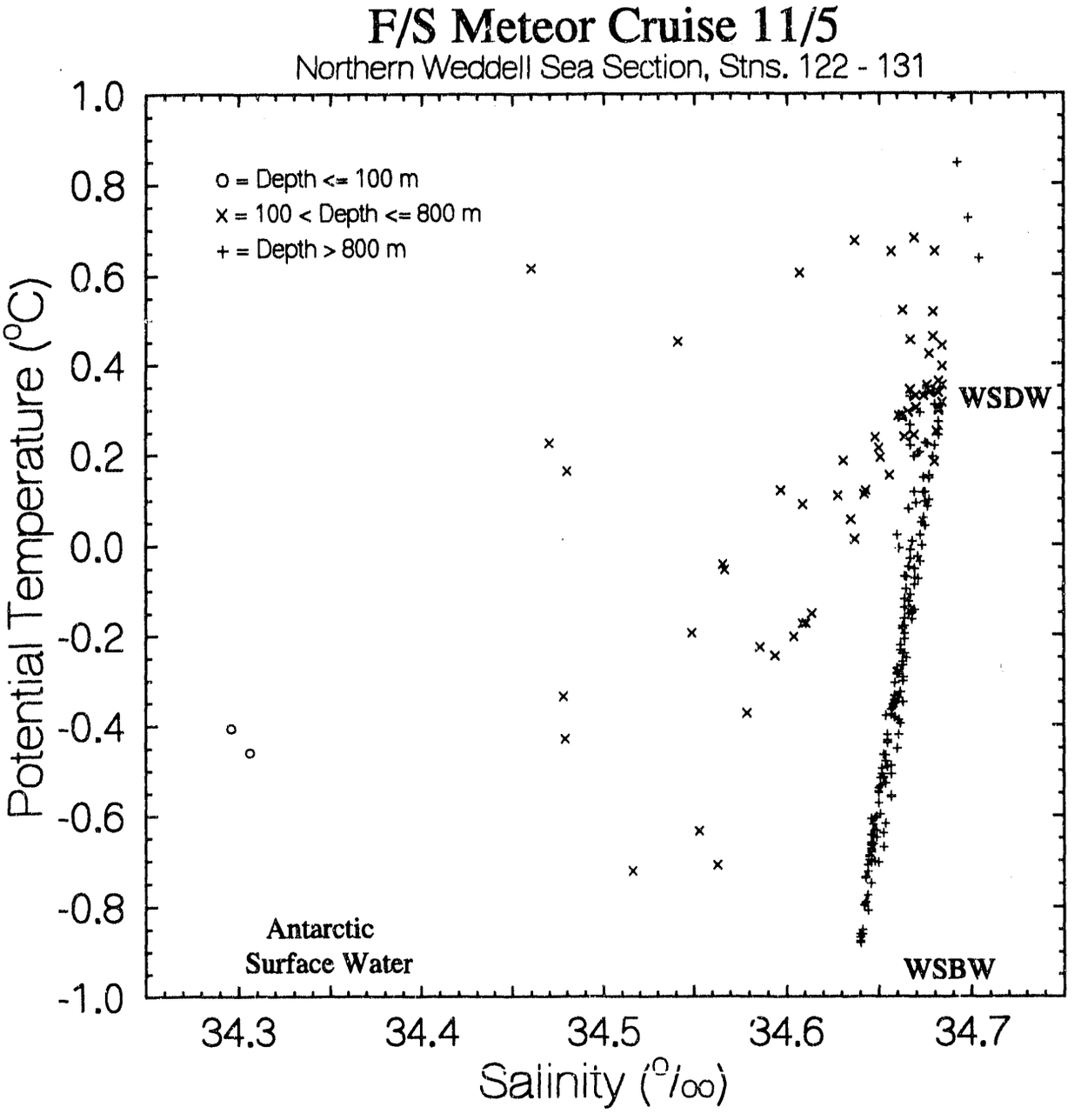

Fig. 21 - **Meteor Cruise 11/5 - Northern Weddell Sea - Stn 122-131**
Sigma 2000

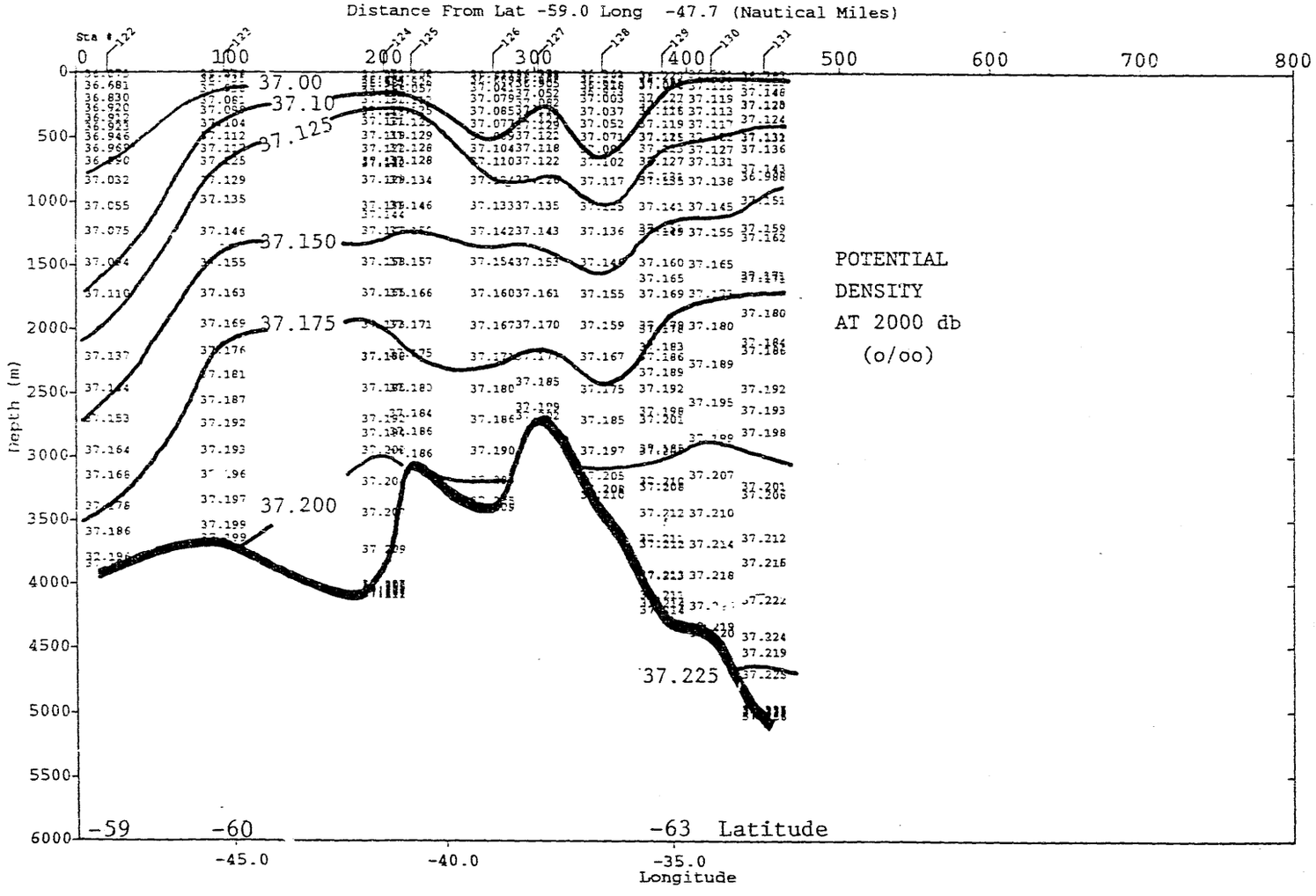

Fig. 22 - Meteor 11/5 Cruise - Northern Weddell Sea Sta 122-131
TCO2 (uM/kg)

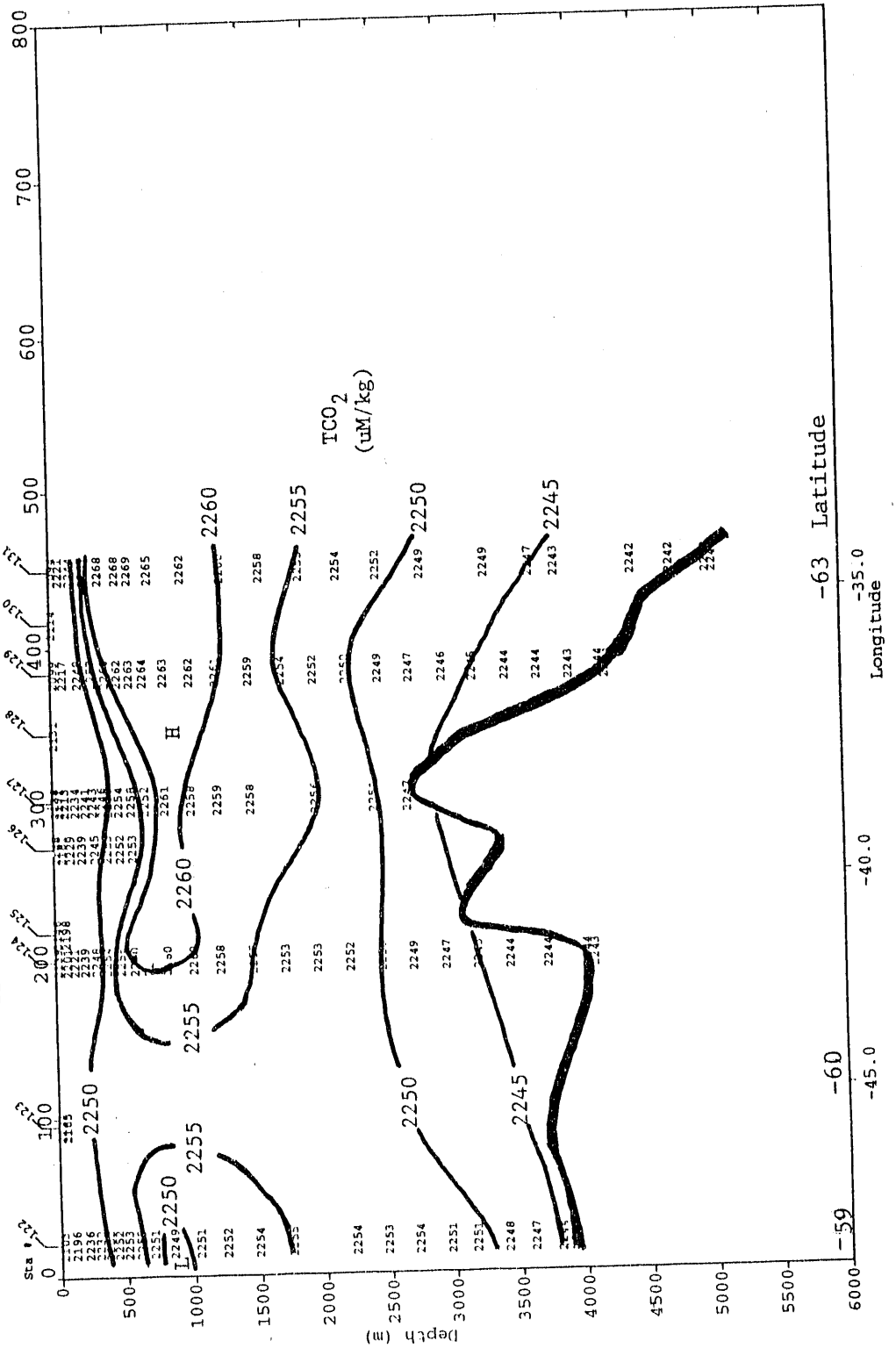

at the respective salinity maximum for the northern layers. Furthermore, the distributions of pCO_2 (Fig. 23), phosphate (Fig. 27) and silica (Fig. 28) appear to indicate that the southern features have separate origins from the warmer layer to the north. The southern layer appears to represent the Weddell Deep Water, which circulates at intermediate depths within the Weddell gyre and is derived from the Circumpolar Deep Water (Jacobs et al., 1985). Since it receives fresh water and is cooled during its circuit around the Weddell Sea, it has lower salinity and temperature but higher pCO_2 and greater concentrations of total CO_2, silica and phosphate than its parent Circumpolar Deep Water. The characteristic chemical properties for these water masses are summarized in Table 2.

Fig. 23 - Meteor 11/5 Cruise - Northern Weddell Sea Sta 122-131
pCO2 in Seawater at 20 Deg C (uAtm)

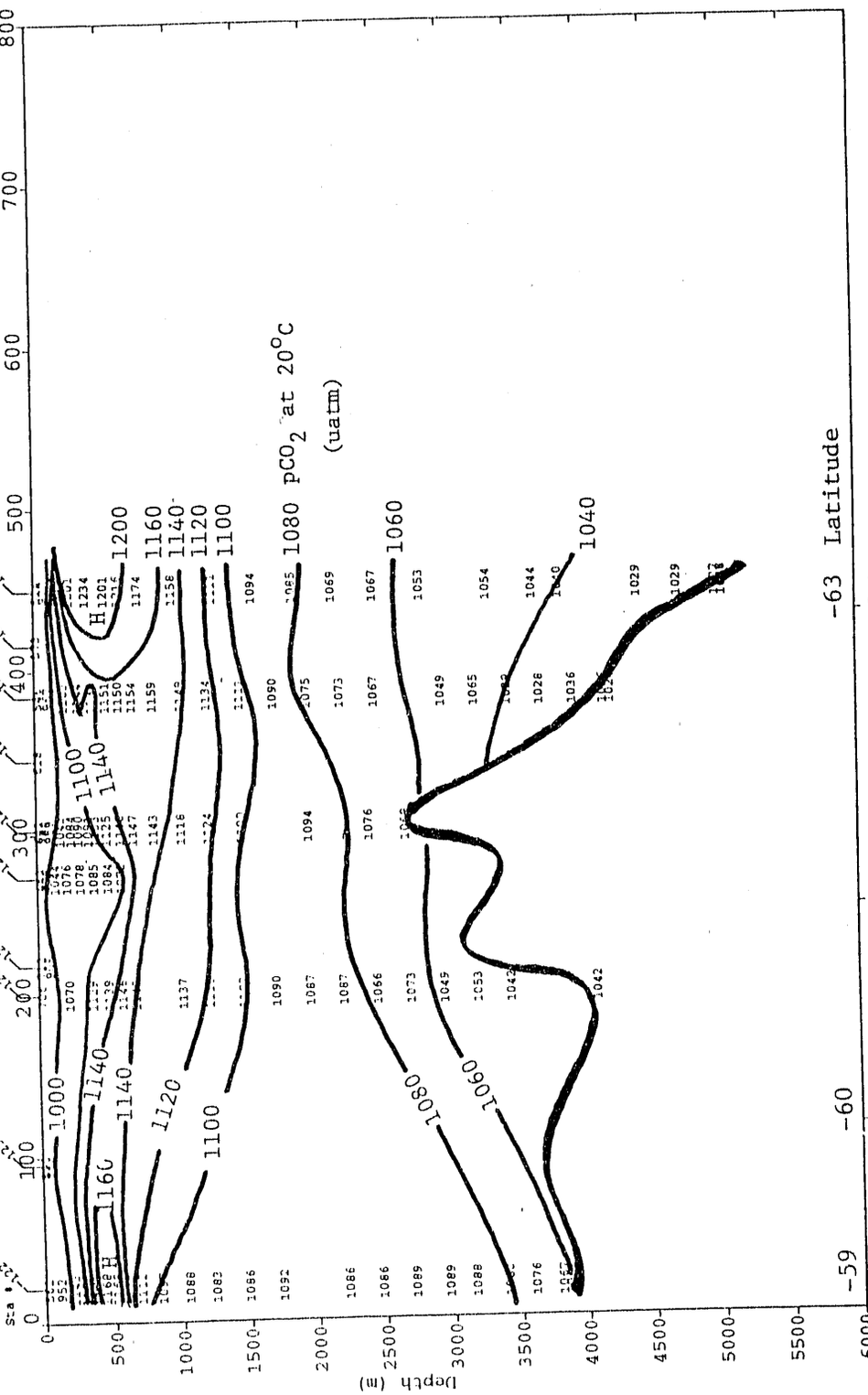

Fig. 24 - Meteor 11/5 Cruise - Northern Weddell Sea Sta 122-131

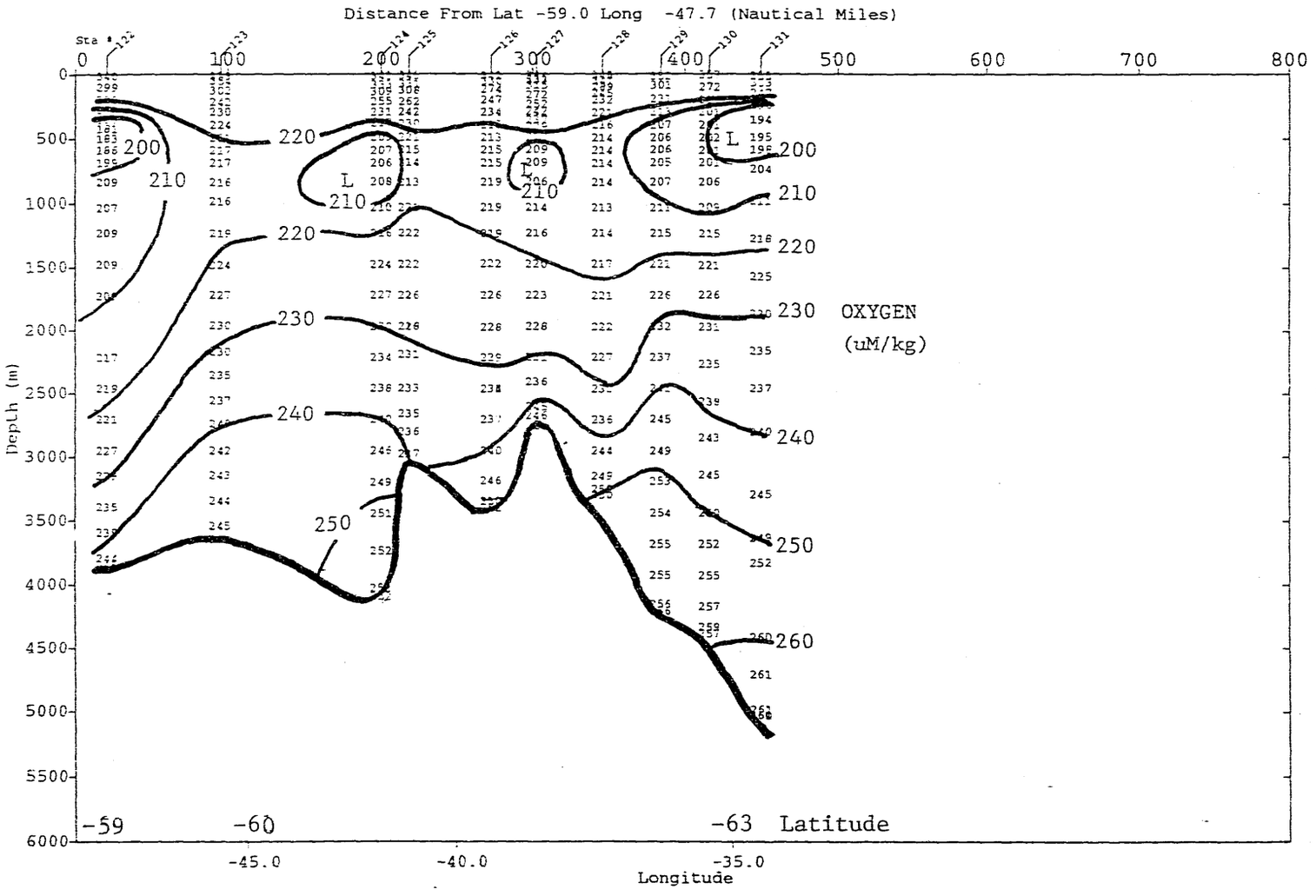

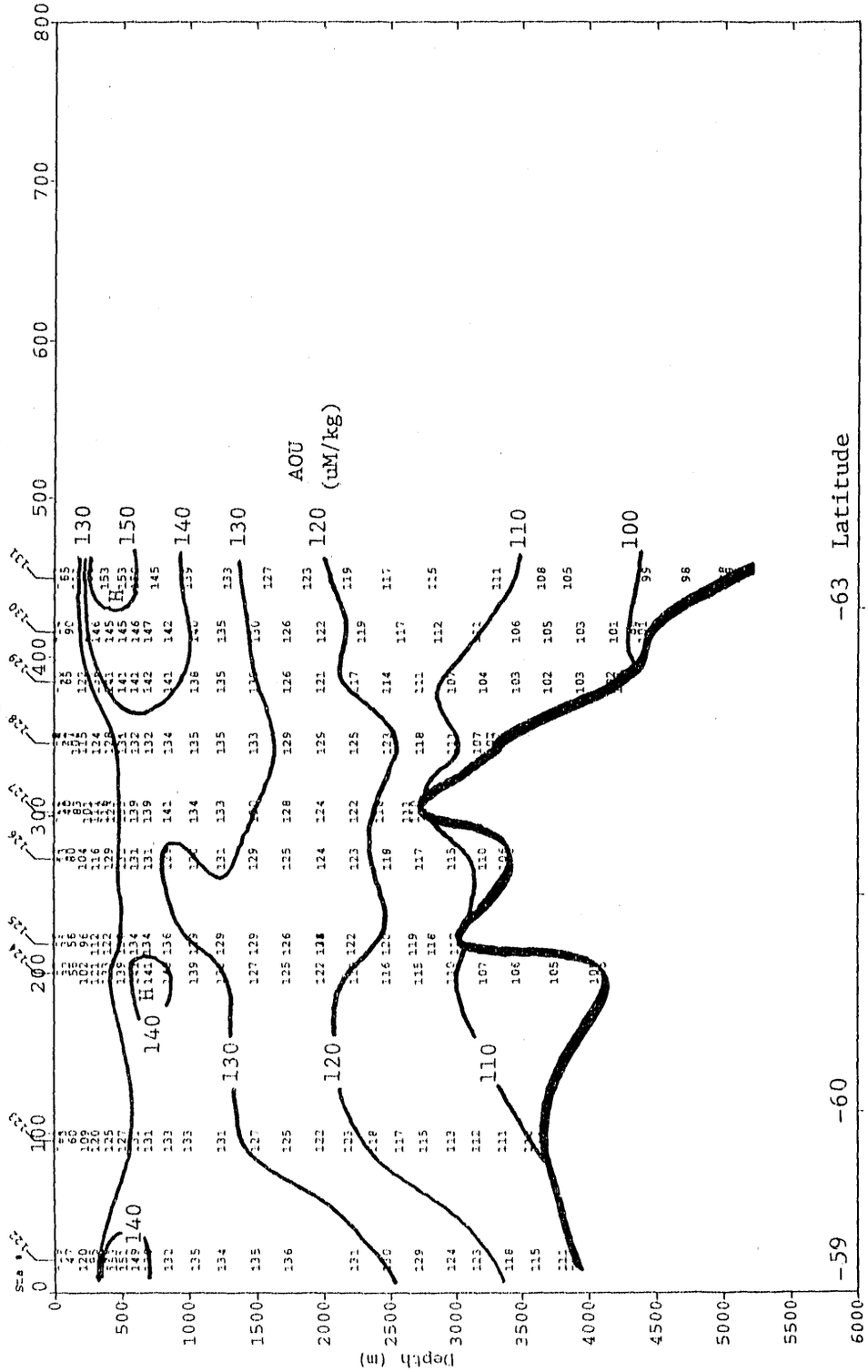

Fig. 25 - Meteor 11/5 Cruise - Northern Weddell Sea Sta 122-131
Apparent Oxygen Utilization (AOU) (uM/kg)

Fig. 26 – **Meteor 11/5 Cruise - Northern Weddell Sea Sta 122-131**
Nitrate Concentration (NO3) (uM/kg)

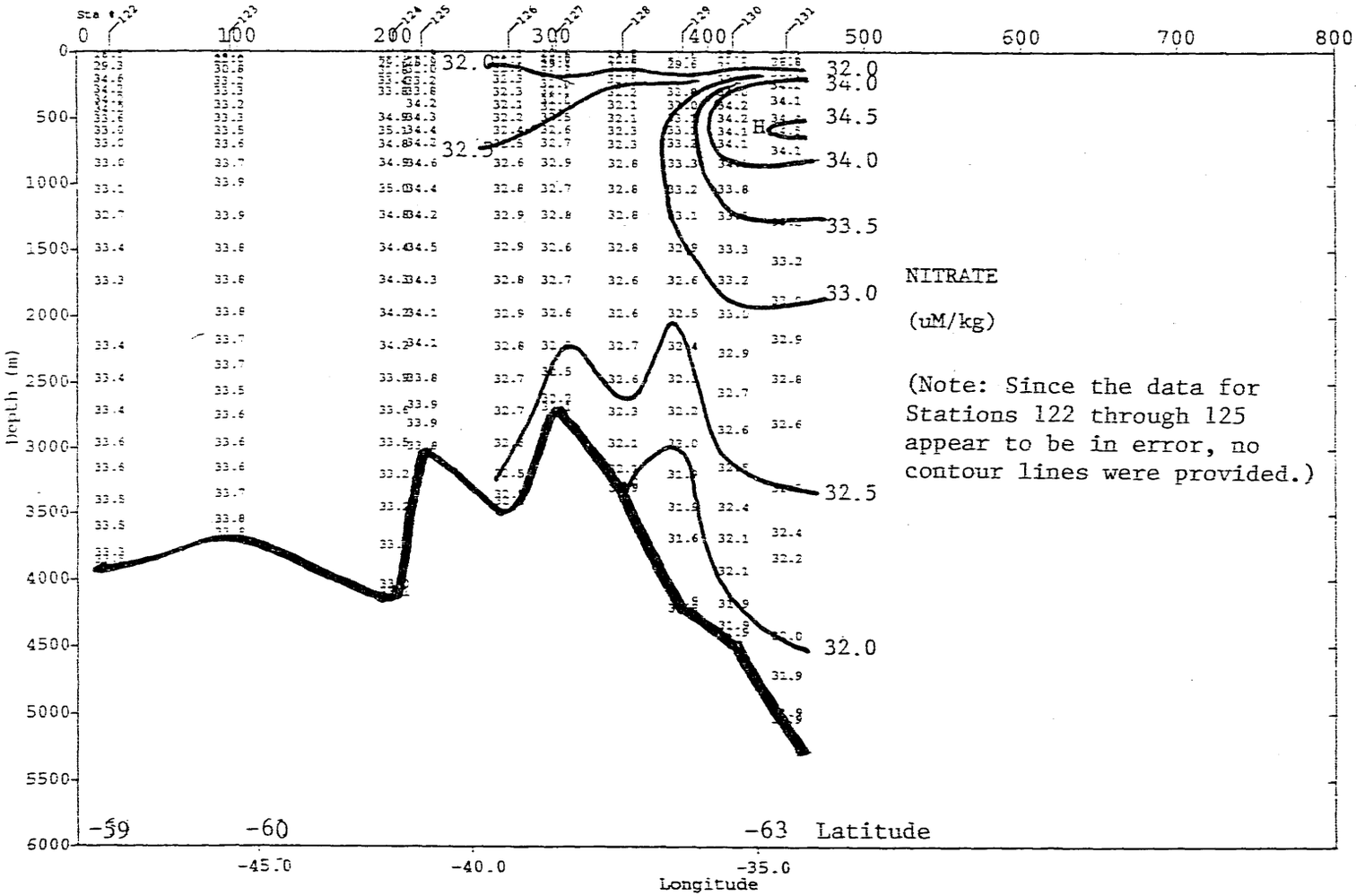

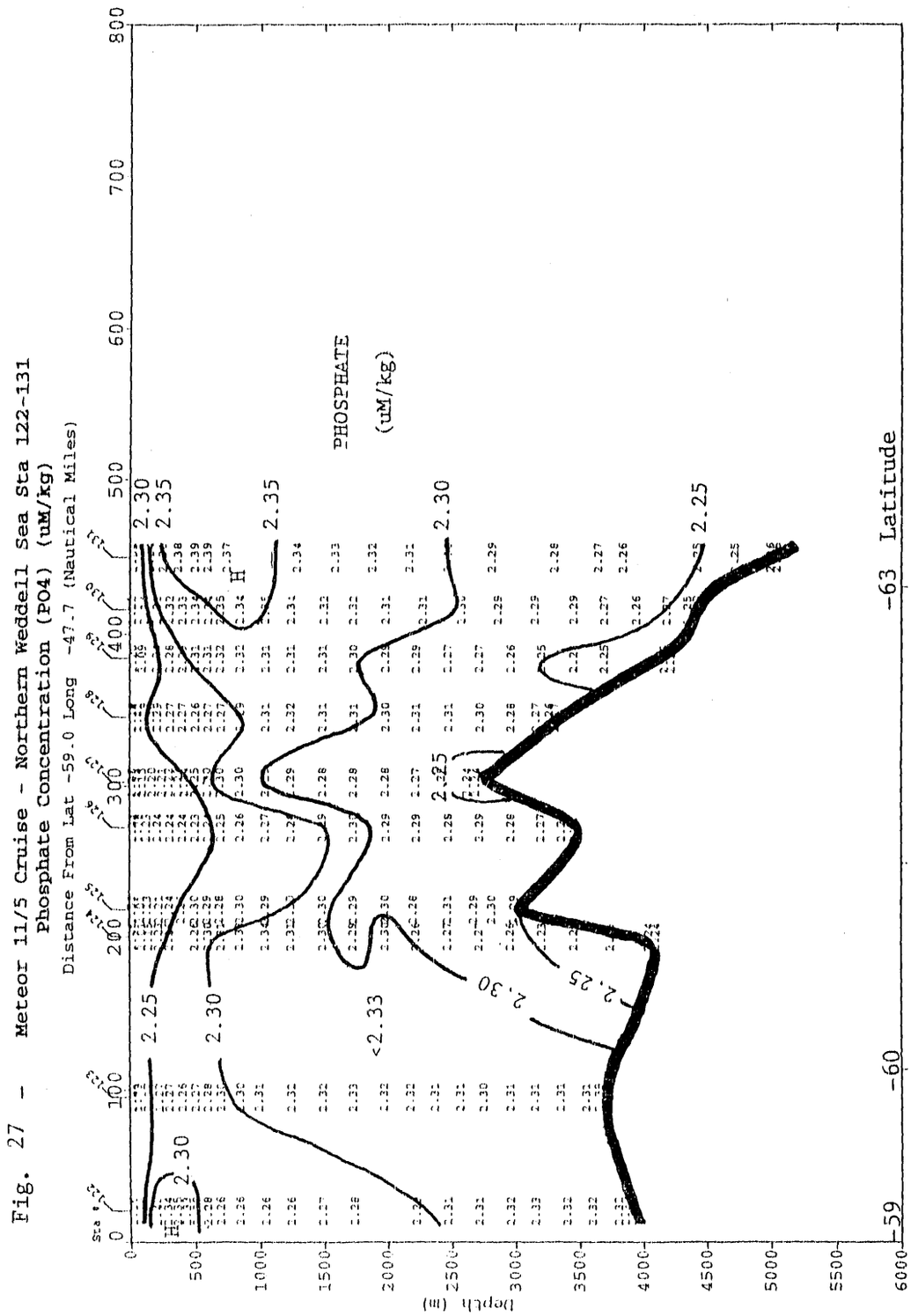

Fig. 27 - Meteor 11/5 Cruise - Northern Weddell Sea Sta 122-131
Phosphate Concentration (PO4) (uM/kg)

Fig. 28 - Meteor 11/5 Cruise - Northern Weddell Sea Sta 122-131
Silicate Concentration (SiO3) (uM/kg)

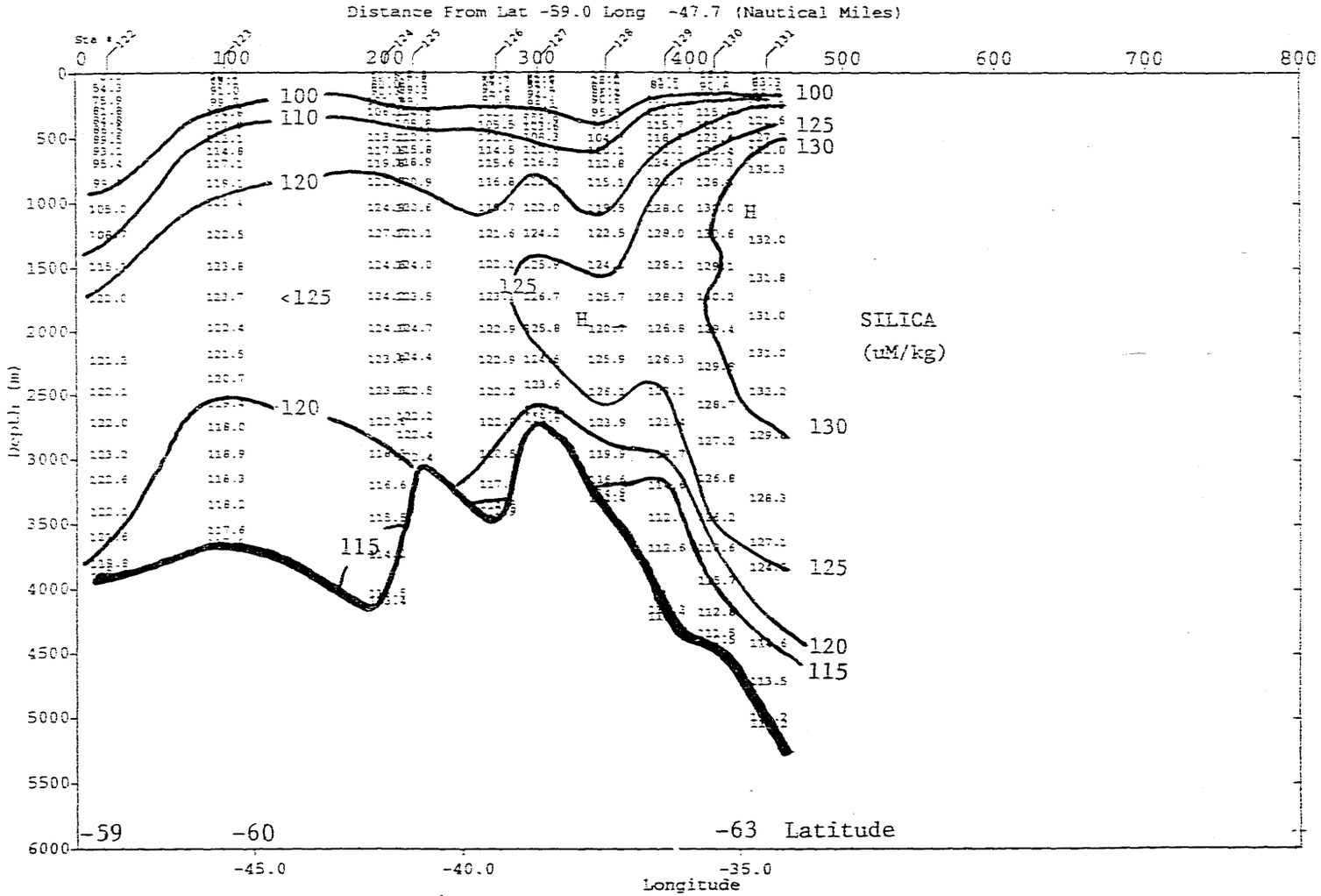

III-4) The 58°S Section (Stations 132-149):

This section represents a E-W zonal section along approximately 58°S between the longitudes of about 25°W and the prime meridian. The temperature and salinity values indicate that this section is dominated by the Circumpolar Deep Water in the upper 1500 meters and the deep and bottom waters from the Weddell Sea below about 1500 meters. The potential temperature-salinity relationships observed in this section are shown in Fig. 31. Wavy patterns of the contour lines are found all the depths in every property including temperature (Fig. 29), salinity (Fig. 30), density (Fig. 32), oxygen (Figs. 35 and 36) and silica (Fig. 39). In a depth range from about 300 and 1000 meters (i.e. Circumpolar Deep Water), strong lateral variations are observed. Warmer waters outlined by the 1.0 and 1.5°C isotherms (Fig. 29) not only have higher salinity values which are outlined by the 34.69 and 34.70 o/oo contours (Fig. 30), but also contain lower oxygen (see the 200 uM/kg contour for oxygen in Fig. 35 and the 140 uM/kg contour for AOU in Fig. 36). These features indicate dynamically active flow of water across this section.

It is noted that the coherent wavy patterns are not observed in the contour lines for the pCO_2 and the concentrations of total CO_2, nitrate and phosphate. In the sections for total CO_2 and pCO_2 (Figs. 33 and 34), it is seen that the measurements were made in deep waters at every other station or only at the even numbered stations. This is because the measurements could not be made fast enough to accommodate the samples taken at every station. Since the wavy patterns observed in the eastern (or right) half of the section, the temperature, salinity, density and oxygen values (see Figs. 29, 30, 32 and 35) tend to exhibit a wave length of two station-distances (or about 2° in longitude), the CO_2 data were obtained only near the bottom of waves but not near the top of waves. Accordingly, the lateral distributions observed for total CO_2 and pCO_2 have been inadvertently smoothed due mainly to undersampling for lateral distances. For future expeditions in this area and other highly dynamic areas, closer station distances must be achieved.

The distributions of nitrate and phosphate shown in Figs. 37 and 38 are not consistent with those for oxygen and silica particularly in waters below about 1000 meters. This is due mainly to the small dynamic range for these two properties. Below 1000 meters, the nitrate and phosphate concentrations vary between 33.5 and 34.0 uM/kg for the former and between 2.30 and 2.35 uM/kg for the latter. The precisions of measurements attained for these quantities during this expedition were not refined enough to resolve the variations satisfactorily.

Fig. 29 - **Meteor 11/5 Cruise - South Atlantic 58 Deg South Section - Sta 132-149**
Potential Temperature at the Surface

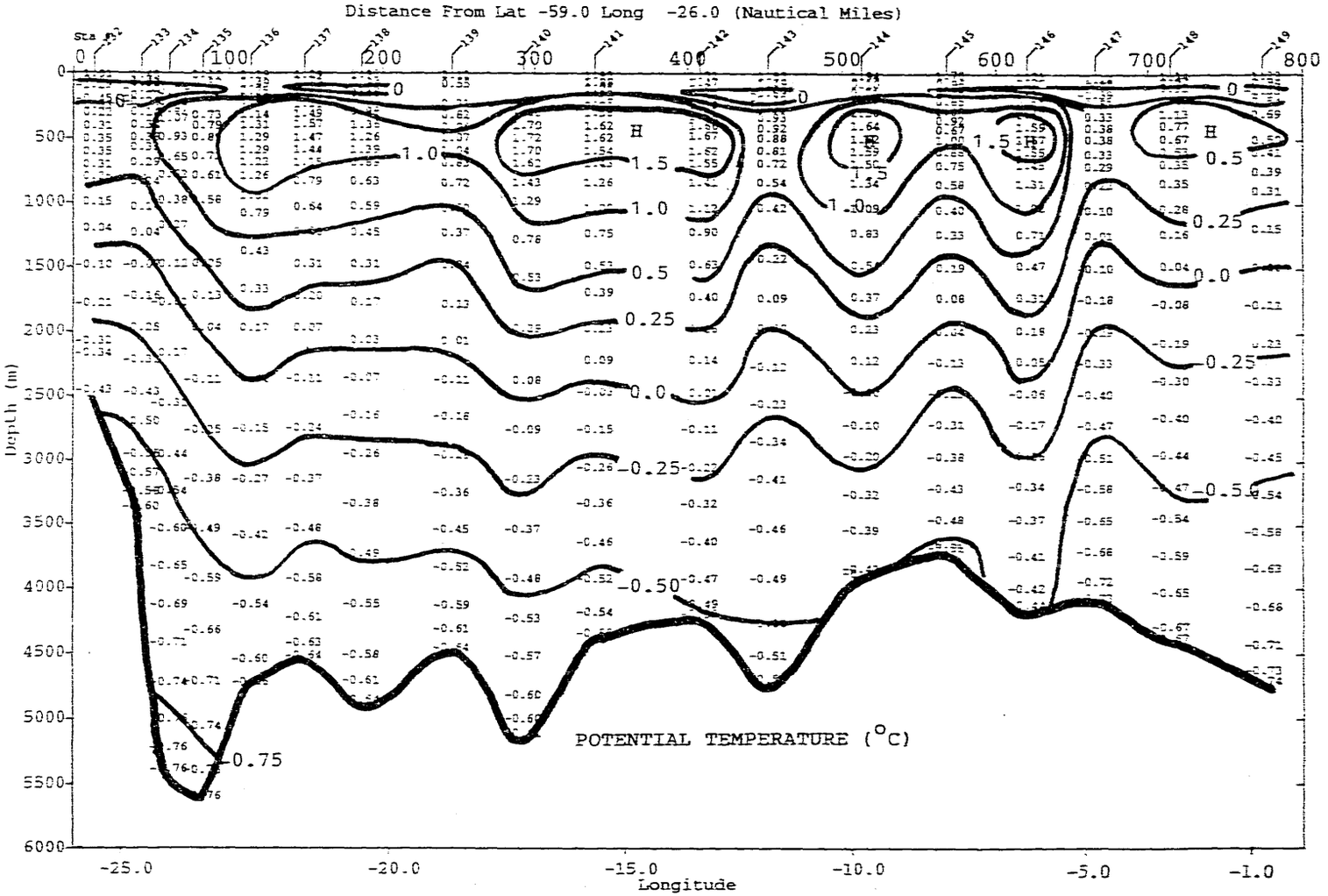

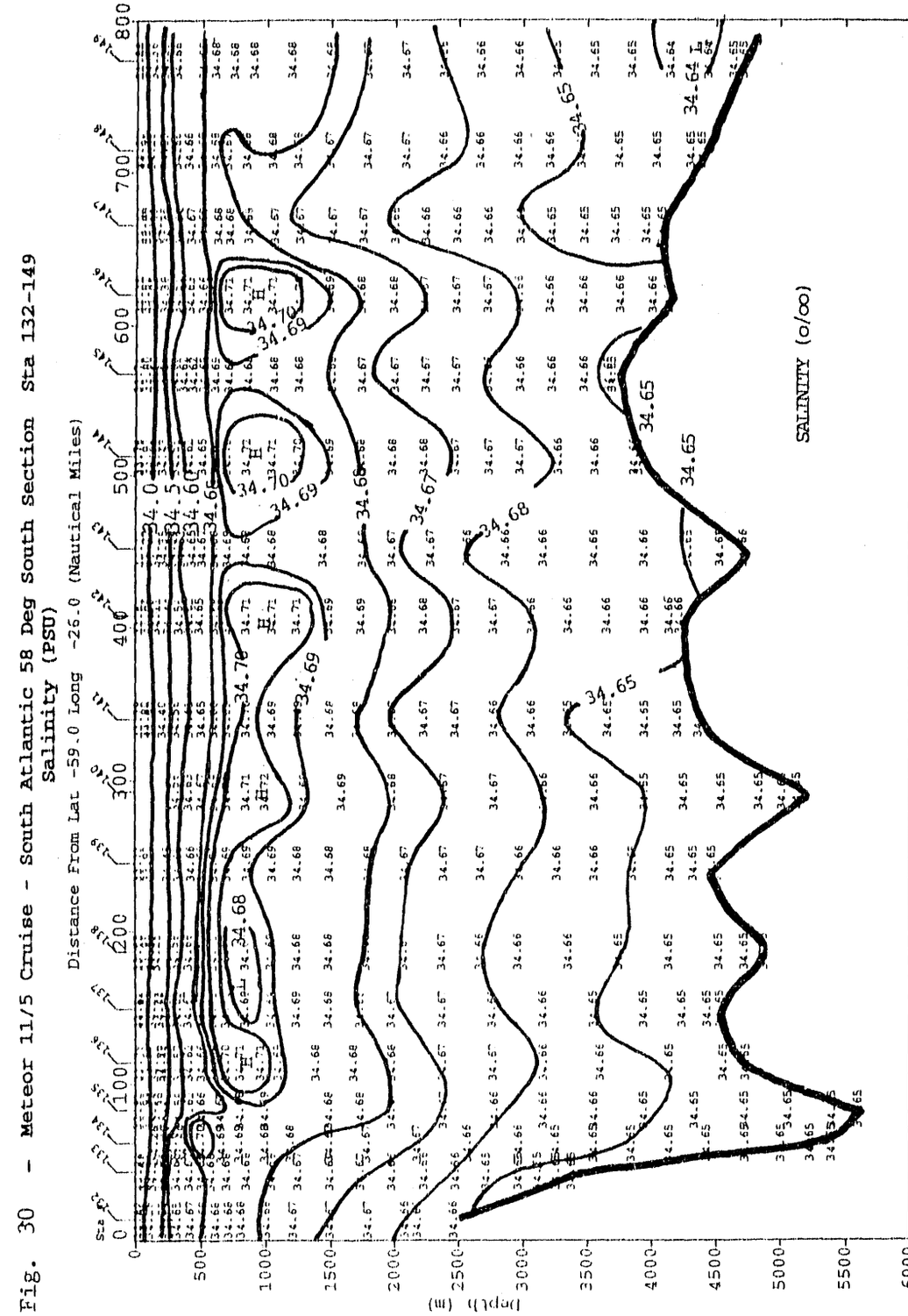

Fig. 30 - Meteor 11/5 Cruise - South Atlantic 58 Deg South Section Sta 132-149
Salinity (PSU)

Fig. 31 - Potential temperature-salinity relationships observed in the 58°S section in the Southern Ocean. CPDW = Circumpolar Deep Water; WSDE = Weddell Sea Deep Water; AABW = Antarctic Bottom Water; WSBW = Weddell Sea Bottom Water.

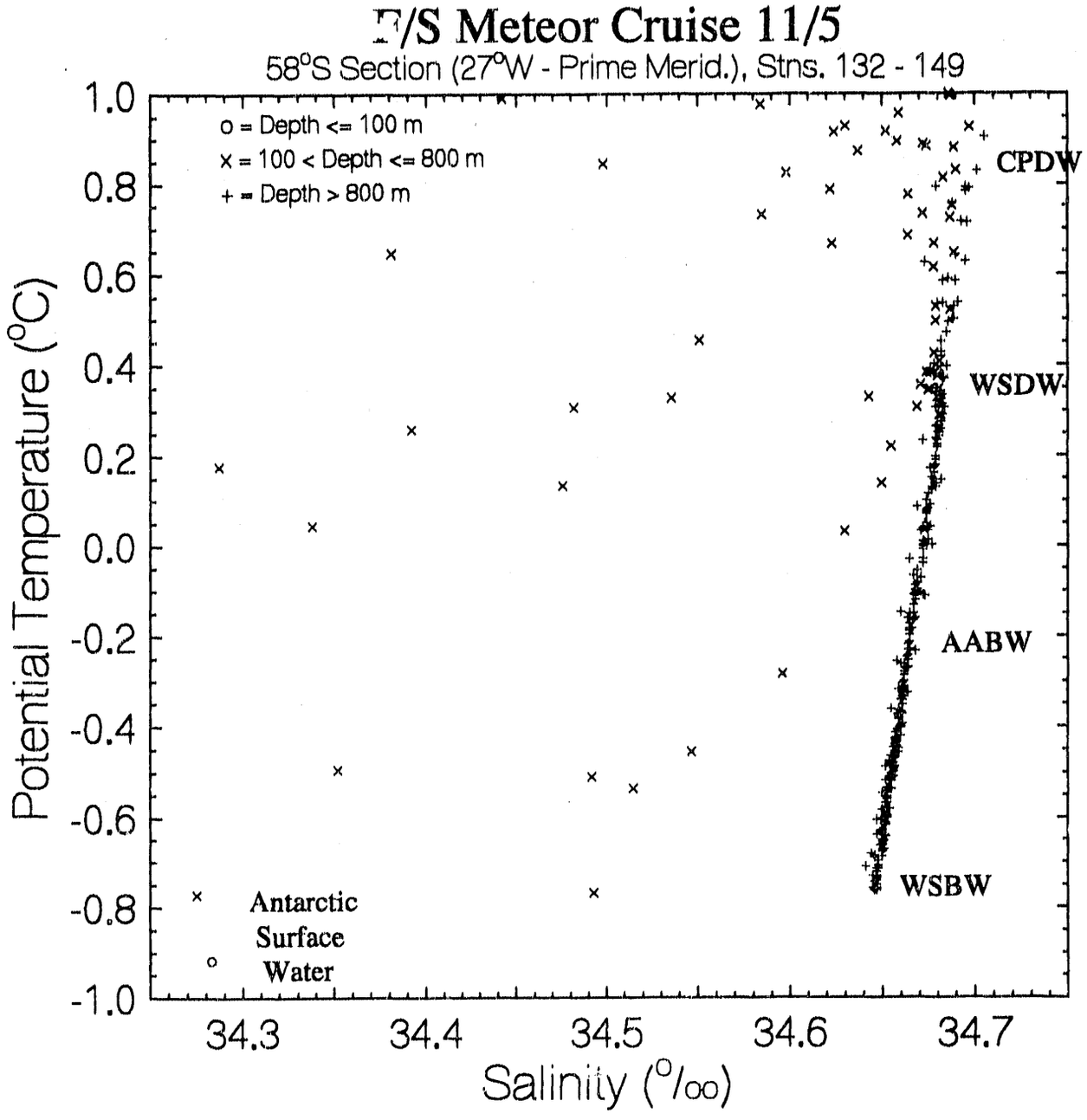

Fig. 32- **Meteor 11/5 Cruise - South Atlantic 58 Deg South Section Sta 132-149**
Potential Density at 2000 Meters (Sigma 2000) (Sigma Units)

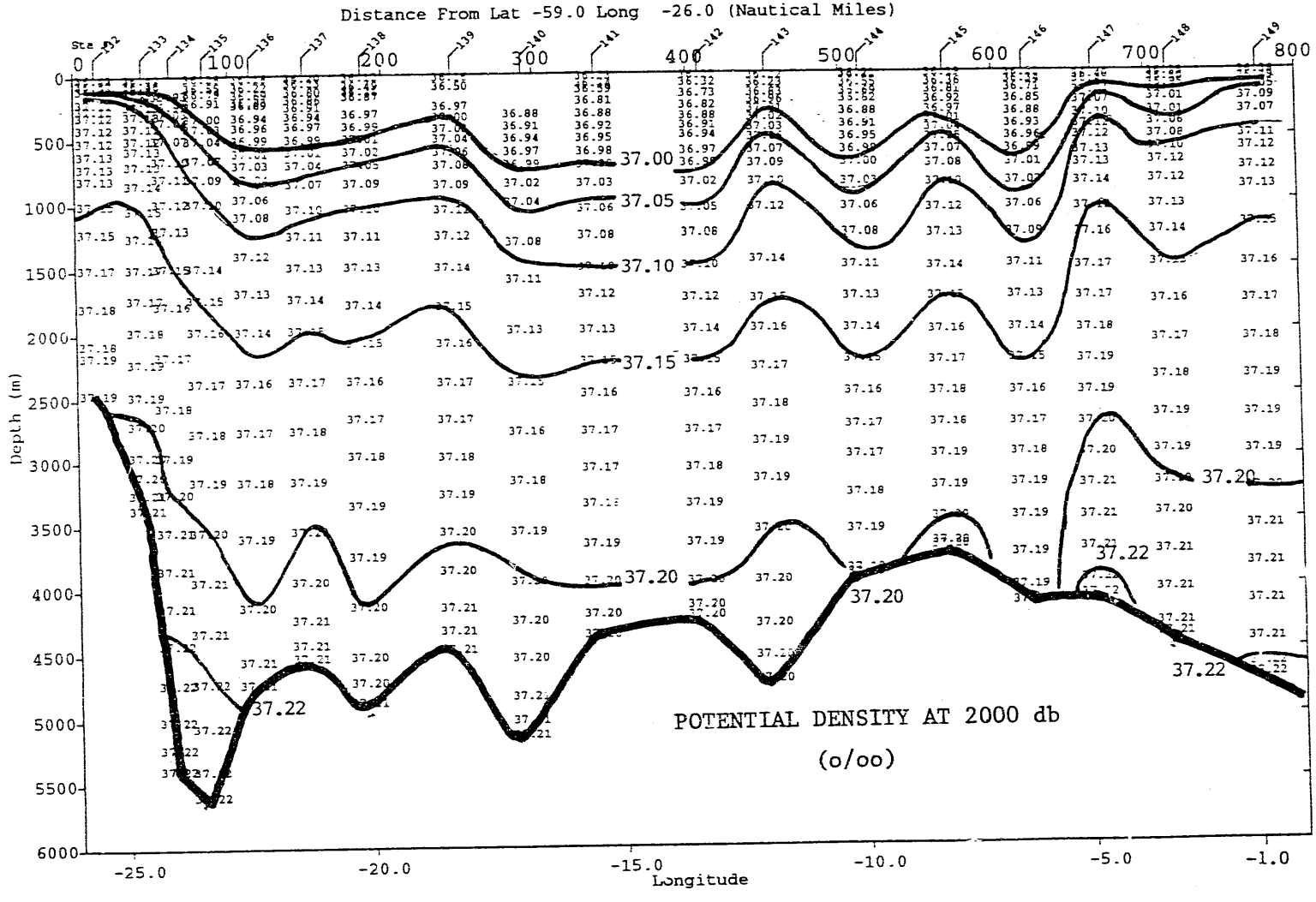

Fig. 33 - Meteor 11/5 Cruise - South Atlantic 58 Deg South Section Sta 132-149
Total CO2 (TCO2) (uM/kg)

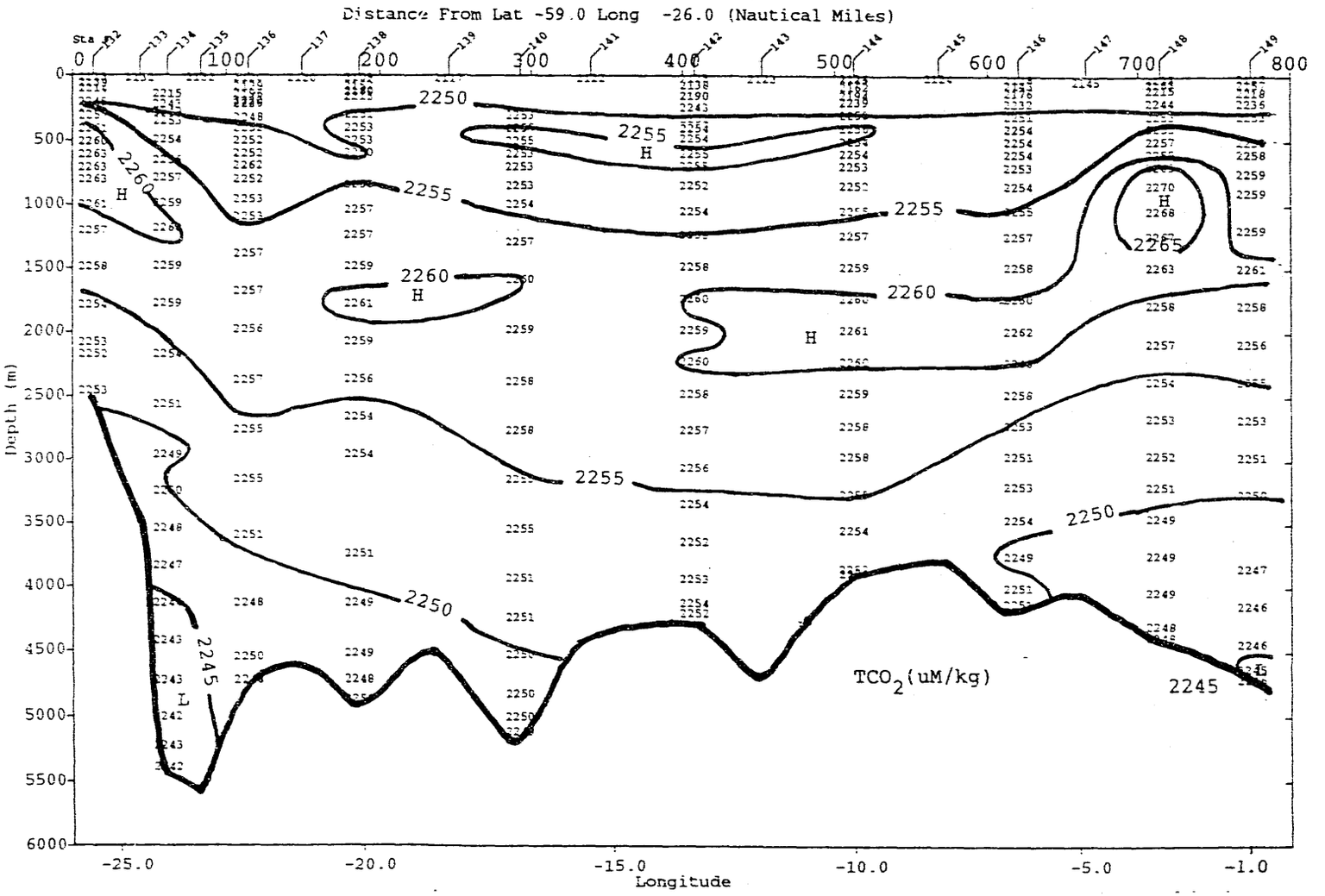

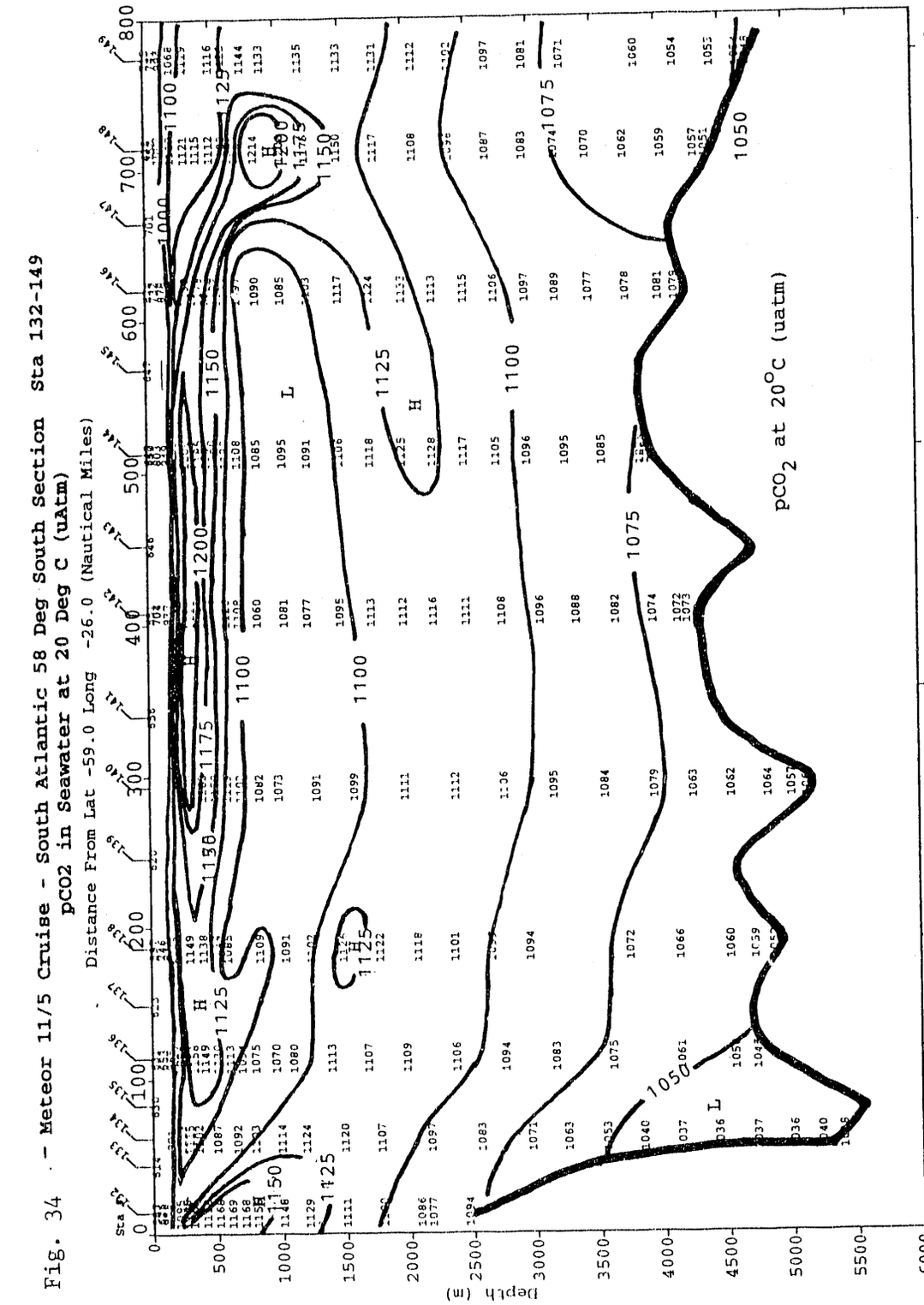

Fig. 34 - Meteor 11/5 Cruise - South Atlantic 58 Deg South Section Sta 132-149
pCO2 in Seawater at 20 Deg C (uAtm)

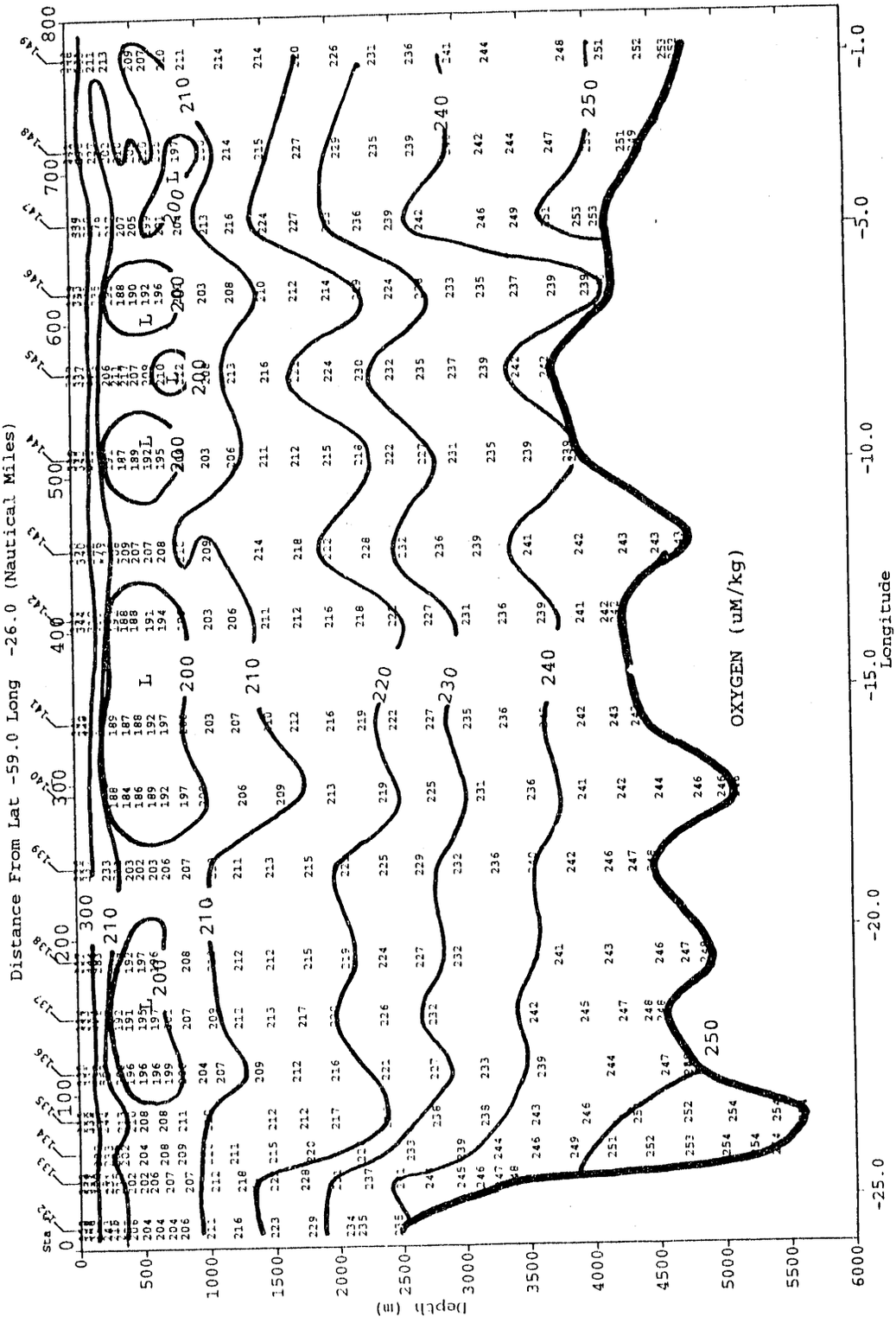

Fig. 35 - Meteor 11/5 Cruise - South Atlantic 58 Deg South Section - Sta 132-149
Oxygen (uM/kg)

Fig. 36 - Meteor 11/5 Cruise - South Atlantic 58 Deg South Section Sta 132-149
Apparent Oxygen Utilization (AOU) (uM/kg)

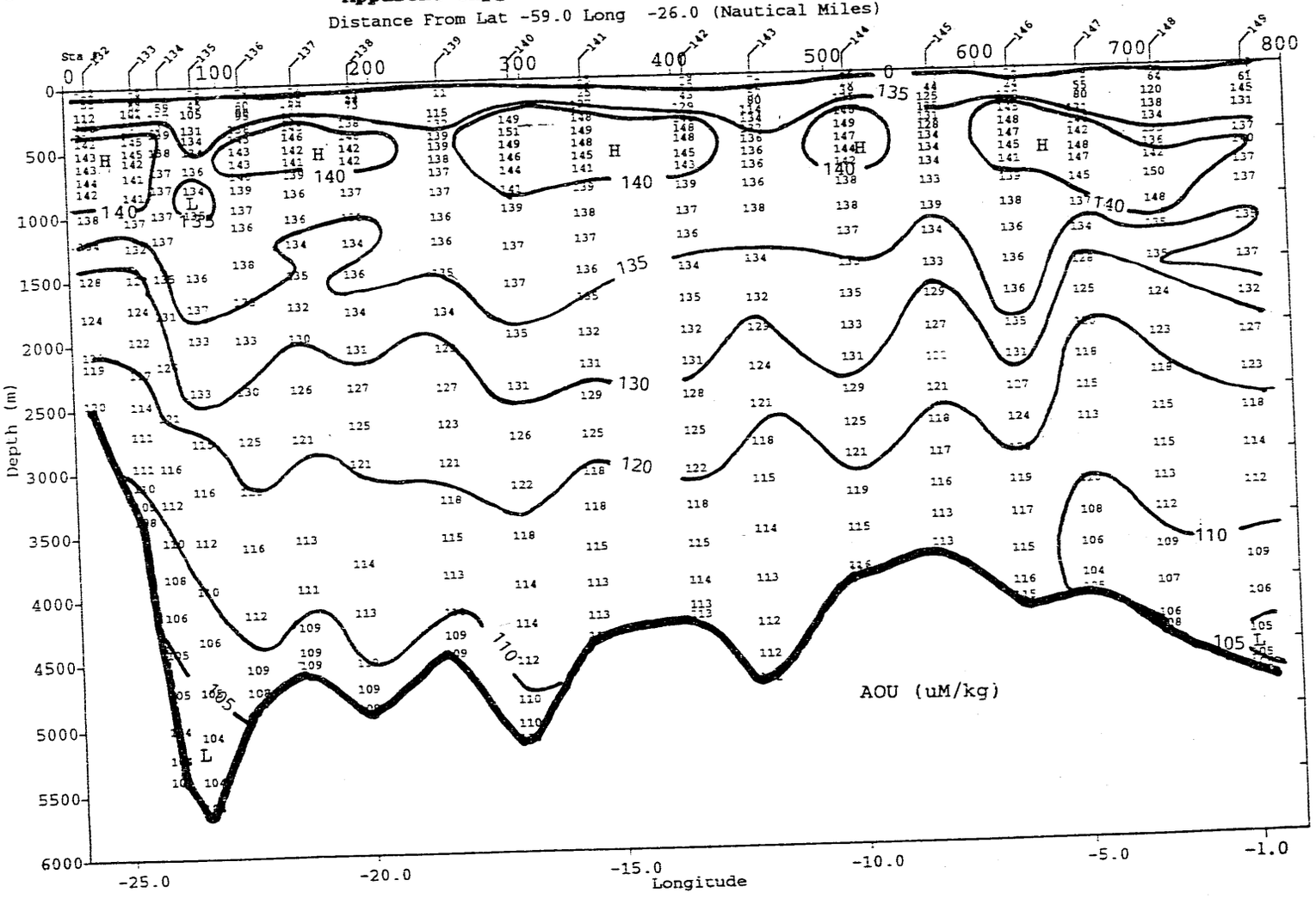

Fig. 37 - Meteor 11/5 Cruise - South Atlantic 58 Deg South Section Sta 132-149
Nitrate Concentration (NO3) (uM/kg)

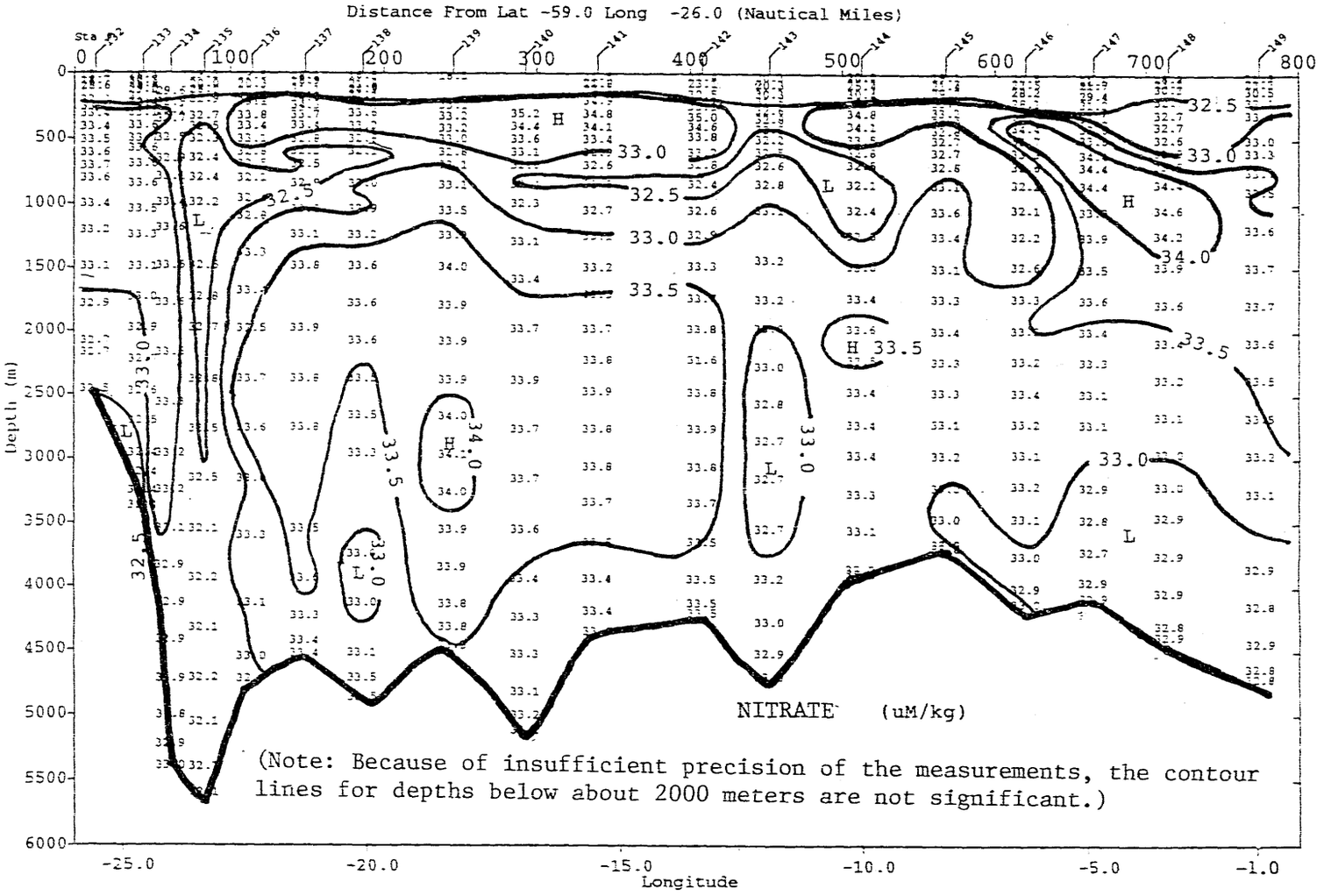

(Note: Because of insufficient precision of the measurements, the contour lines for depths below about 2000 meters are not significant.)

Fig. 38 – Meteor 11/5 Cruise - South Atlantic 58 Deg South Section Sta 132-149
Phosphate Concentration (PO4) (uM/kg)

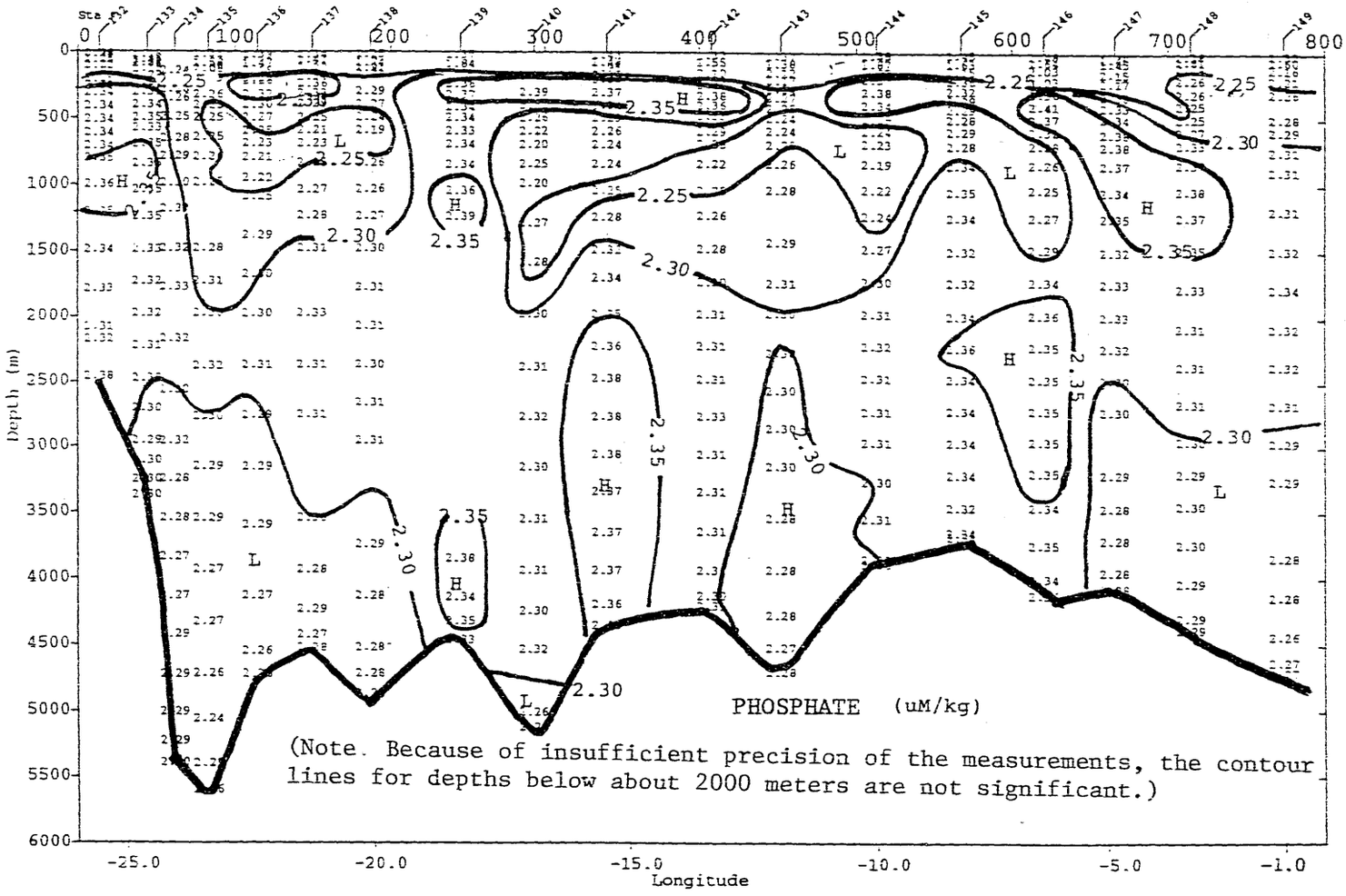

(Note. Because of insufficient precision of the measurements, the contour lines for depths below about 2000 meters are not significant.)

Fig. 39 - Meteor 11/5 Cruise - South Atlantic 58 Deg South Section Sta 132-149
Silicate Concentration (SiO3) (uM/kg)

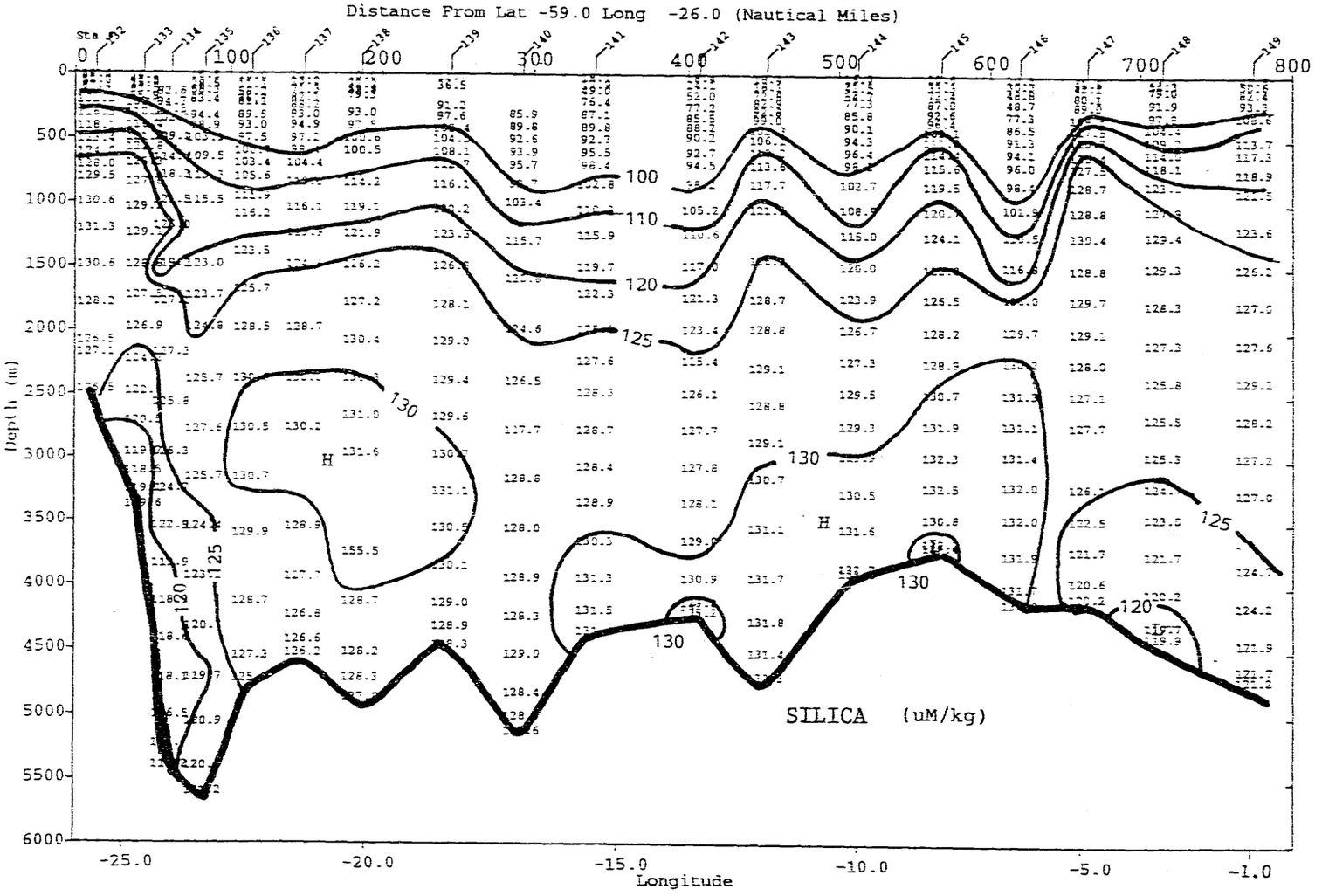

In this section around 3000 meters deep, there is a layer of water with a typical temperature (-0.25 ~ -0.50) and salinity (34.65 ~ 34.67 o/oo) range for the Antarctic Bottom Water (AABW. This is commonly found in abyssal depths throughout the western basin of the South Atlantic Ocean. As seen in Fig. 31, the temperature and salinity values for the AABW fall between the warmer Weddell Sea Deep Water and the colder Weddell Sea Bottom Water. This suggests that the AABW consists roughly of a 1:1 mixture of the WSDW and WSBW. The characteristic chemical properties for the AABW are listed in Table 2.

III- 5) The Capetown-Weddell Section (Stations 149-179):

This section represents a near-meridional section from the northeastern Weddell Sea (58°S and the prime meridian) to Capetown (35°S and 18°E). In order to provide a better lateral resolution for the large distances covered by this section, it has been divided into two segments: the southern segment consisting of Stations 149 to 164 (47°S and 8°E) and the northern segment consisting of Stations 164 to 179.

III-5-a) Southern Capetown-Weddell Section (Stations 149-164):

This segment represents a meridional section for a latitudinal range from about 59°S to 46°S. In the area south of about 51°S, a well defined temperature minimum layer with sub-zero temperatures (about 100 meters thick, outlined by the 0.0°C contour in Fig. 40) is present around 200 meters deep. This appears to represent remnants of cold winter mixed layer water, which is, in turn, underlain by a warmer and more saline layer. The temperature minimum deepens north of about 52°S and disappears totally north of 50°S (see Fig. 40) as described by Gordon (1971-b). In the area north of about 51°S, the surface and intermediate waters are both several degrees warmer and the deep waters by 1°C compared to the southern half. The transition in surface water temperature takes place between 51°S and 52°S representing the polar front separating the subantarctic and antarctic waters (Gordon, 1971-b). A layer of warm (2.3 ~ 3.0°C) and less saline (34.0 ~ 34.3 o/oo) water is found between 300 and 800 meters deep in the area north of 50°S. This appears to represent the Antarctic Intermediate Water (AAIW), which is formed in this latitudinal range and spreads northward eventually beyond the equator. The potential temperature and salinity relationships are shown in Fig. 42.

In the southern half of this segment, there is a well defined temperature maximum which is centered around about 300 meters deep and outlined by the 1.0, 1.5 and 2.0°C isotherms (Fig. 40). This temperature maximum layer is located above the salinity maximum layer (Fig. 41), which appears to be derived from the high salinity NADW depicted by the 34.75 and 34.78 o/oo isohalines in the northern half of this section between 2000 and 3000 meters deep. The temperature maximum water has a σ_2 density of about 36.95 and also is associated with a local maximum in the total CO_2, pCO_2, AOU, nitrate and phosphate and with a local minimum in the oxygen concentration. On the basis of the density, temperature, salinity and other chemical values (Tables 1 and 3), this water appears to represent the upper Circumpolar Deep Water (Reid et al., 1977). Immediately below this, the saline

TABLE - 3 Summary of the physical and chemical characteristics of various water masses observed during the Meteor 11/5 expedition in the South Atlantic and northern Weddell Sea areas. The values represent extreme values observed during the expedition, but do not necessarily indicate the values for the "pure" end members of water mass. UCPDW = Upper Circumpolar Deep Water; NADW = North Atlantic Deep Water; LCPDW = Lower Circumpolar Deep Water; CBBW = Cape Basin Bottom Water. (+) and (-) signs indicate that the values listed comprise a local maximum and minimum respecitvely.

Water Masses	UCPDW	NADW	LCPDW	CBBW
Sections Observed	Cape-Weddell	Cape-Weddell	Cape-Weddell	Cape-Weddell
Stations	158-161	177-178	152-154	176-179
Depths (meters)	1000-1500	2000-3000	1200-1700	>4400
Pot. Temp. (°C)	2.0-2.5	2.0-2.5	0.2-0.3	<0.6
Salinity (o/oo)	34.5-34.7	34.80-34.85(+)	34.68-34.70	<34.73
Denisty (σ_t)	27.74-27.80	27.80-27.84	27.82-27.84	>27.85
Denisty (σ_2)	36.7-36.9	36.95-37.05	37.07-37.13	>37.13
TCO_2 (uM/kg)	2220-2250(+)	2200-2210(-)	2260(+)	>2250
pCO_2 @ 20°C (uatm)	1100-1180(+)	850-900(-)	1100-1125(+)	>1010
O_2 (uM/kg)	180-200(-)	220-230(+)	210-220	<219
AOU (uM/kg)	140-150(+)	100-110(-)	135	125
NO_3 (uM/kg)	34-35(+)	25-26(-)	33-34	>31
PO_4 (uM/kg)	2.4-2.5(+)	1.7-1.8(-)	2.3	2.1
SiO_3 (uM/kg)	70-80	50-60(-)	120-127	>108
TALK (uEq/kg)*	2335-2340	2335-2340	2360	>2370
Pot.ALK (uEq/kg)**	2400(+)	2378(-)	2415-2417	>2420

*/ Total alkalinity (TALK) values computed using the total CO_2 concentration and pCO_2 @ 20°C data at observed salinities.
**/ Potential alkalinity (Pot.ALK) computed as [(TALK) + (NO_3^-)] and normalized to a salinity of 35.00 o/oo.

Fig. 40 - Meteor 11/5 Cruise - Southern Part of Eastern N/S Section - Sta 149-164
Potential Temperature at the Surface (Deg C)

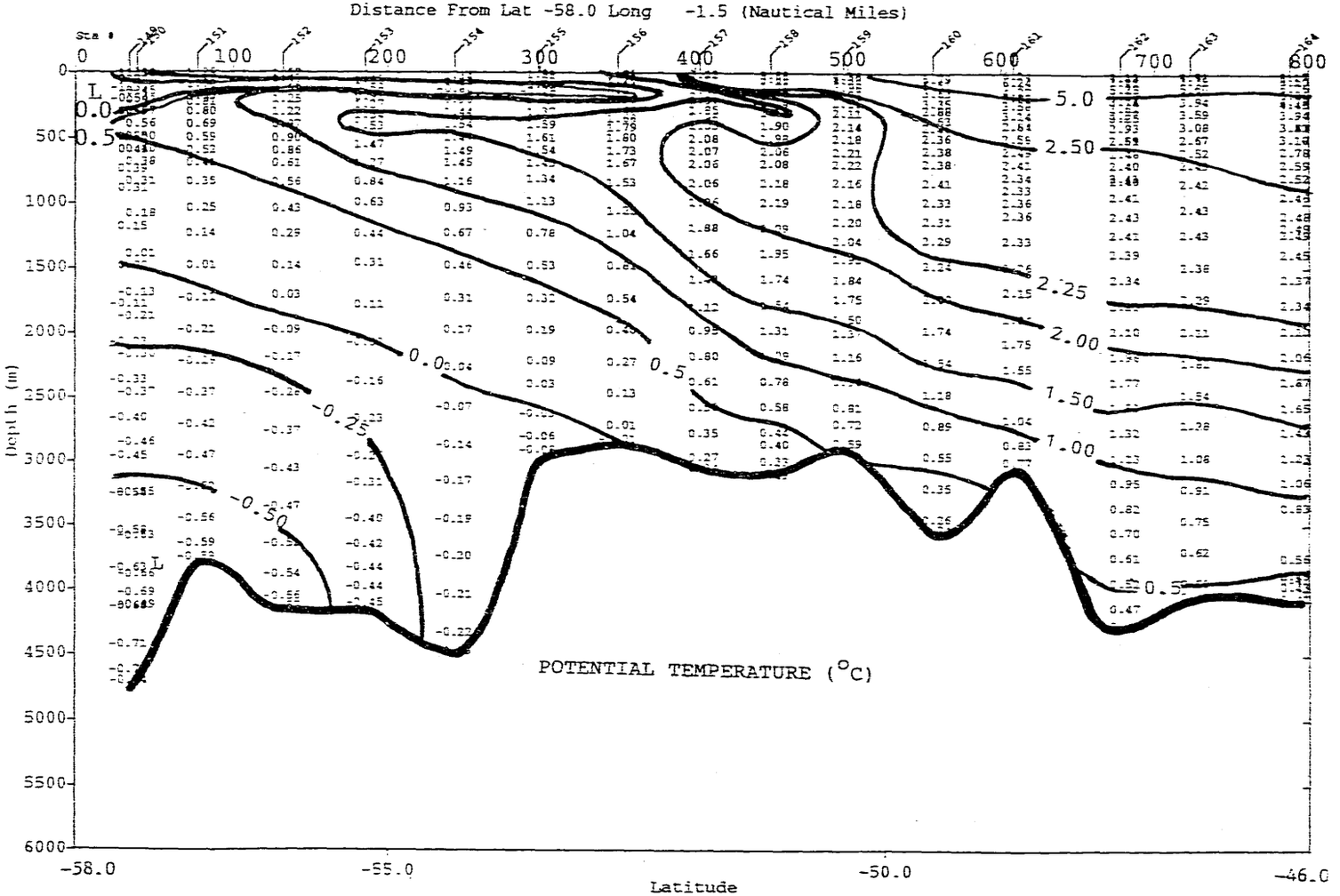

Fig. 41 - Meteor 11/5 Cruise - Southern Part of Eastern N/S Section Sta 149-164
Salinity (PSU)

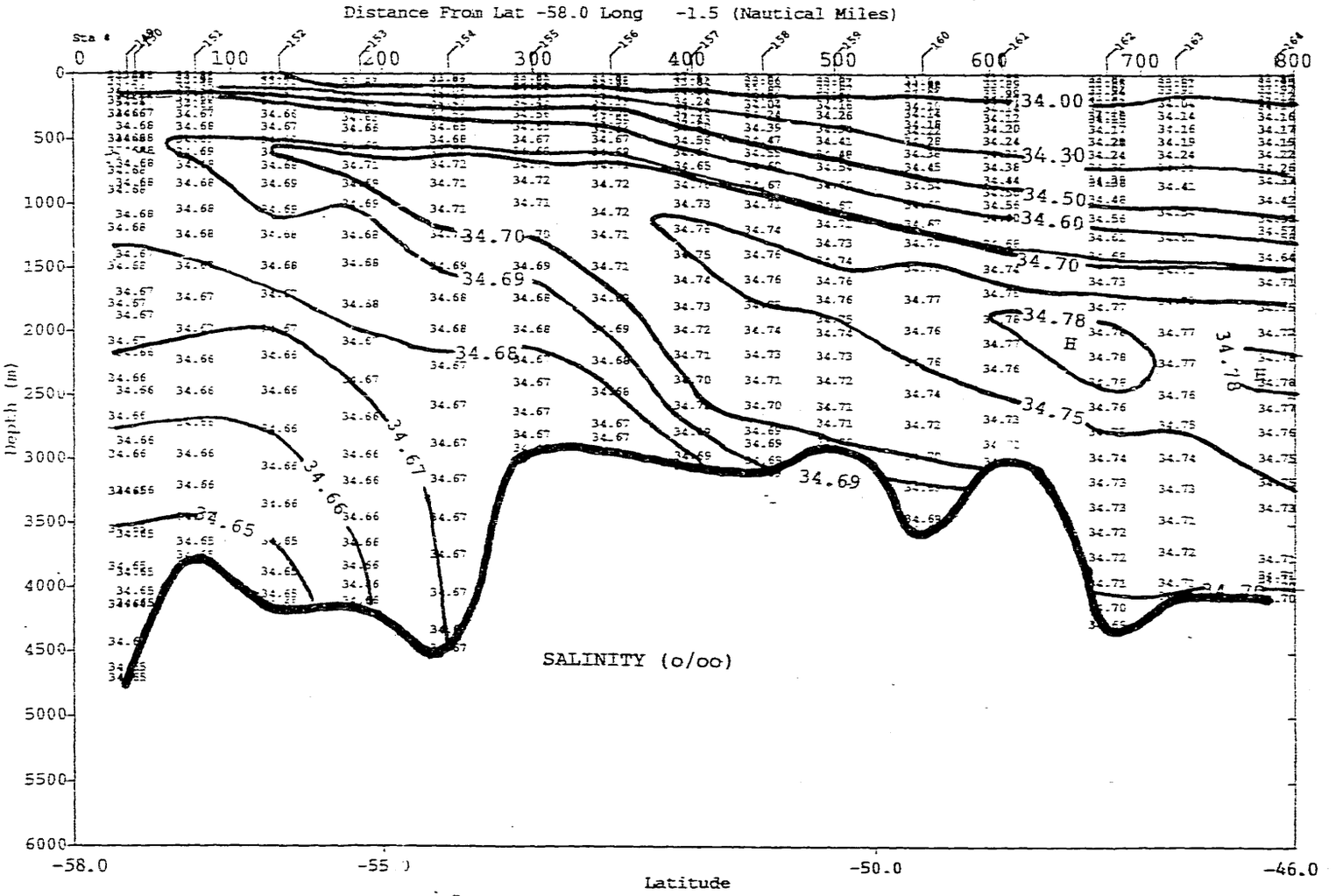

Fig. 42 - Potential temperature-salinity relationships observed in the Capetown-Weddell Sea section (southern segment). AAIW = Antarctic Intermediate Water; NADW = North Atlantic Deep Water; CPDW = Circumpolar Deep Water; AABW = Antarctic Bottom Water; WSBW = Weddell Sea Bottom Water.

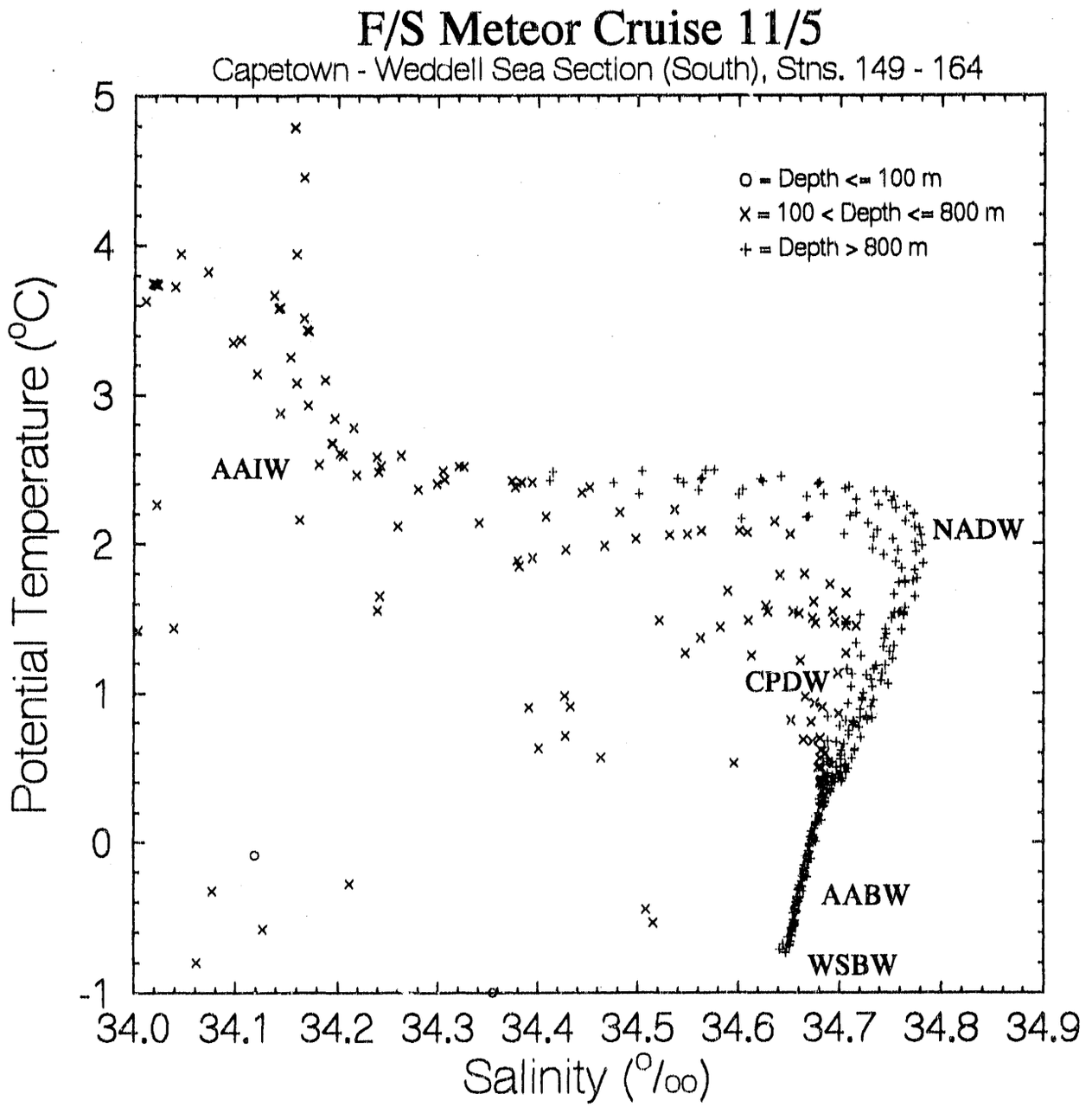

North Atlantic Deep Water (NADW) is found. It appears to intrude southward as indicated by the long upward extension of the 34.70 and 34.69 o/oo isohaline contours (Fig. 41). At the northernmost station, Stn. 164, in this section, the NADW has a σ_2 density range of 36.96 to 37.05 (Fig. 43) and is characterized by a minimum in TCO_2 (about 2230 uM/kg, Fig. 44), pCO_2 (980 to 1000 uatm, Fig. 45), AOU (130 uM/kg, Fig. 47), nitrate (29 ~ 30 uM/kg, Fig. 48) and phosphate (2.0 uM/kg, Fig. 49). Because of the similarity in densities, it appears that the NADW mixes with the Circumpolar Water and thus is responsible for the high salinity values of the latter.

Below the NADW, a layer of colder and lower salinity water is present. This gives an appearance of the NADW wedging itself between the two layers of the Circumpolar Deep Water. This feature can be best illustrated in Figs. 44 and 45 by the TCO_2 and pCO_2 contours seen between 300 and 2000 meters deep in the southern (i.e. left) half of this section. Based upon the distribution of oxygen and phosphate in the western South Atlantic and Scotia Sea, Reid et al. (1977) observed splitting of the Circumpolar Deep Water into two branches above and below the NADW and named the Upper and Lower Circumpolar Deep Water. The chemical characteristics of these water masses are summarized in Table 3.

The waters below about 3000 meters in the southern half of this segment is dominated by the Antarctic and Weddell Sea waters, i.e. as cold as -0.71°C and as fresh as 34.65 o/oo. They are characterized by relatively low TCO_2 (2245 uM/kg), pCO_2 (1050 uatm), AOU (105 uM/kg) values and high oxygen values (255 uM/kg), indicating strong influence of the Weddell Bottom Water.

Fig. 43 - **Meteor 11/5 Cruise - Southern Part of Eastern N/S Section Sta 149-164**
Potential Density at 2000 Meters (Sigma 2000) (Sigma Units)

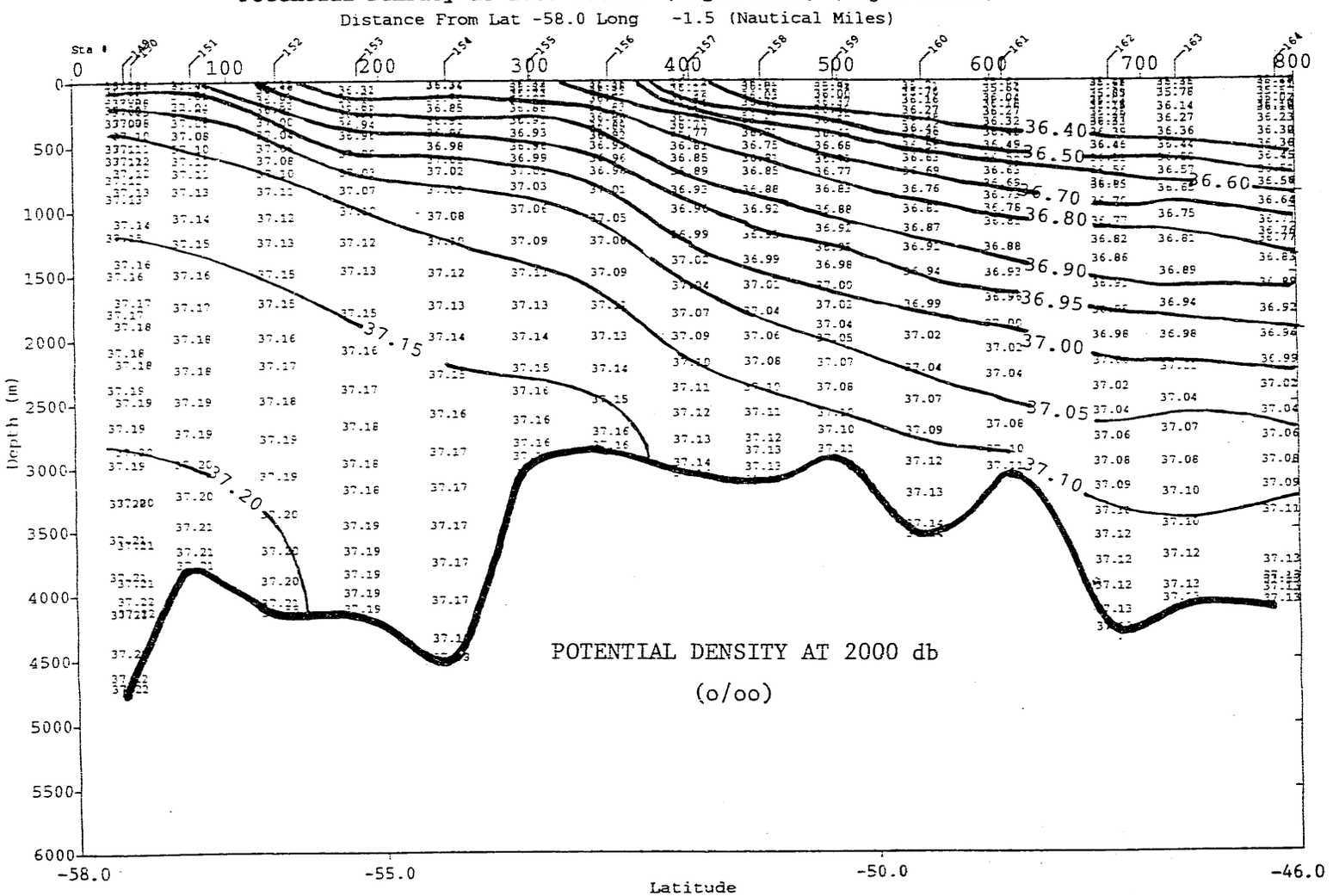

Fig. 44 - Meteor 11/5 Cruise - Southern Part of Eastern N/S Section Sta 149-164
Total CO2 (TCO2) (uM/kg)

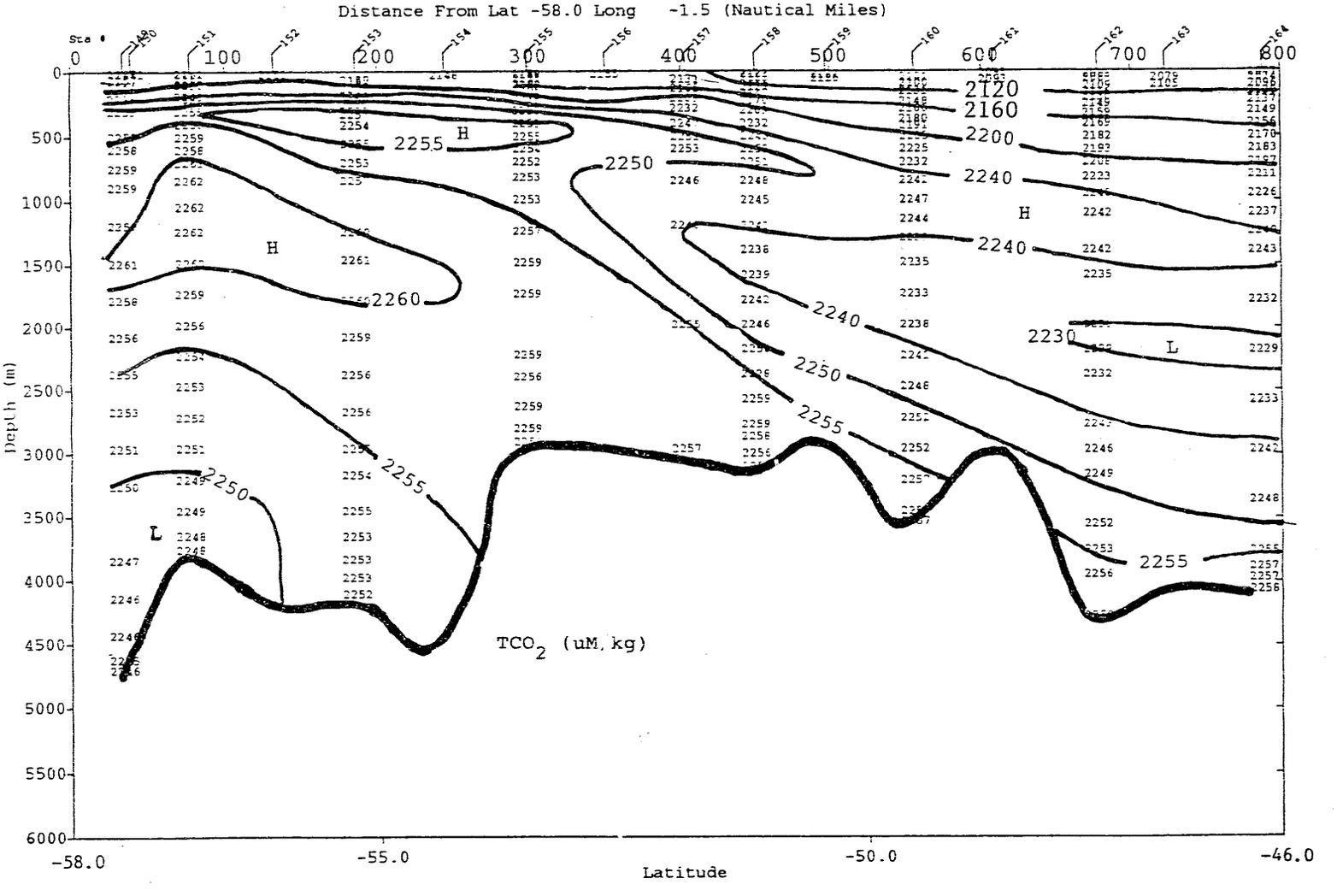

Fig. 45 - **Meteor 11/5 Cruise - Southern Part of Eastern N/S Section Sta 149-164**
pCO2 in Seawater at 20 deg C (uAtm)

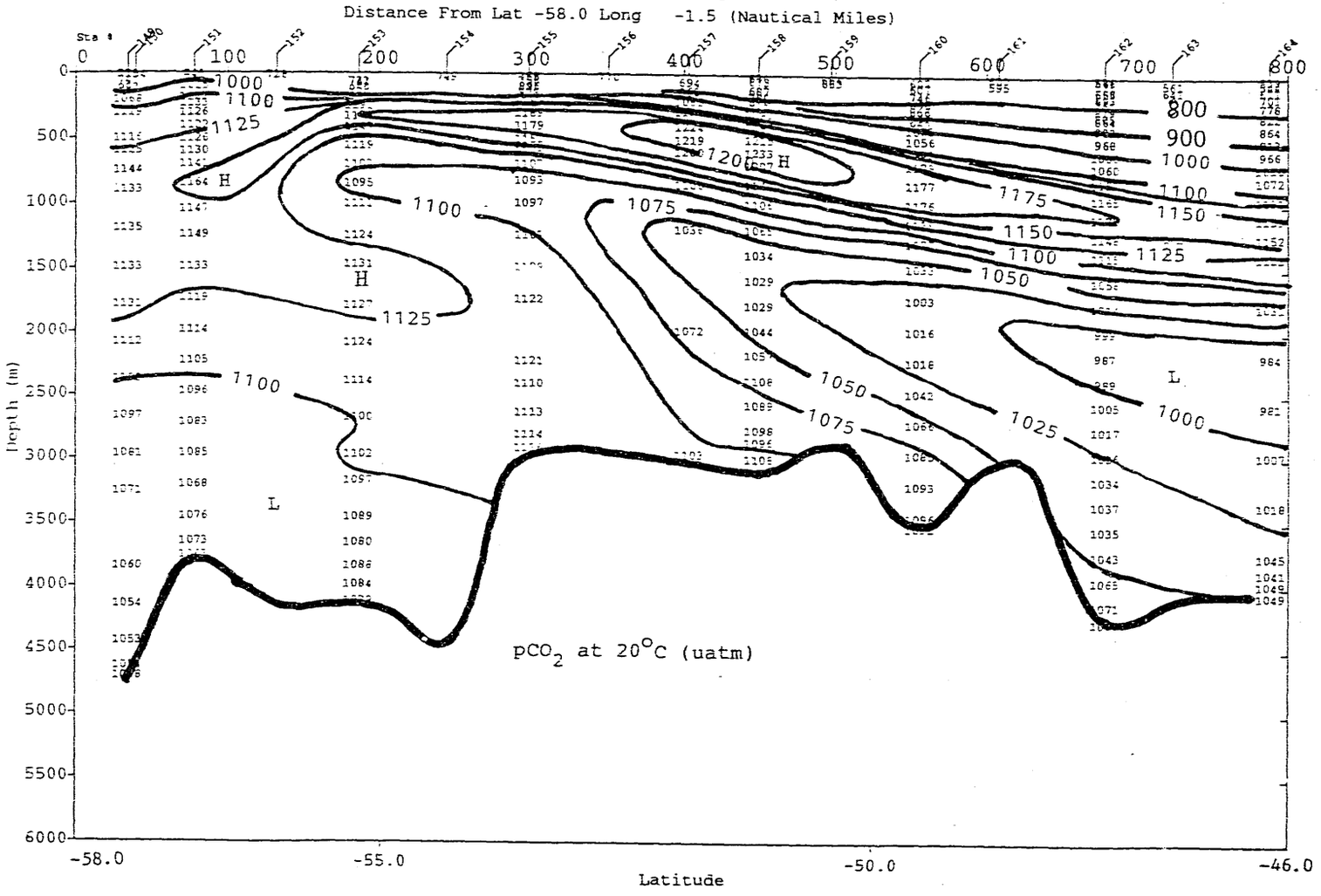

Fig. 46 - Meteor 11/5 Cruise - Southern Part of Eastern N/S Section - Sta 149-164

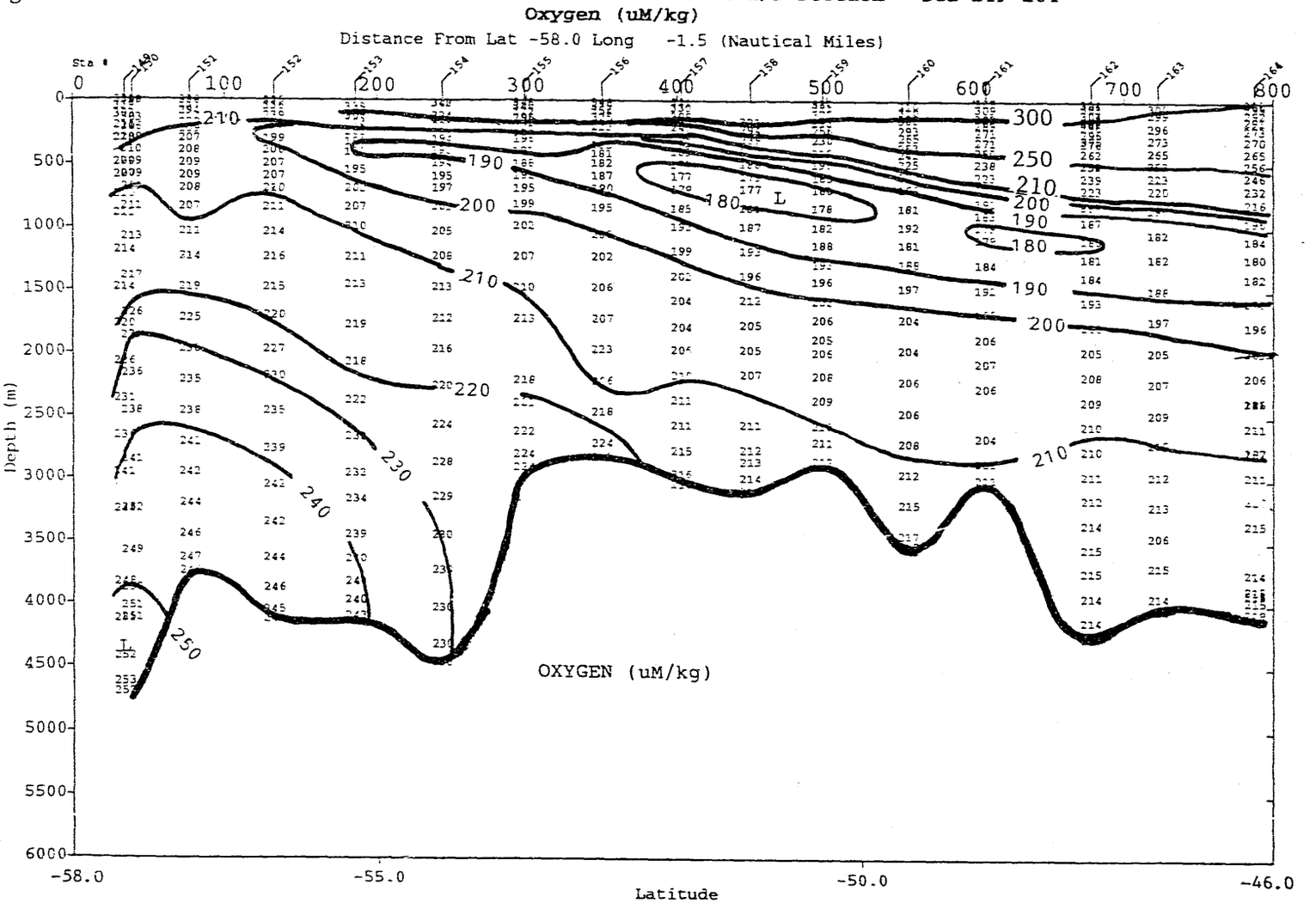

Fig. 47 - Meteor 11/5 Cruise - Southern Part of Eastern N/S Section Sta 149-164
Apparent Oxygen Utilization (AOU) (uM/kg)

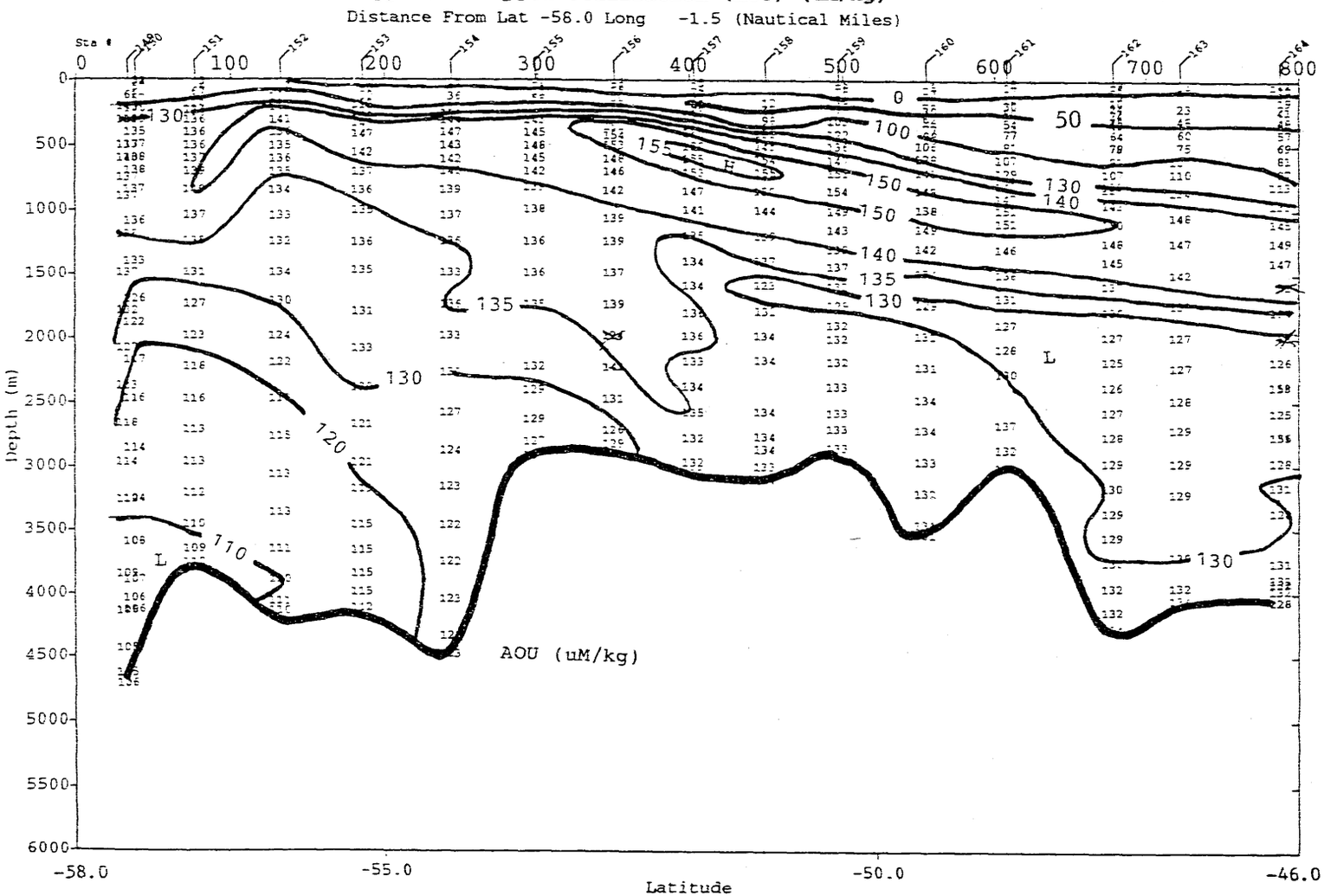

Fig. 48 - Meteor 11/5 Cruise - Southern Part of Eastern N/S Section Sta 149-164

Nitrate Concentration (NO3) (uM/kg)

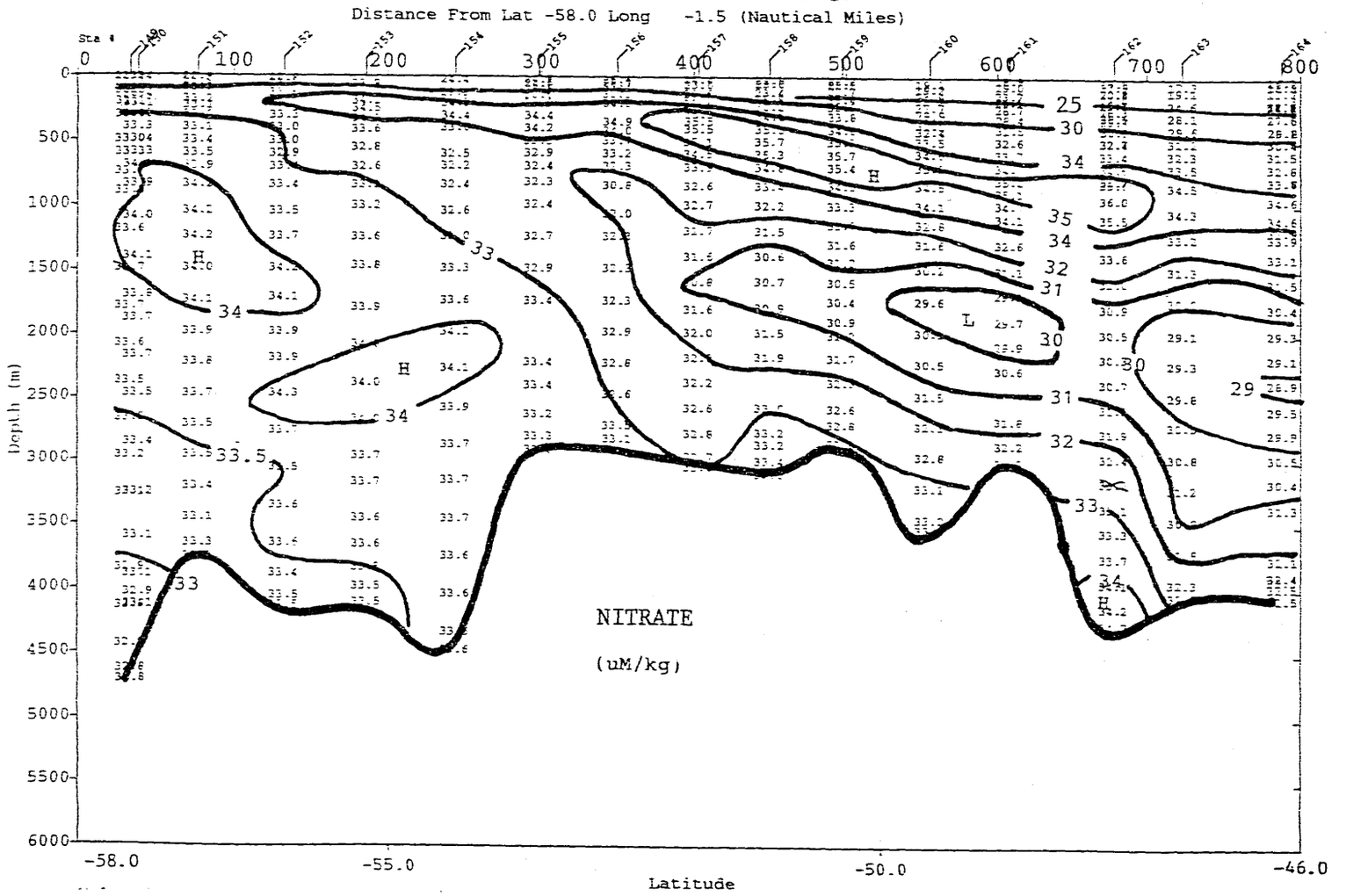

Fig. 49 - Meteor 11/5 Cruise - Southern Part of Eastern N/S Section Sta 149-164
Phosphate Concentration (PO4) (uM/kg)

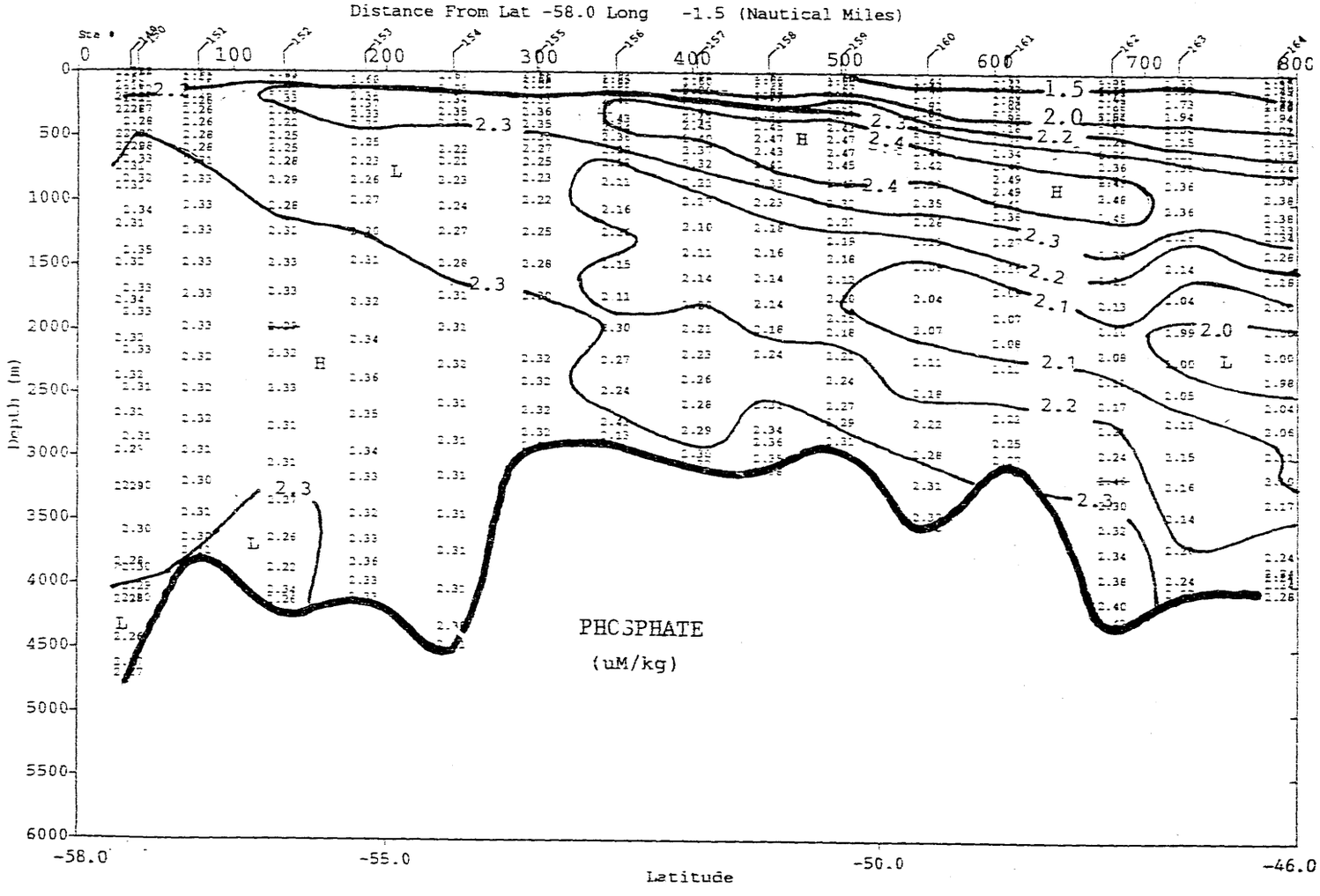

Fig. 50 - Meteor 11/5 Cruise - Southern Part of Eastern N/S Section Sta 149-164
Silicate Concentration (SiO3) (uM/kg)

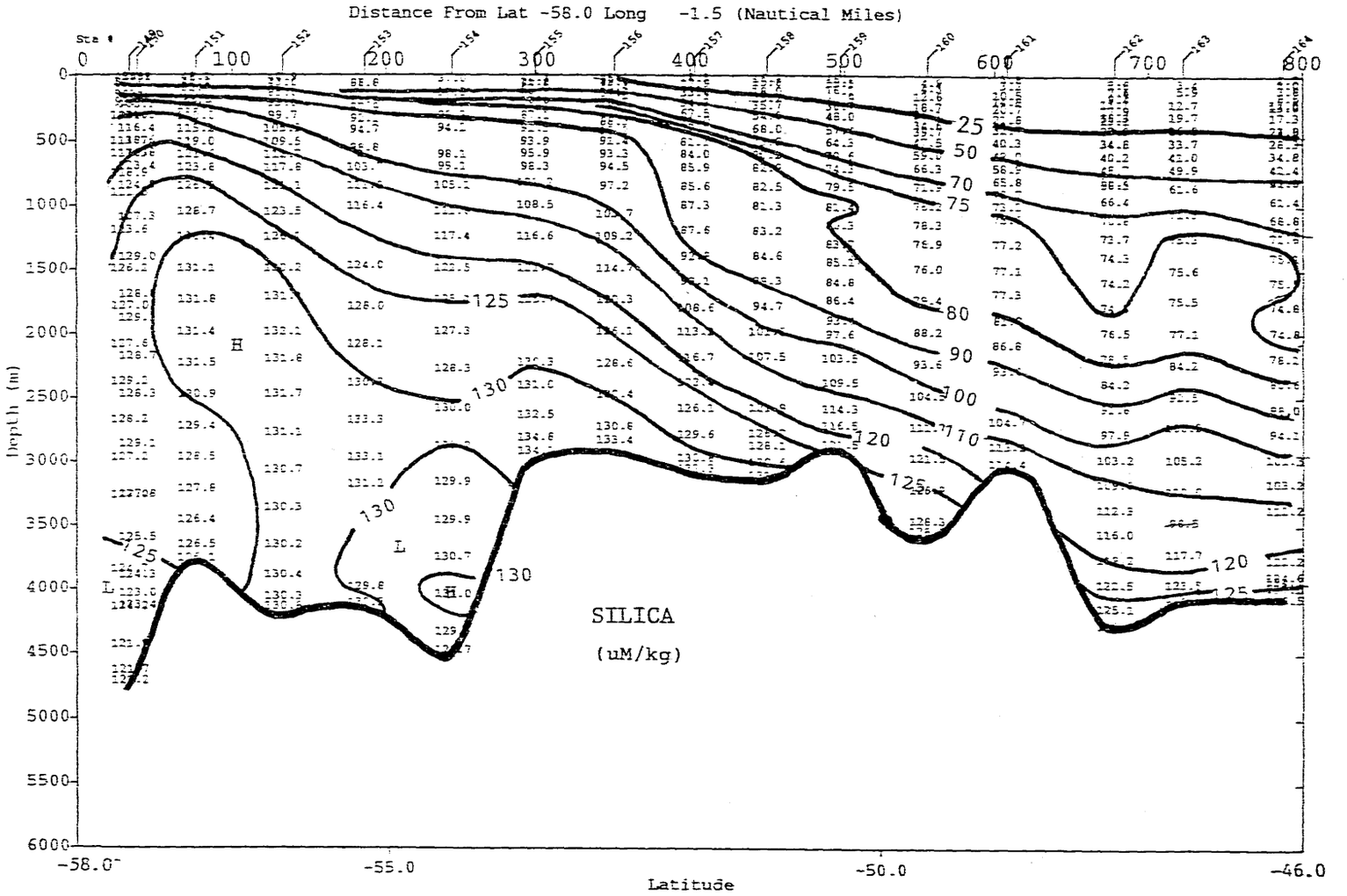

III-5-b) Northern Capetown-Weddell Section (Stations 164-179):

This segment covers a latitudinal range from 46°S to 37°S in the eastern South Atlantic Ocean. The temperature and salinity both continue to increase northward ranging from about 0.5°C and 34.7 o/oo near the southernmost sea floor to 20°C and 35.5 o/oo for the northernmost surface waters. In the upper 1000 meters, the Antarctic Intermediate Water (AAIW) is shown with a salinity minimum which is clearly outlined with the 34.3 and 34.4 o/oo isohalines centered around 500 meters deep near 45°S and 1000 meters deep near 37.5°S. The temperature for the AAIW ranges from about 3 to 5°C. However, this water mass does not exhibit local minima or maxima in other properties besides the salinity.

Immediately below the AAIW, there exists a layer of water with a temperature of about 2.5°C and a salinity of 34.6 o/oo at a depth of about 1500 meters. It has a σ_2 density between 36.8 and 36.9 (Fig. 54). While this layer does not show a local maximum or minimum in salinity or temperature, it exhibits a clear minimum in the oxygen concentration (see the 180 and 190 uM/kg contours in Fig. 57) and a clear maximum in the total CO_2 concentration (see the 2230 and 2240 uM/kg contours in Fig. 55), pCO_2 (see the 1100 and 1150 uatm contours in Fig. 56), AOU (see the 140 uM/kg contours in Fig. 58), nitrate (see the 33 and 34 uM/kg contours in Fig. 59), phosphate (see the 2.2 and 2.3 uM/kg contours in Fig. 60). On the other hand, the silicate concentration (Fig. 61) does not exhibit an extremum at these depths, and ranges between 68 and 73 uM/kg. Since these features match with those for the Upper Circumpolar Deep Water (UCPDW) listed in Table 3, this layer is identified as UCPDW. In the eastern basin of the South Atlantic, this water mass has been traced as far north as 20°S or equatorward of the Rio Grande Rise) (see page 70 in Reid et al., 1977). Our study in the eastern Atlantic shows that the UCPDW also extends further north beyond 37°S.

The deep regime is dominated by the North Atlantic Deep Water (NADW) which is characterized by a salinity maximum outlined with the 34.80 and 34.85 o/oo contours. The NADW exhibits a maximum in the oxygen concentration (see 220 and 230 uM/kg contours in Fig. 57) and a minimum in the total CO_2 concentration (see 2210 contour in Fig. 55), pCO_2 (see 850 and 900 uatm contours in Fig. 56), AOU (see 100 and 110 uM/kg contours in Fig. 58), nitrate (see 25 and 26 uM/kg contours), phosphate (see 1.7 and 1.8 uM/kg contours in Fig. 60) and silica (see 60 and 70 uM/kg contours in Fig. 61). These chemical properties are summarized in Table 3 and the potential temperature-salinity relationships observed in this section are shown in Fig. 53.

Fig. 51 – Meteor 11/5 Cruise – Northern Part of Eastern N/S Section – Sta 164-179
Potential Temperature at the Surface (Deg C)

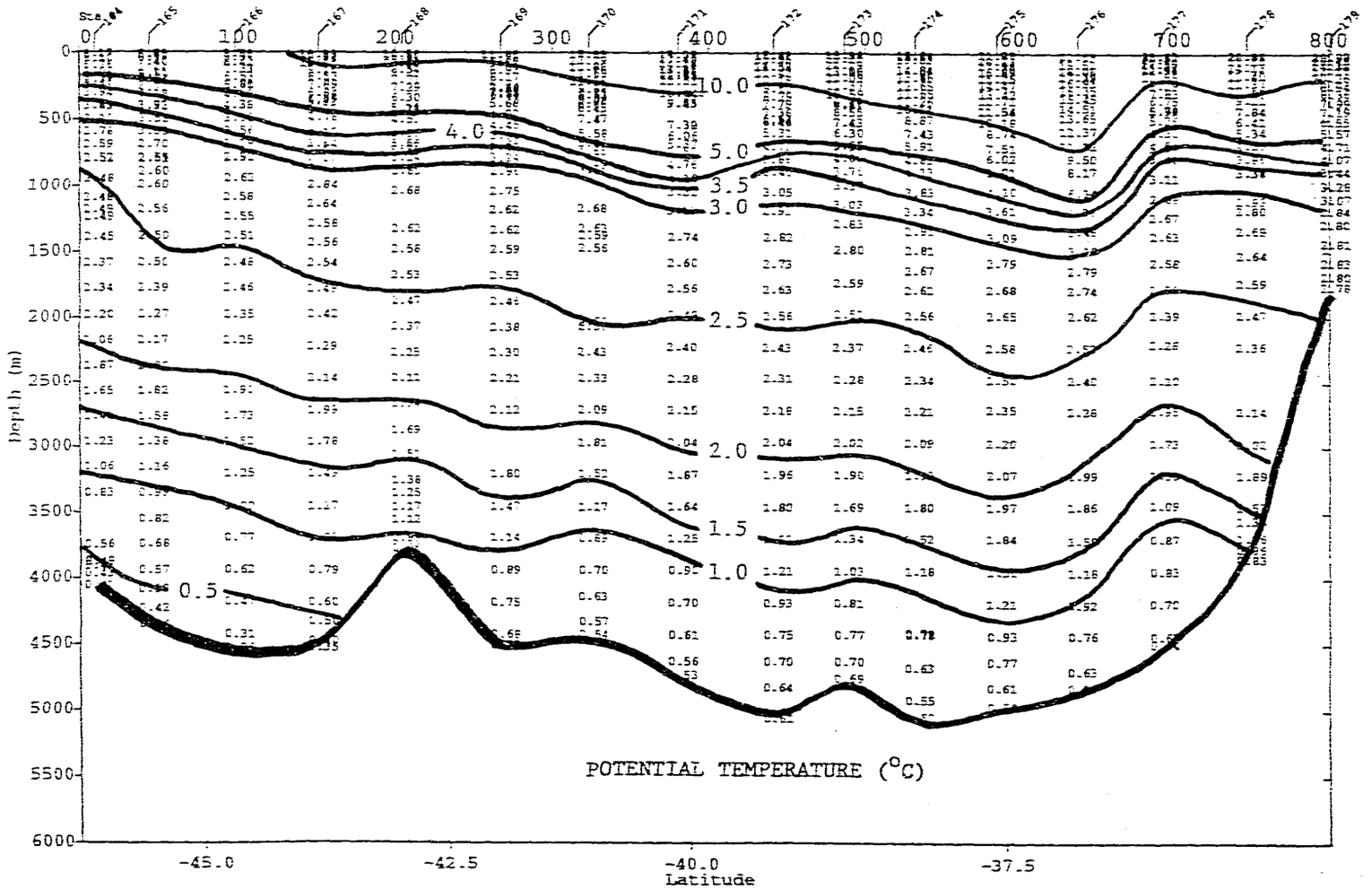

Fig. 52 – Meteor 11/5 Cruise - Northern Part of Eastern N/S Section Sta 164-179
Salinity (PSU)

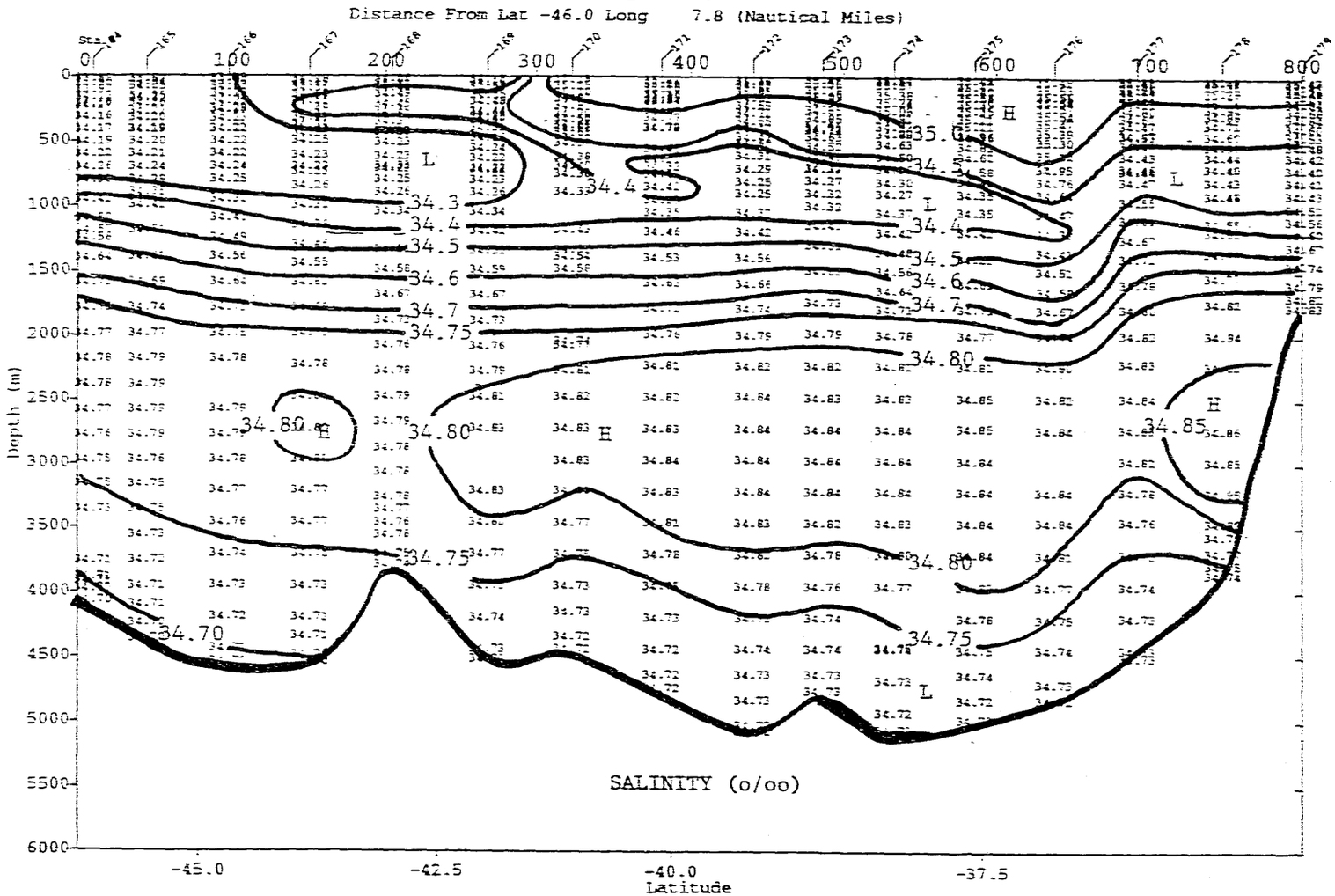

Fig. 53 - Potential temperature-salinity relationships observed in the Capetown-Weddell Sea section (northern segment). AAIW = Antarctic Intermediate Water; NADW = North Atlantic Deep Water; AABW = Antarctic Bottom Water.

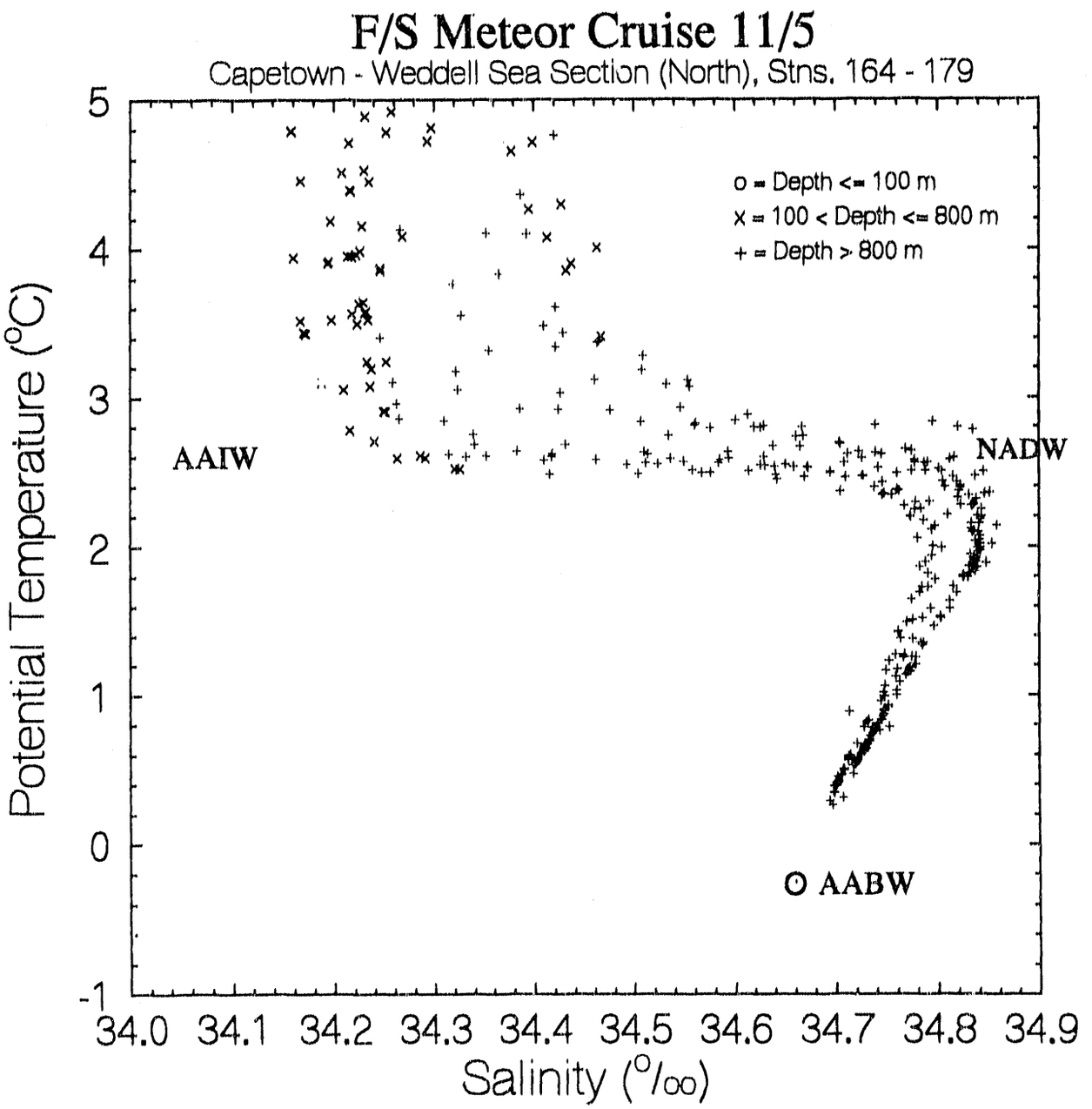

Fig. 54 – **Meteor 11/5 Cruise - Northern Part of Eastern N/S Section Sta 164-179**
Potential Density at 2000 Meters (Sigma 2000)

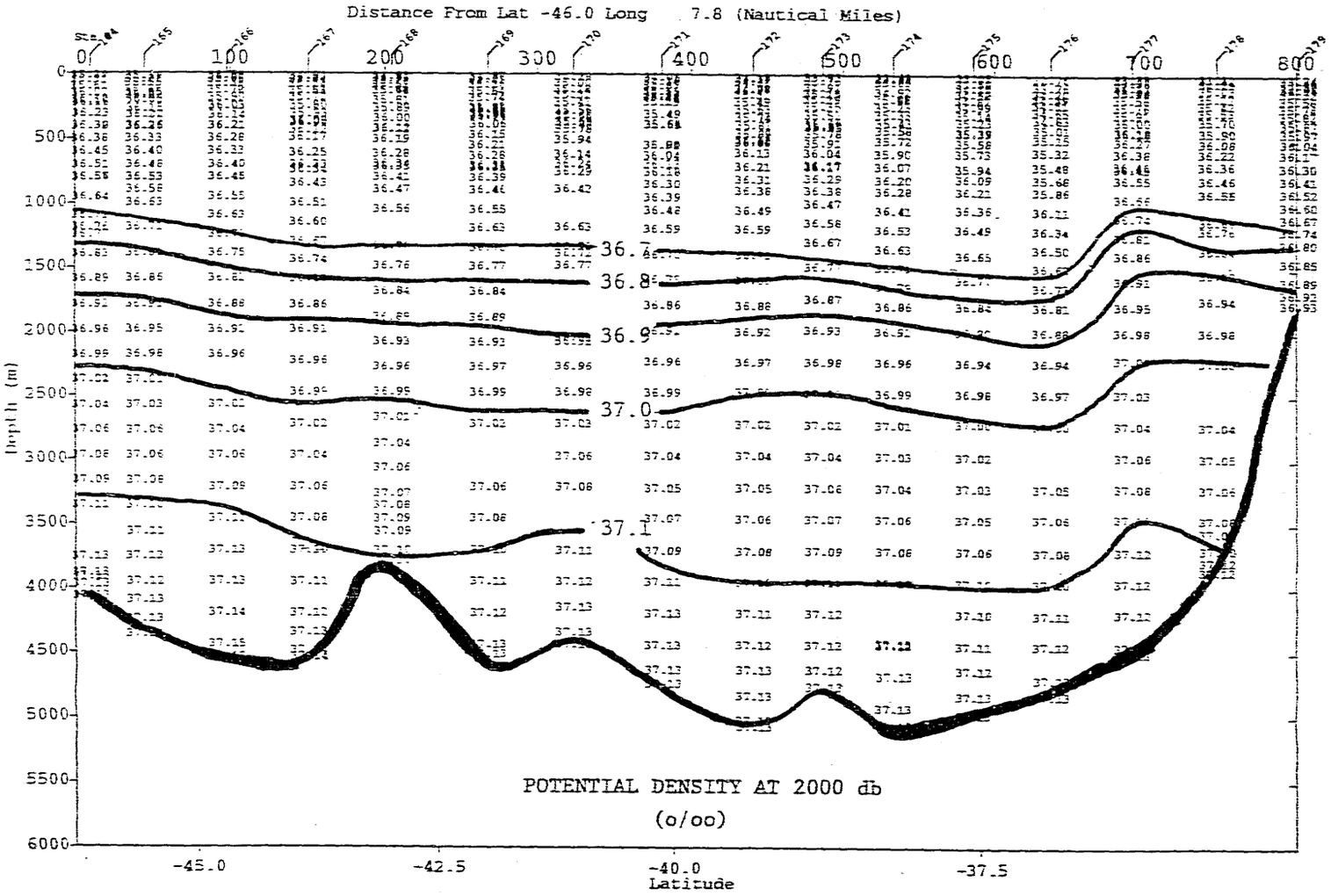

Fig. 55 - Meteor 11/5 Cruise - Northern Part of Eastern N/S Section Sta 164-179
Total CO2 (TCO2) (uM/kg)

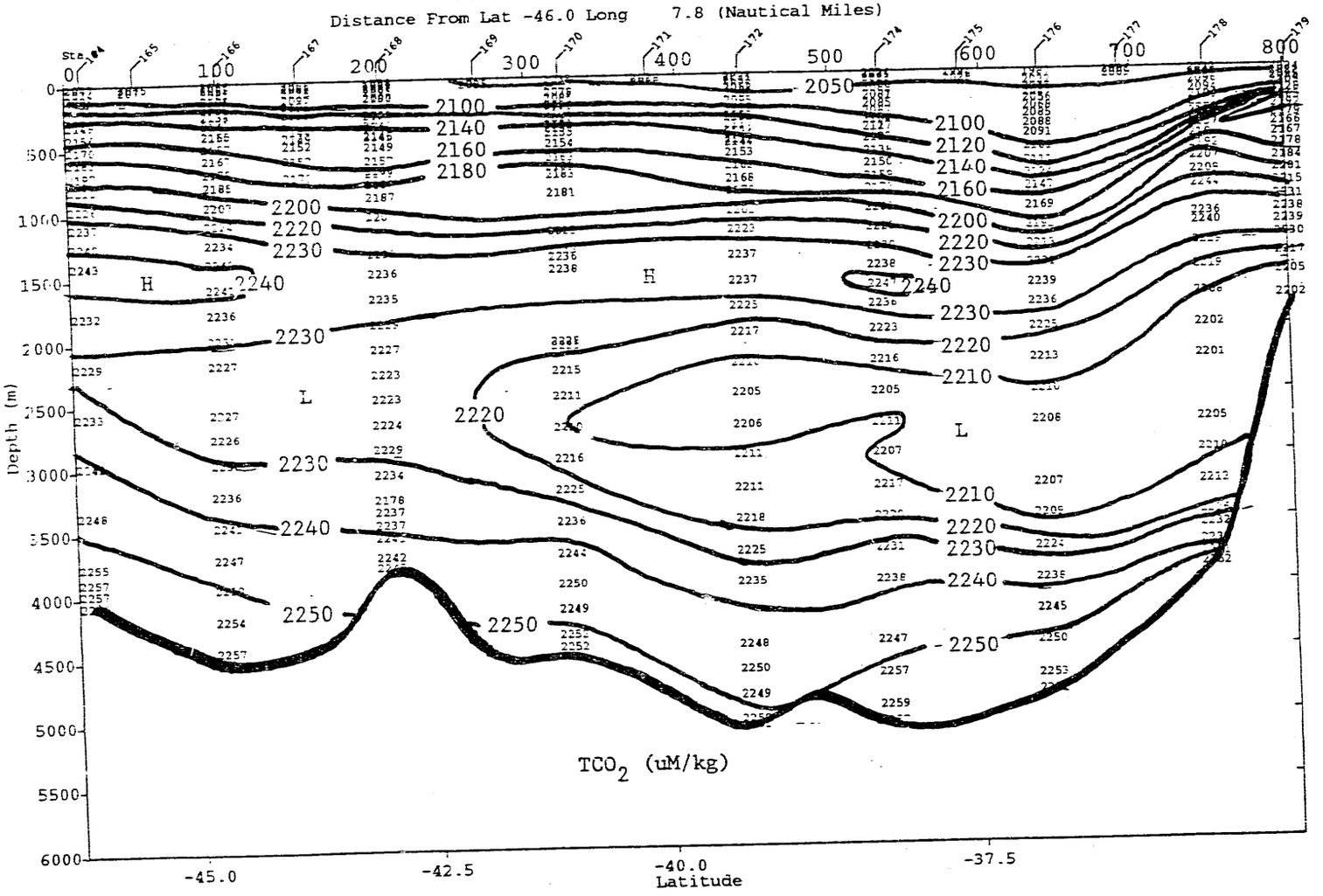

Fig. 56 - **Meteor 11/5 Cruise - Northern Part of Eastern N/S Section Sta 164-179**
pCO2 in Seawater at 20 Deg C (uAtm)

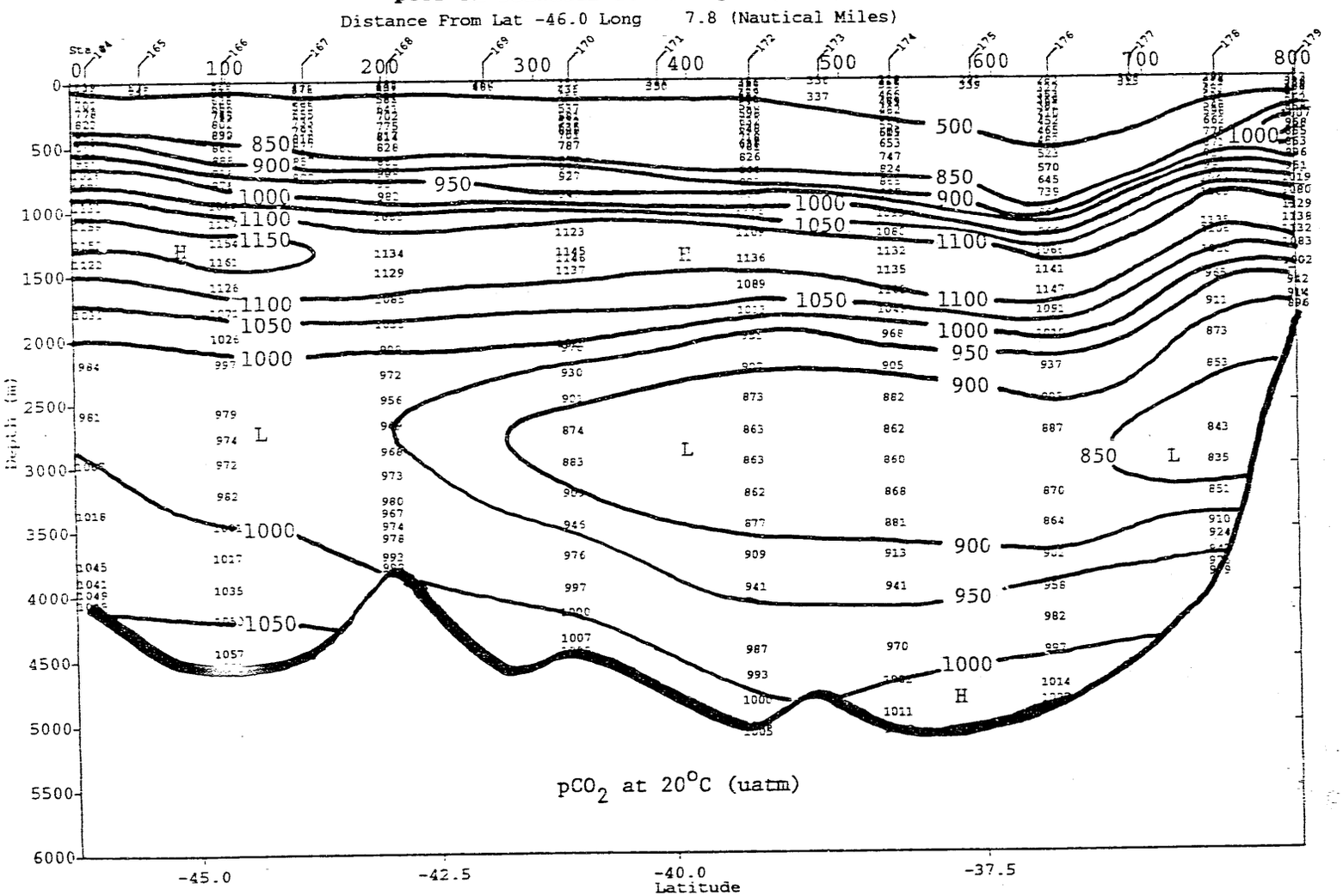

Fig. 57 - Meteor 11/5 Cruise - Northern Part of Eastern N/S Section - Sta 164-179
Oxygen (uM/kg)

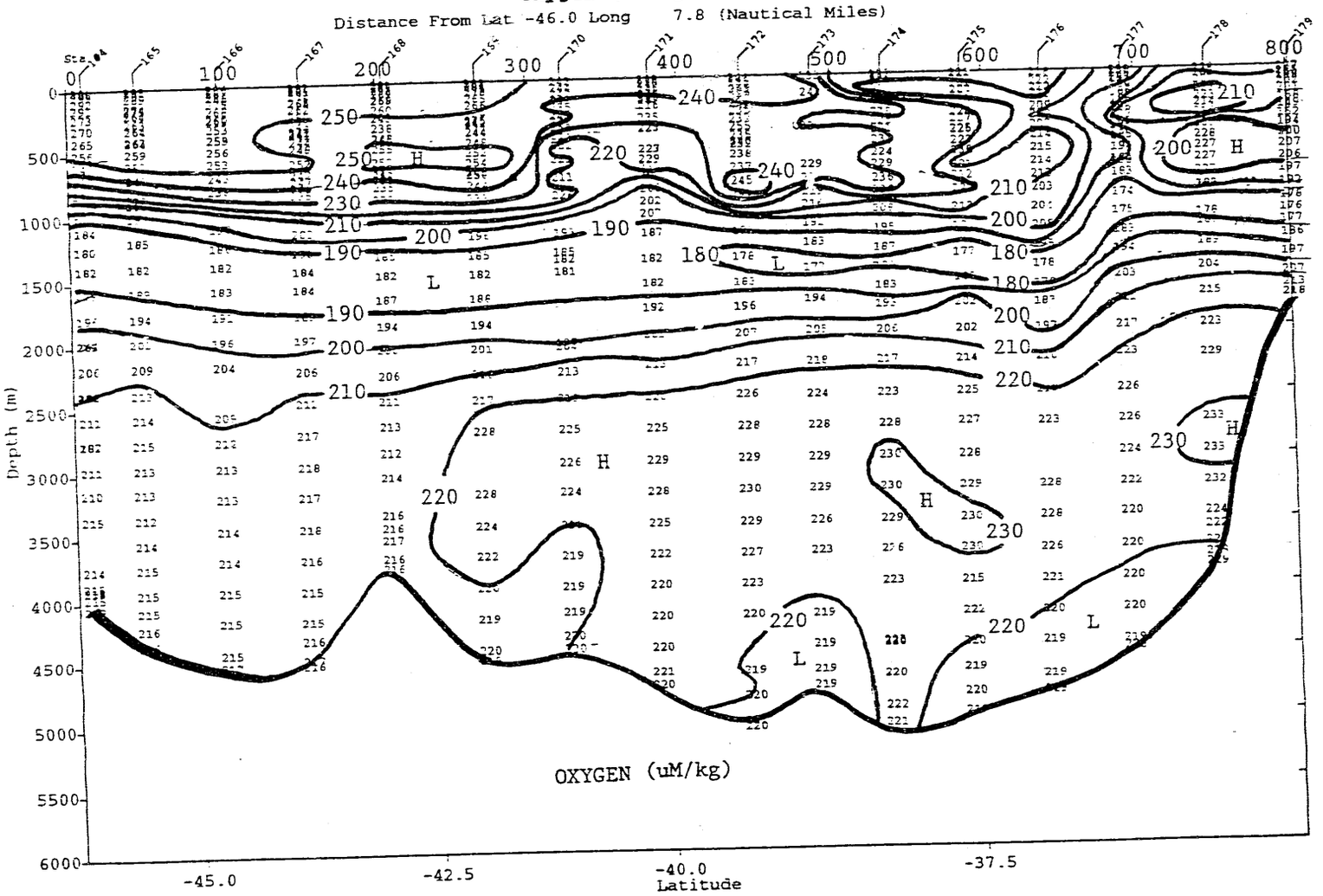

Fig. 58 - Meteor 11/5 Cruise - Northern Part of Eastern N/S Section Sta 164-179
Apparent Oxygen Utilization (AOU) (uM/kg)

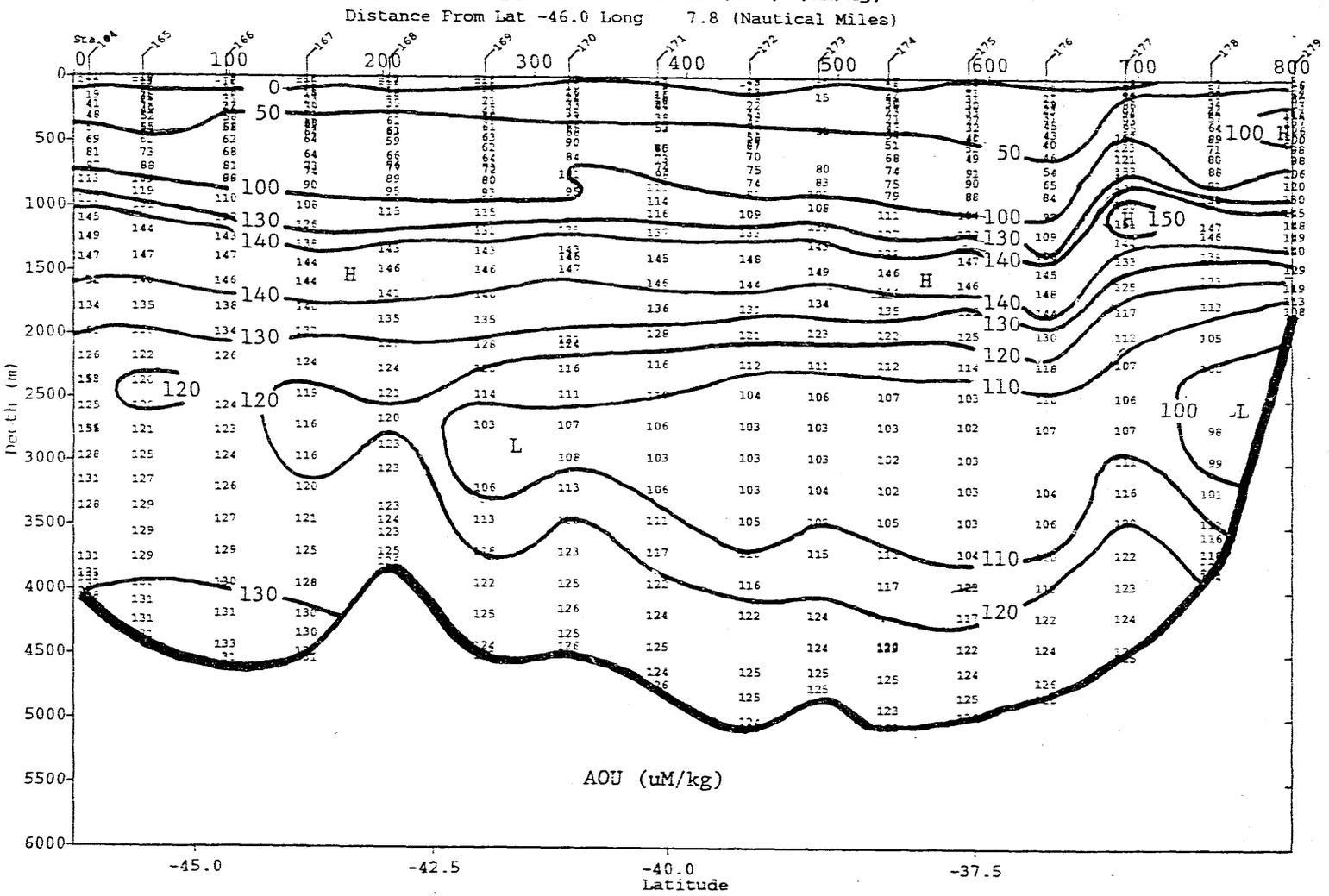

Fig. 59 - **Meteor 11/5 Cruise - Northern Part of Eastern N/S Section Sta 164-179**
Nitrate Concentration (NO3) (uM/kg)

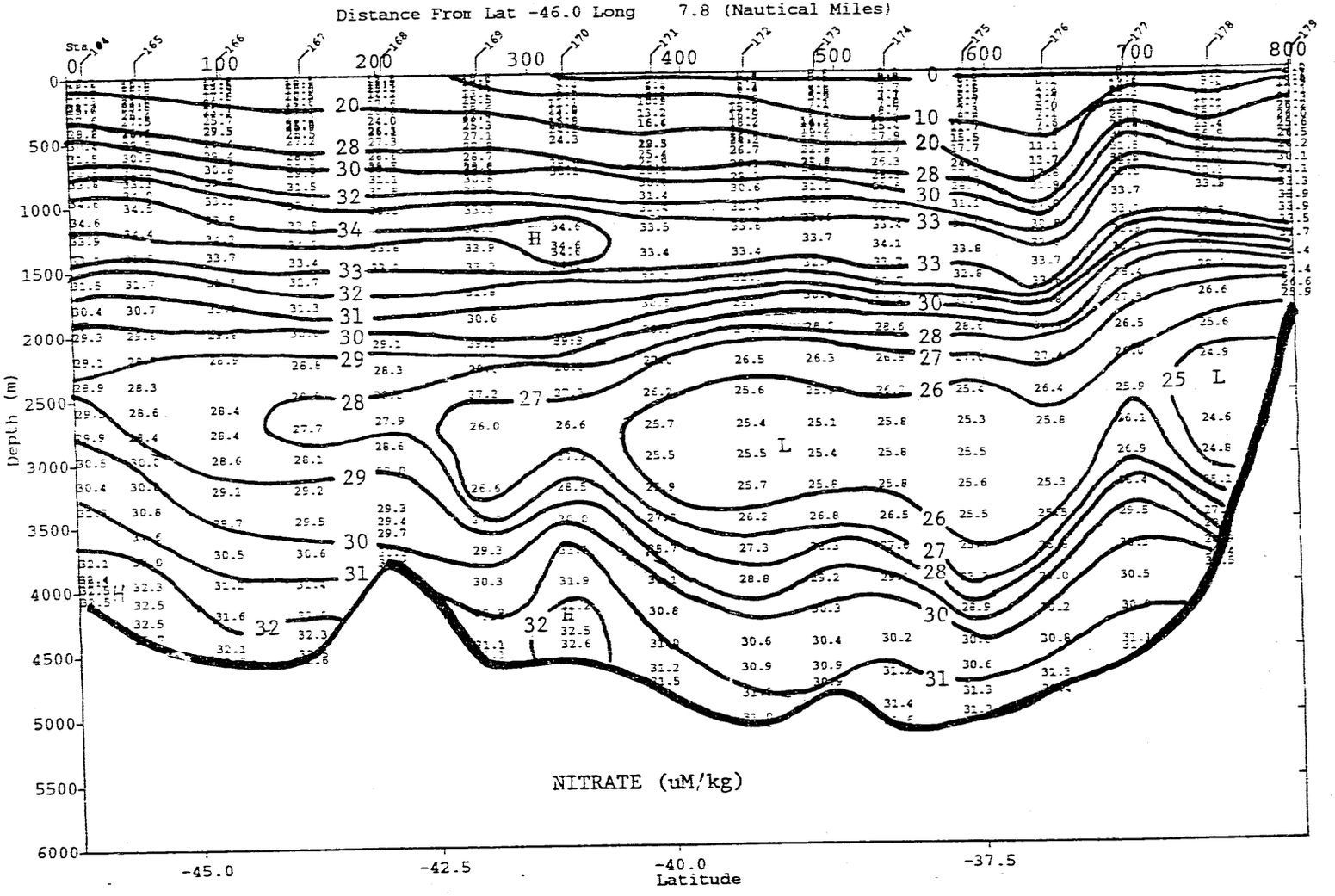

Fig. 60 - Meteor 11/5 Cruise - Northern Part of Eastern N/S Section Sta 164-179
Phosphate Concentration (PO4) (uM/kg)

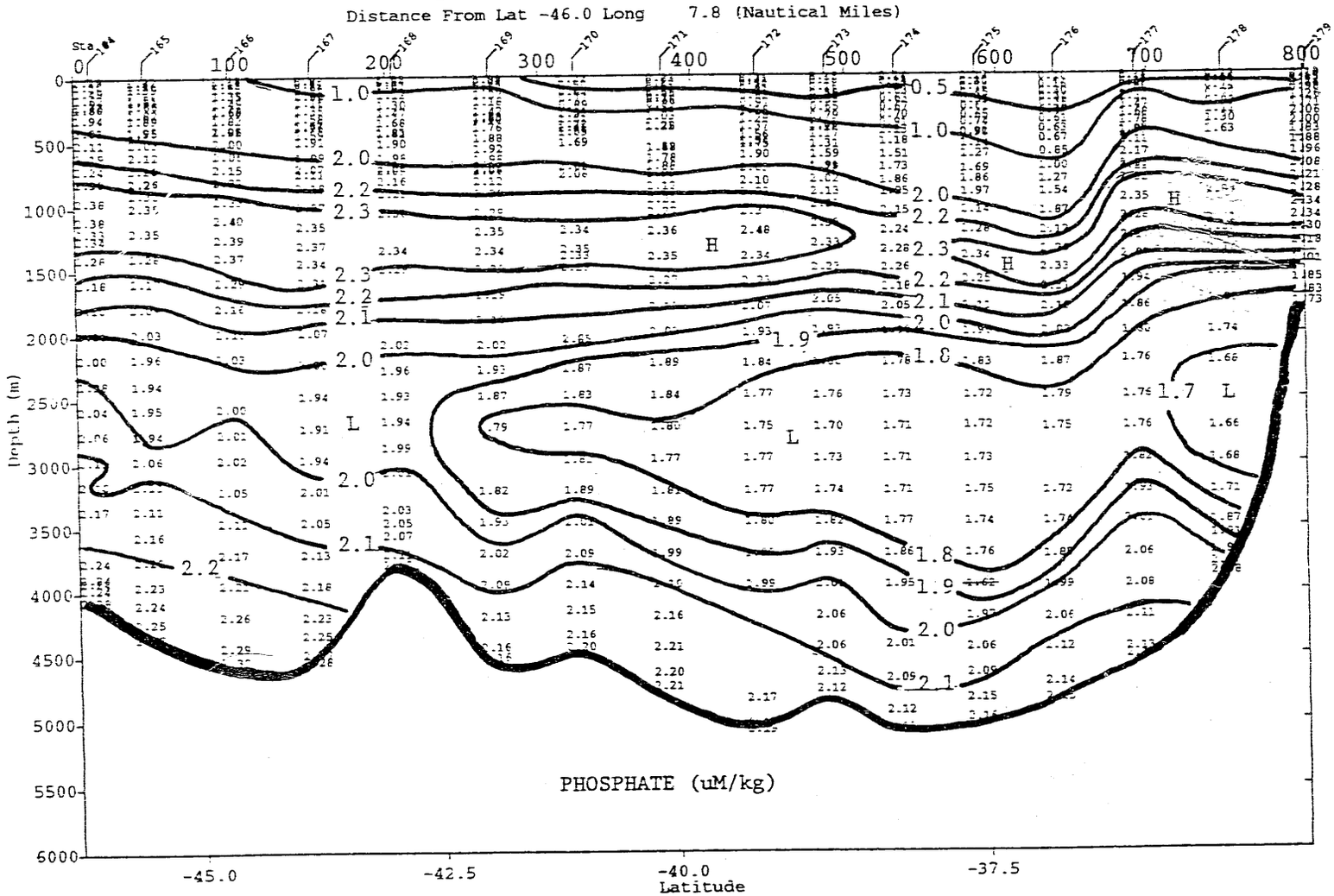

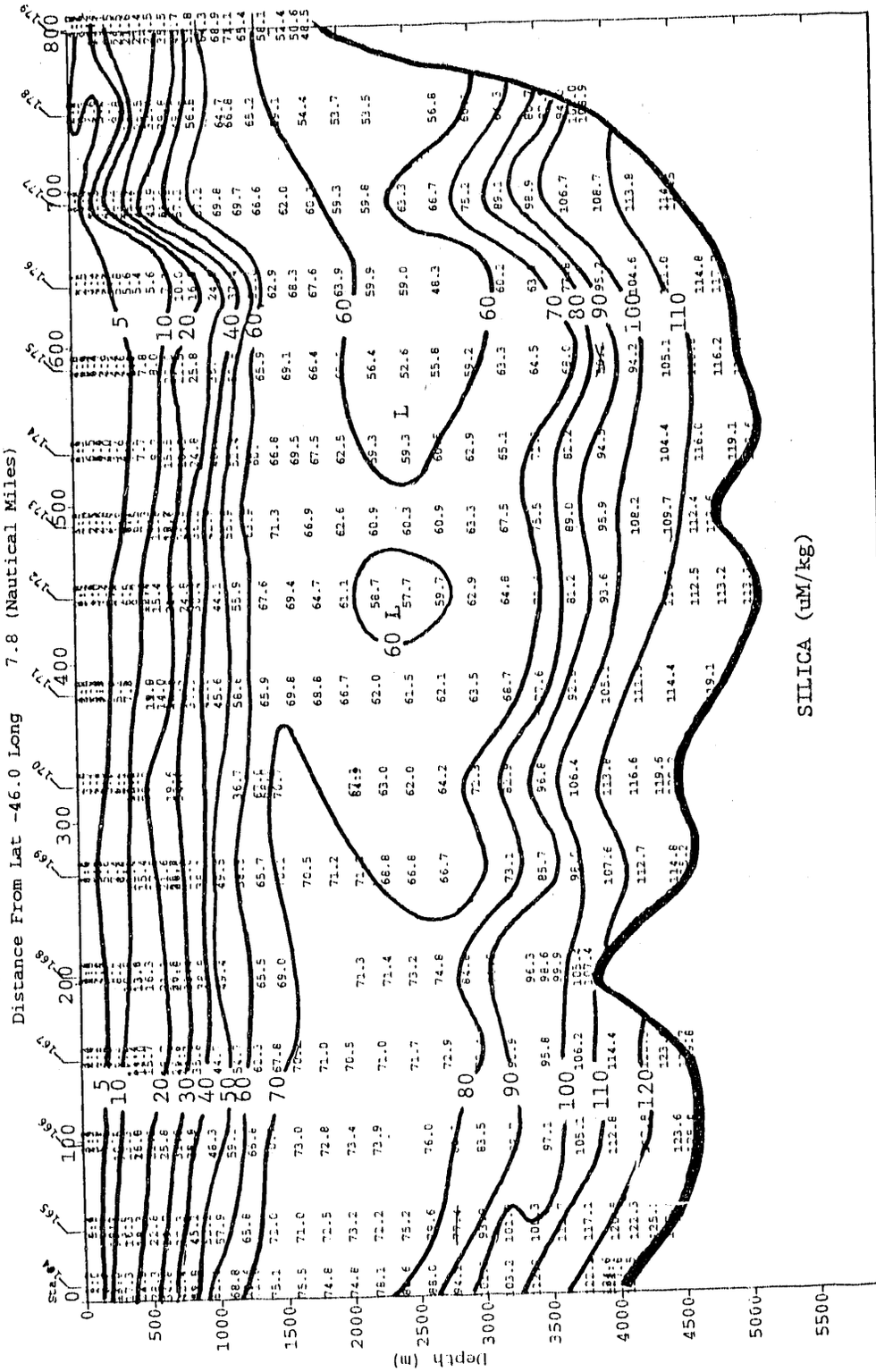

Fig. 61 - Meteor 11/5 Cruise - Northern Part of Eastern N/S Section Sta 164-179
Silicate Concentration (SiO3) (uM/kg)

VI. PROPERTY-PROPERTY RELATIONSHIPS

The oceanographic data obtained during this expedition have been analyzed using property-property relationships in order to show processes controlling various biologically mediated quantities as well as their relationships with water masses and other oceanographic features such as the polar front and meridional temperature distribution.

Fig. 62 shows the potential temperature-salinity relationships observed during this expedition and includes all the data, which have been presented in parts in Figs. 10, 20, 31, 42 and 53. Among surface waters, the South Atlantic subtropical water is warmest and most saline (23°C and 35.5 o/oo), whereas the least saline water (33.3 o/oo) was observed close to the South American coast in the Drake Passage. The winter Antarctic surface water as cold as -1.8°C has been identified as the near-surface sub-zero temperature minimum layer. This represents remnants of cold surface waters of the previous winter season. The densest water mass observed in this study is the Weddell Sea Bottom Water (WSBW), which is characterized by temperatures lower than about -0.75°C indicating contributions from cold ice-shelf waters (-1.9°C) of the southern Weddell Sea. The North Atlantic Deep Water (NADW) which originated in the high latitude North Atlantic is clearly depicted by the salinity maximum at temperatures in the vicinity of 2°C.

Fig. 63 shows the relationships between the partial pressure of CO_2 (at 20°C) and the total CO_2 concentration. Natural logarithm of these quantities are used, so that the slope of trends indicate the Revelle factor ($\gamma = (\partial \ln pCO_2 / \partial \ln TCO_2)$). The mean trend observed for surface waters (indicated by open circles) of the subtropical and subantarctic regions shows a typical value of 8 for the Revelle factor. It increases to 10 for the thermocline water and to 17 for the surface and deep waters of the Antarctic origin. The observed increase in the Revelle factor with depth suggests that the concentration of CO_2 increases with depth faster than the alkalinity. Increases in CO_2 may be attributed to the oxidation of organic debris and/or mixing with waters with greater CO_2 concentrations; and increases in alkalinity to the dissolution of $CaCO_3$ and/or mixing with waters with higher alkalinity values.

Fig. 64 shows the relationships between the total CO_2 concentration and potential temperature. The former is normalized to a salinity of 35.00 o/oo. A linear trend is observed for the surface waters (indicated by open circles) of the subtropical, subantarctic and antarctic regions: $(TCO_2)_{s=35}$ (uM/kg) = -11.5 T (°C) + 2227. Although the data points scatter more widely around this mean line in the Antarctic waters (south of the Polar Front Zone), the mean deviation for the waters warmer than about 3°C is about 10 uM/kg. The highest total CO_2 concentrations observed during this expedition are associated with the

Fig. 62 - Potential temperature-salinity relationships observed during the F/S Meteor 11/5 Expedition in the South Atlantic Ocean and northern Weddell Sea, January-March, 1990. NADW = North Atlantic Deep Water; AABW = Antarctic Bottom Water; WSBW = Weddell Sea Bottom Water.

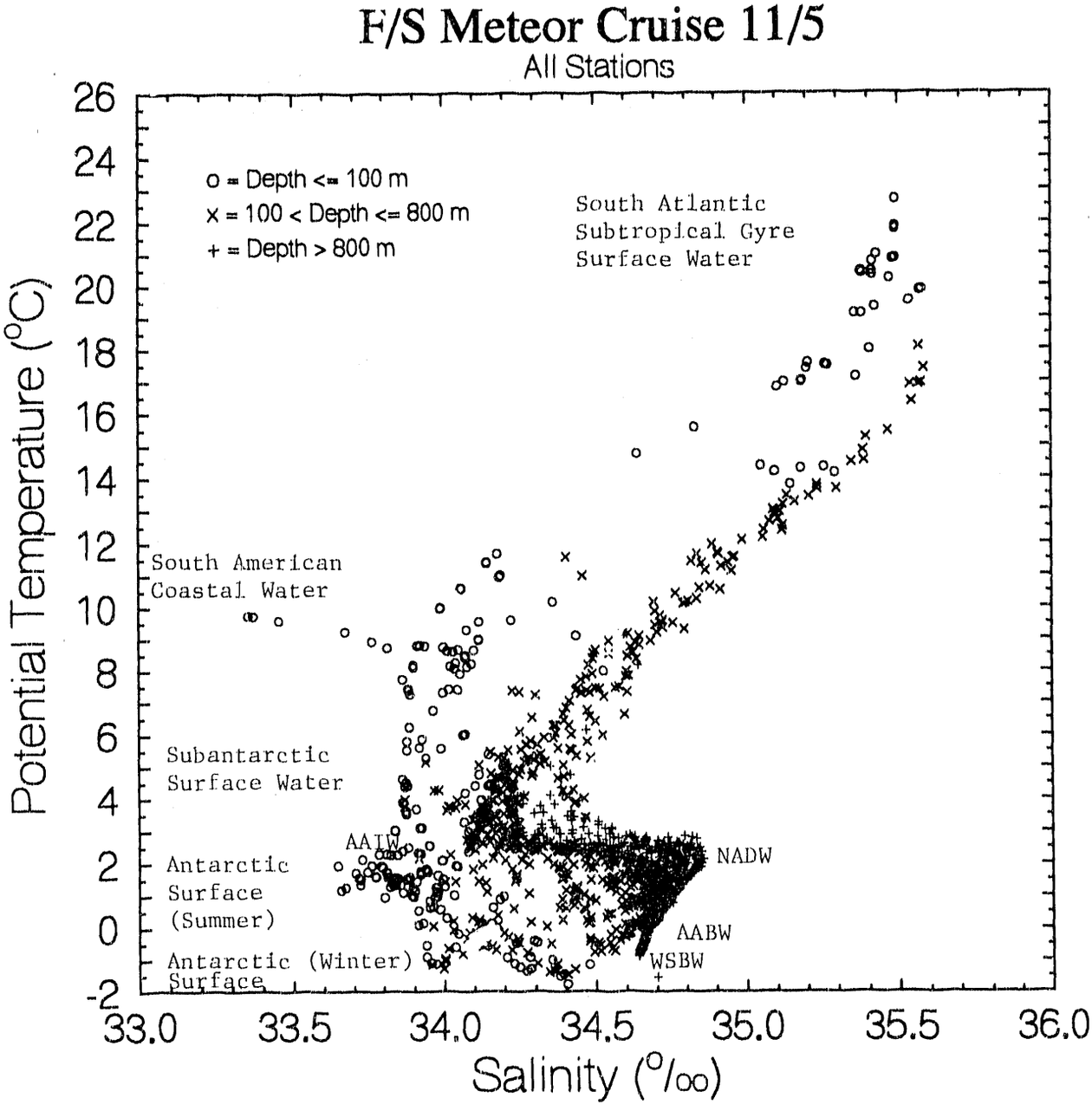

Fig. 63 - Relationshipbs between pCO_2 at 20°C and the total CO_2 concentration (normalized to a salinity of 35.00 o/oo) observed during the F/S Meteor Expedition in the South Atlantic and northern Weddell Sea. Natural logarithm of the quantities is plotted, so that the slopes of the regression lines indicate the Revelle factor.

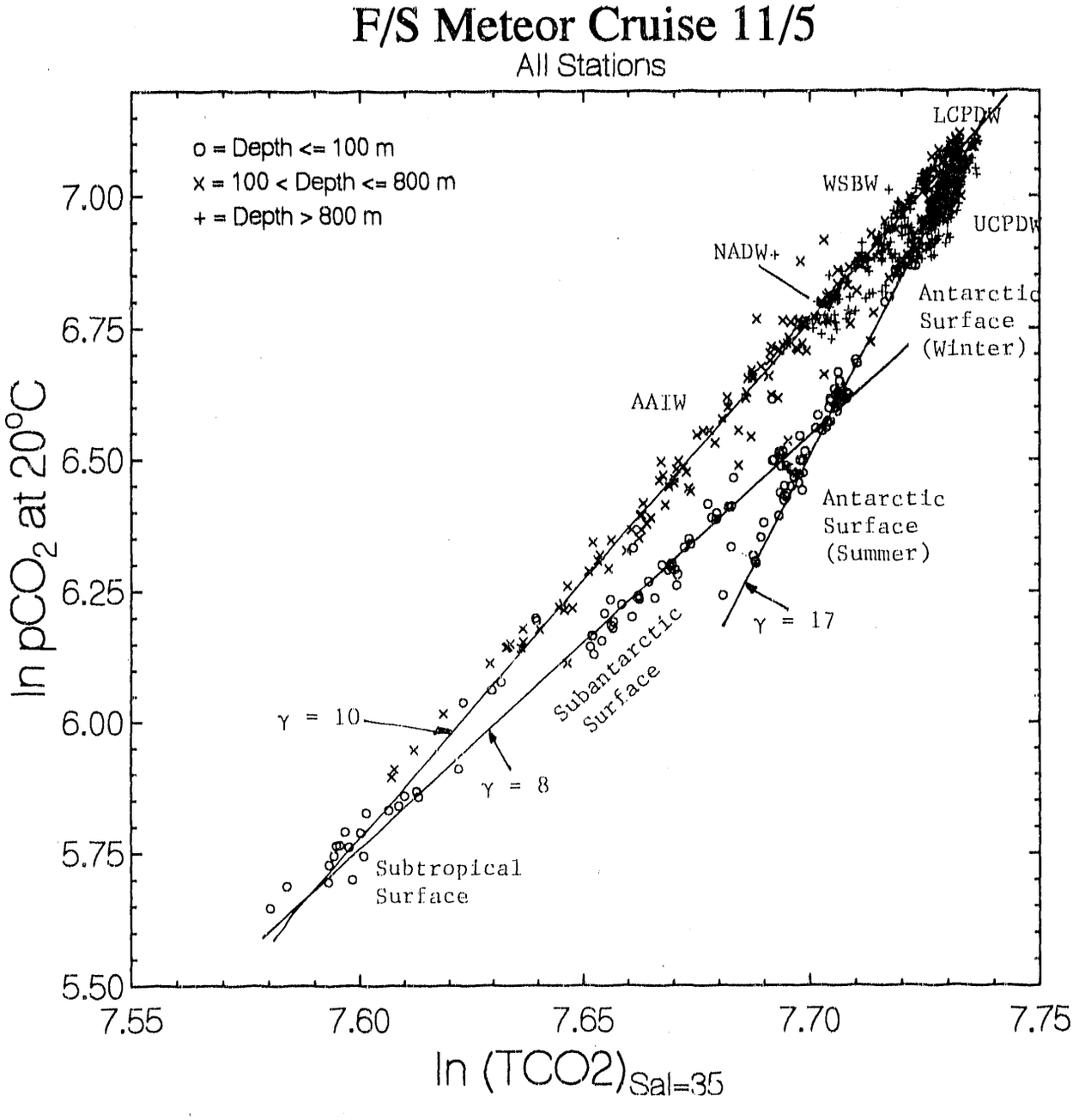

Fig. 64 - Total CO_2-potential temperature relationships observed during the F/S Meteor Expedition, Jan.-March, 1990, in the South Atlantic Ocean and northern Weddell Sea. LCPDW and UCPDW = Lower and Upper Circumpolar Deep Water; SPLOW = Southeast Pacific Low Oxygen Water; WSBW = Weddell Sea Bottom Water; NADW = North Atlantic Deep Water; AASW (Winter) and AASW (Summer) = Winter and Summer Antarctic Surface Waters.

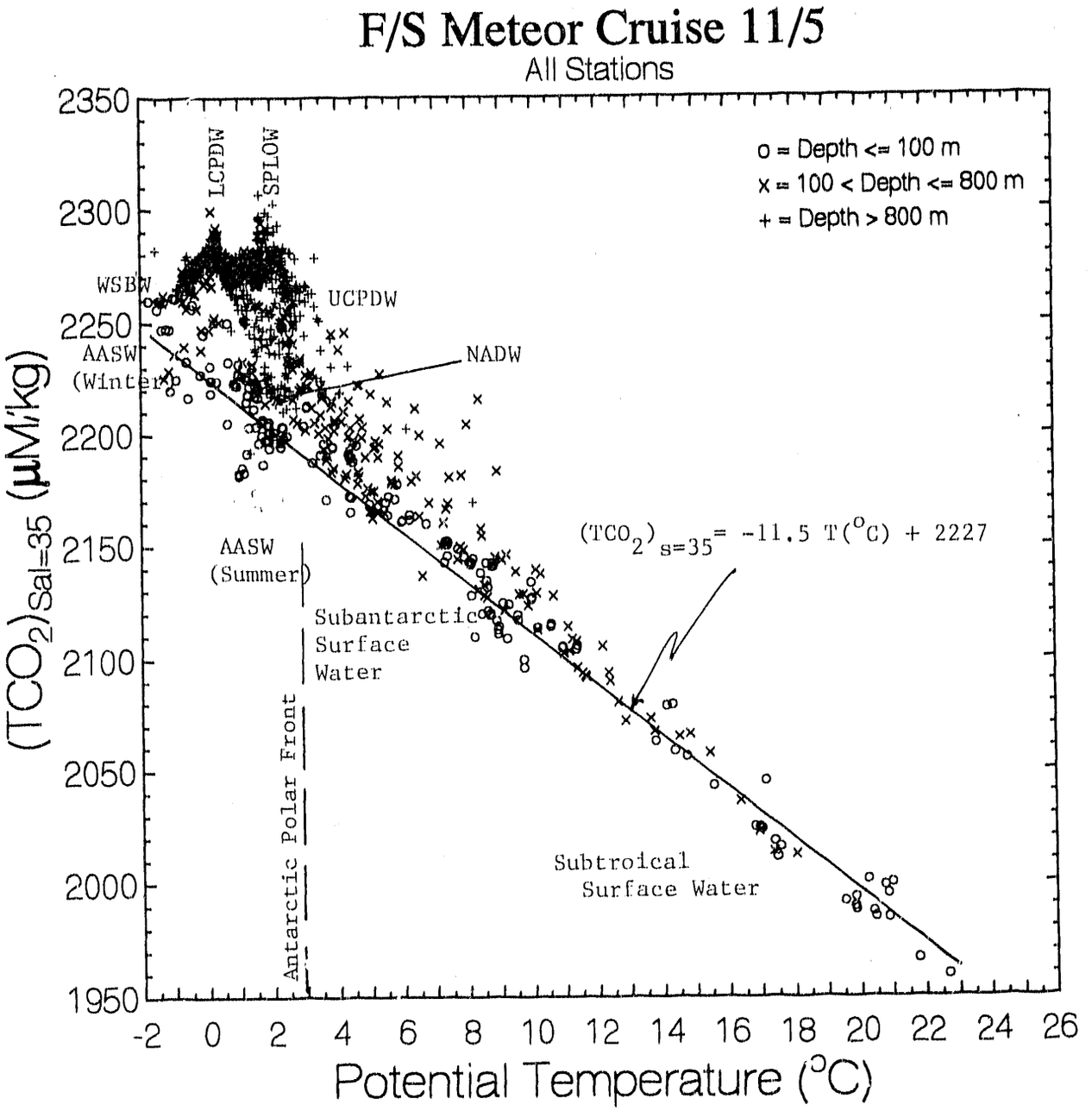

Lower Circumpolar Deep Water (LCPDW) and Southeast Pacific Low Oxygen Water. The former is found in the Northern Weddell Sea and South Atlantic (Table 3) and the latter is found in the Drake Passage (Table 1).

Fig. 65 shows the relationships between the concentrations of oxygen and total CO_2 dissolved in seawater. Warmer surface waters have lower oxygen and CO_2 concentrations, whereas colder surface waters have greater oxygen and CO_2 concentrations. This may be attributed mainly to the effect of temperature on gas solubilities. The Antarctic winter surface water, which is represented by the sub-zero temperature minimum layer near the surface, tends to have the oxygen and CO_2 values closer to the deep water values. This may be due either to the oxidation of organic debris occurred since the previous winter, or to the mixing with deep water caused by deep winter convection.

The Southeast Pacific Low Oxygen Water (SPLOW, Table 1), which was presumably originated in the high productivity areas along the Chilean coast, has the highest total CO_2 and lowest oxygen values. Among the Antarctic waters, the Weddell Sea Bottom Water (WSBW) has the highest oxygen concentration indicating contributions of young waters from ice-shelf.

Fig. 66 shows the relationships between the concentration of nitrate and total CO2 in seawater. The subtropical and subantarctic surface waters exhibit two separate trends due mainly to large salinity differences. These two trends, however, collapse into one when the total CO_2 concentrations normalized to 35.00 o/oo salinity are used. Such a relationship is illustrated in Fig. 67 with the phosphate-total CO_2 data.

The Upper Circumpolar Deep Water (UCPDW) has the highest nitrate concentration, and the Southeast Pacific Low Oxygen Water (SPLOW) has the highest total CO_2 concentration observed during this study. The North Atlantic Deep Water (NADW) shows as a nitrate minimum in the vicinity of 2220 uM/kg in the total CO_2 concentration.

Fig. 67 shows the relationships between the phosphate concentration and the total CO_2 concentration normalized to a salinity of 35.00 o/oo. The surface water values exhibit three trends: the subtropical trend for temperatures warmer than about 12°C has a $\Delta CO2/\Delta P$ ratio of 150, the subantarctic water has the ratio of 93 and the Antarctic (mostly summer surface waters in the Weddell Sea) the ratio of 63. The $\Delta CO_2/\Delta P$ ratio is influenced by the lateral and vertical water mixing, biological assemblage and air-sea CO_2 flux. However, presently the regional differences observed in the ratio can not be quantitatively accounted for.

Fig. 65 - Relationships between the concentrations of oxygen and total CO_2 observed during the F/S Meteor Expedition, Jan.-March, 1990, in the South Atlantic Ocean and northern Weddell Sea. WSBW = Weddell Sea Bottom Water; AABW = Antarctic Bottom Water; WSDW = Weddell Sea Deep Water; LCPDW and UCPDW = Lower and Upper Circumpolar Deep Water; SPLOW = Southeast Pacific Low Oxygen Water; NADW = North Atlantic Deep Water; AAIW = Antarctic Intermedimate Water.

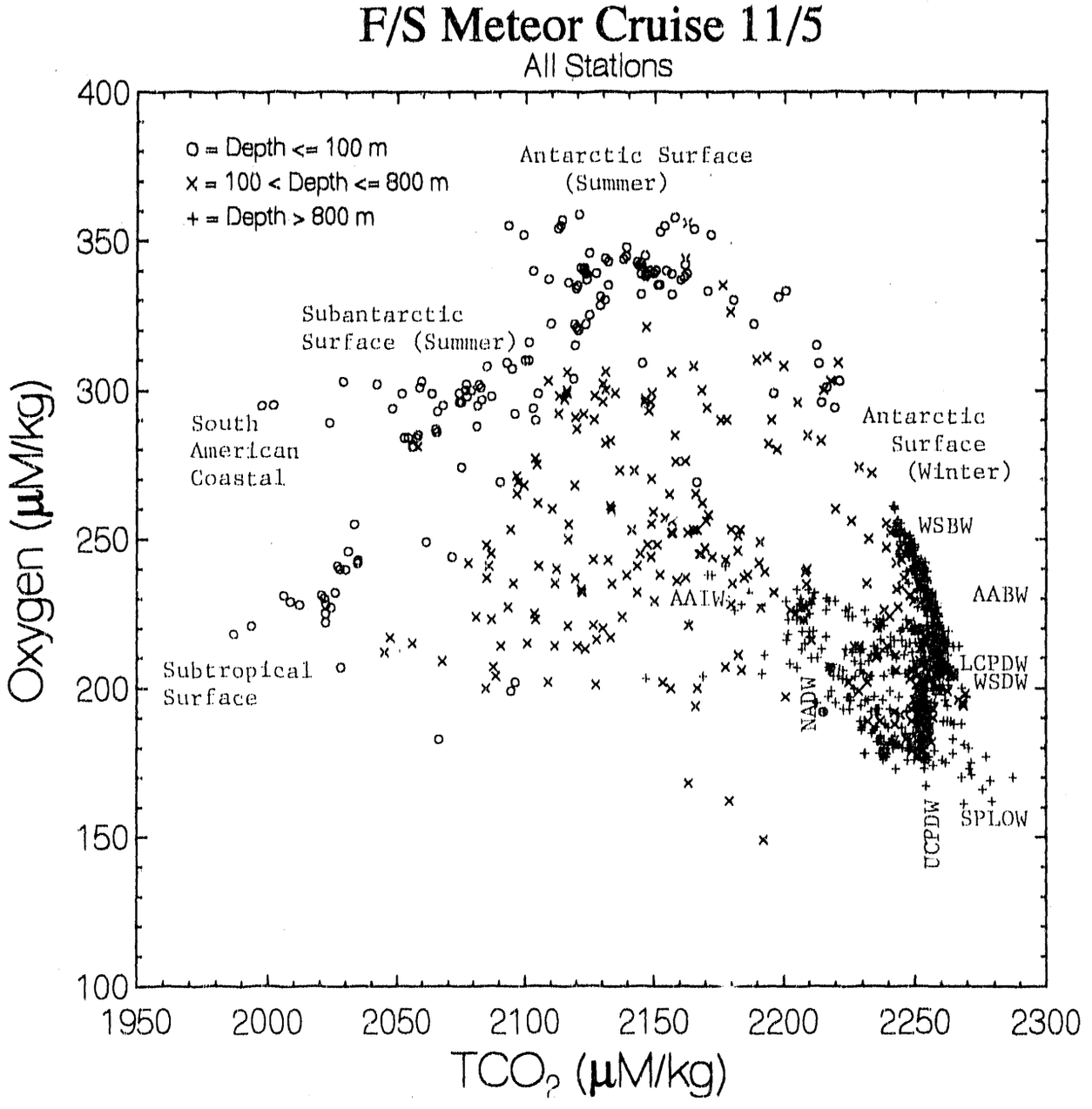

Fig. 66 - Relationships between the concentrations of nitrate and total CO_2 observed during the F/S Meteor Expedition, Jan.-March, 1990, in the South Atlantic Ocean and northern Weddell Sea. UCPDW and LCPDW = Upper and Lower Circumpolar Deep Water; SPLOW = Southeast Pacific Low Oxygen Water; AABW = Antarctic Bottom Water; WSBW = Weddell Sea Bottom Water; NADW = North Atlantic Deep Water; AAIW = Antarctic Intermediate Water.

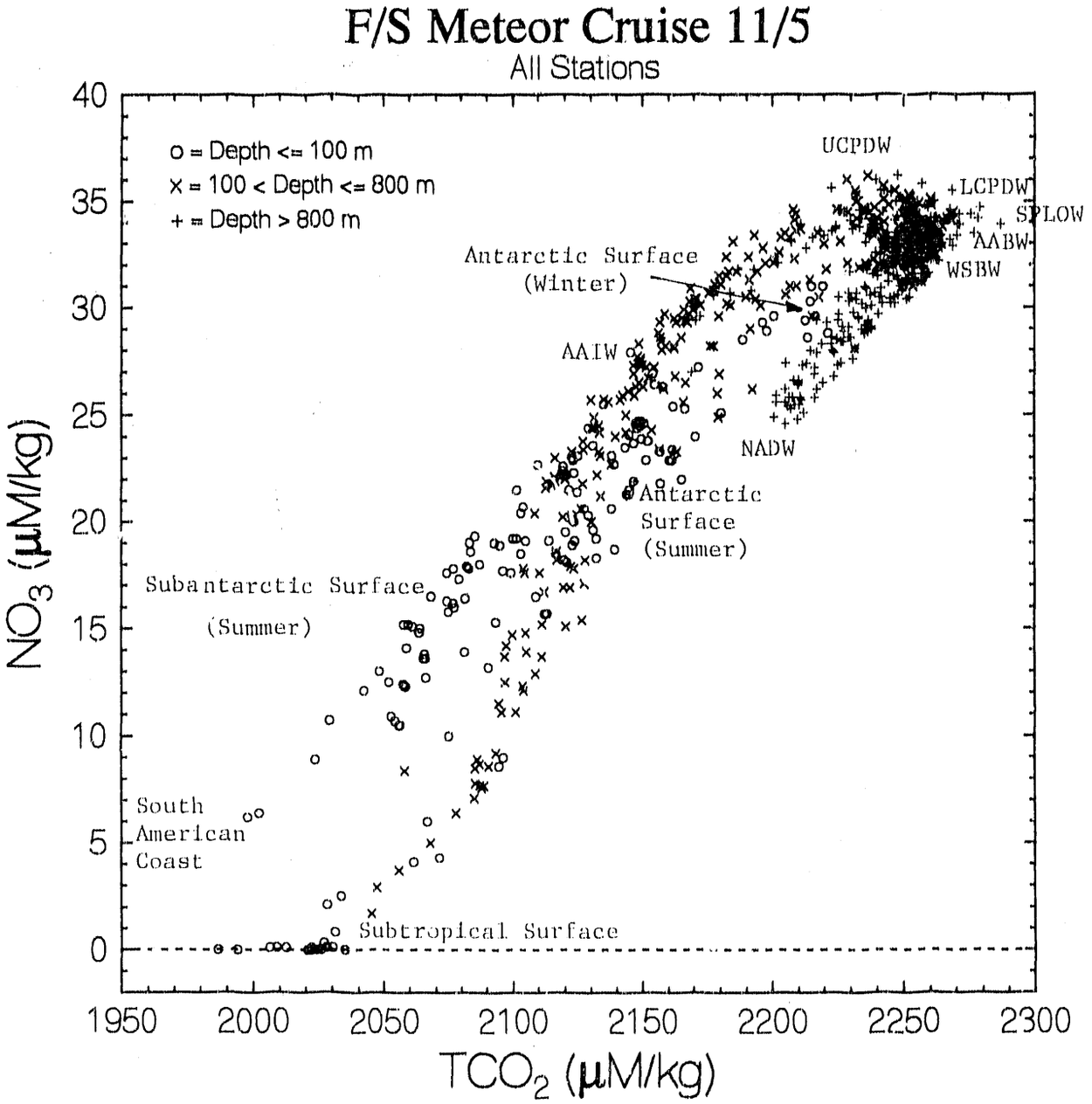

Fig. 67 - Relationships between the concentrations of phosphate and total CO_2 normalized to a salinity of 35.00 o/oo, observed during the F/S Meteor Expedition, Jan.-March, 1990, in the South Atlantic Ocean and northern Weddell Sea. UCPDW and LCPDW = Upper and Lower Circumpolar Deep Water; SPLOW = Southeast Pacific Low Oxygen Water; WSBW = Weddell Sea Bottom Water; AABW = Antarctic Bottom Water; AAIW = Antarctic Intermediate Water; NADW = North Atlantic Deep Water.

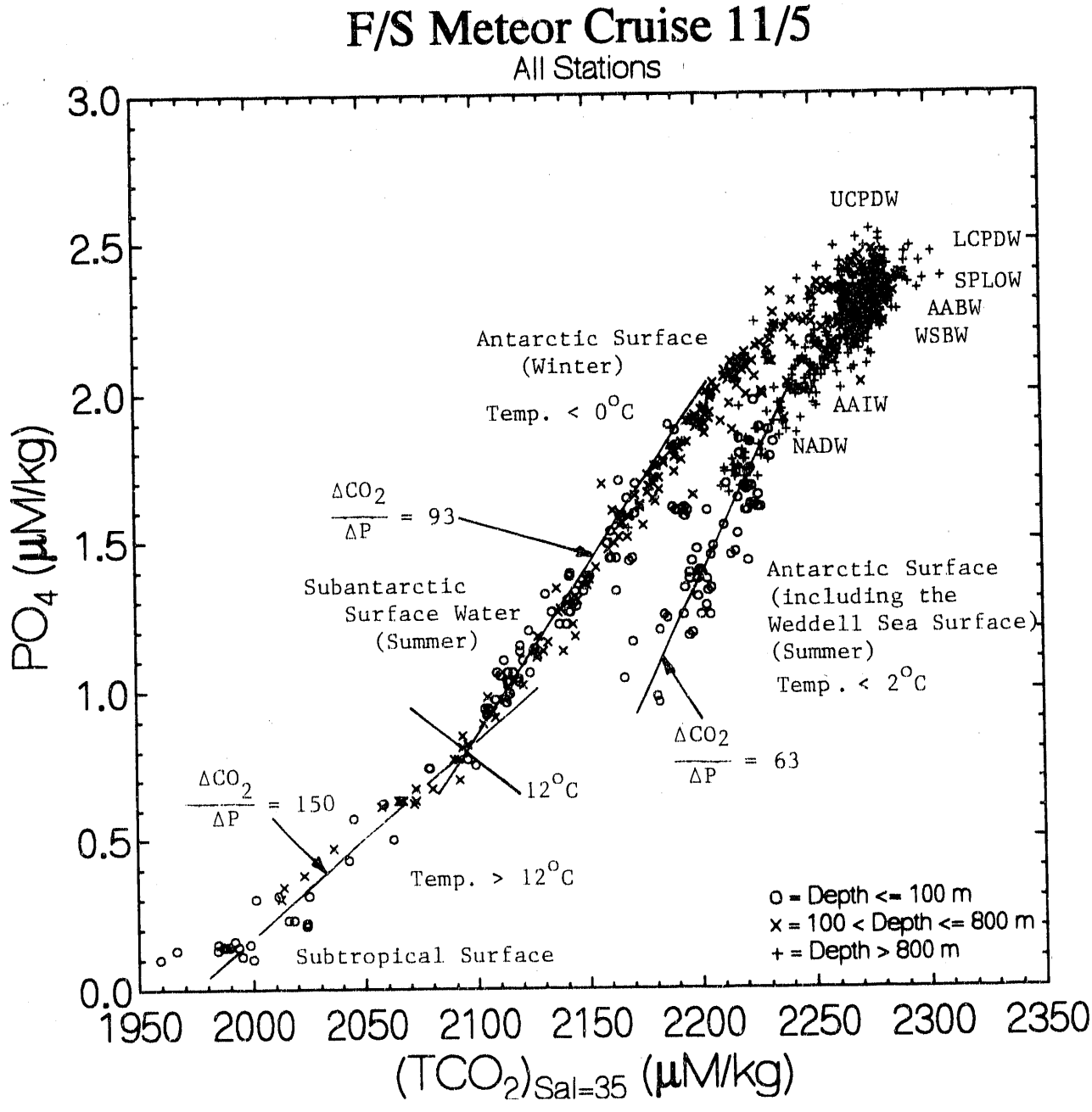

Fig. 68 shows the relationships between the natural logarithm of pCO_2 at 20°C and the concentration of phosphate. The data for surface waters in the antarctic (winter and summer), subantarctic and subtropical regions exhibits a linear trend: ln (pCO_2 at 20°C) = 0.52 (PO_4) + 5.70. As shown in Fig. 67, there are three distinctly different trends observed for the total CO_2-phosphate concentrations in surface water. In addition, a linear relationship is observed for the logarithmic plot for pCO_2 and total CO_2 concentration (Fig. 63) in surface waters. Therefore, in order to have a linear trend for ln pCO_2 and phosphate, the alkalinity of surface water must change regionally in such a way to offset changes in the total CO_2-phosphate trends.

Fig. 69 shows the relationships between the potential alkalinity and total CO_2 concentration. Both of these quantities are normalized to a salinity of 35.00 o/oo. The potential alkalinity is defined as [(Total Alkalinity) + (Nitrate)] (Brewer and Goldman, 1976). It is changed by dissolution and precipitation of $CaCO_3$, but remains constant for the photosynthetic utilization of CO_2 and nutrient salts or the oxidation of biological debris. The surface water data (see open circles) exhibits a linear trend with a slope of 0.423. The observed trend may be interpreted as floows; the surface water formed by the winter upwelling of deep waters loses CO_2 and potential alkalinity by photosynthesis and biogenic production of $CaCO_3$ shells as it is transported northward and incorporated eventually into the subtropical gyre water. If the air-sea CO_2 flux is neglected (normally less than 10% of the biological CO_2 utilization), the slope of the surface water trend gives a (organic carbon fixation)/($CaCO_3$ production) ratio of about 4 or 80% of carbon removal by organic carbon formation and 20% by calcareous shell production.

The highest potential alkalinity values were observed in the near bottom water in the Cape Basin, north of the Atlantic-Indian Ridge. The Cape Basin Bottom Water (CBBW) has a potential temperature and salinity of about 0.6°C and 34.73 o/oo, and hence is warmer and more saline than the Antarctic Bottom Water (AABW) and the Weddell Sea Bottom Water (WSBW). However, it contains as much oxygen as the AABW, but distinctly less silica. Its total CO_2, pCO_2, oxygen, nitrate, phosphate and silica concentrations are similar to those for the WSBW. Accordingly, it appears to represent a portion of WSBW, which entered into the Cape Basin through a fracture across the Atlantic-Indian Ridge system and received additional alkalinity by the dissolution of $CaCO_3$ sediments on the Cape Basin floor. Since the GEOSECS alkalinity data for the Indian Ocean do not show the presence of high alkalinity abyssal waters, the high alkalinity values in the CBBW do not appear to be derived from the Indian Ocean.

Fig. 70 shows the relationships between the concentrations of nitrate and phosphate. A linear regression of the entire data set yields a mean slope of 15.47 (±0.04) with a root mean square deviation of ±0.9 uM/kg NO_3. This slope is consistent with the Redfield N/P ratio of 16.

Fig. 68 - Relationships between pCO_2 at 20°C and the concentration of phosphate observed during the F/S Meteor Expedition, Jan.-March, 1990, in the South Atlantic Ocean and the northern Weddell Sea. UCPDW and LCPDW = Upper and Lower Circumpolar Deep Water; AABW = Antarctic Bottom Water; WSBW = Weddell Sea Bottom Water; NADW = North Atlantic Deep Water; AAIW = Antarctic Intermediate Water.

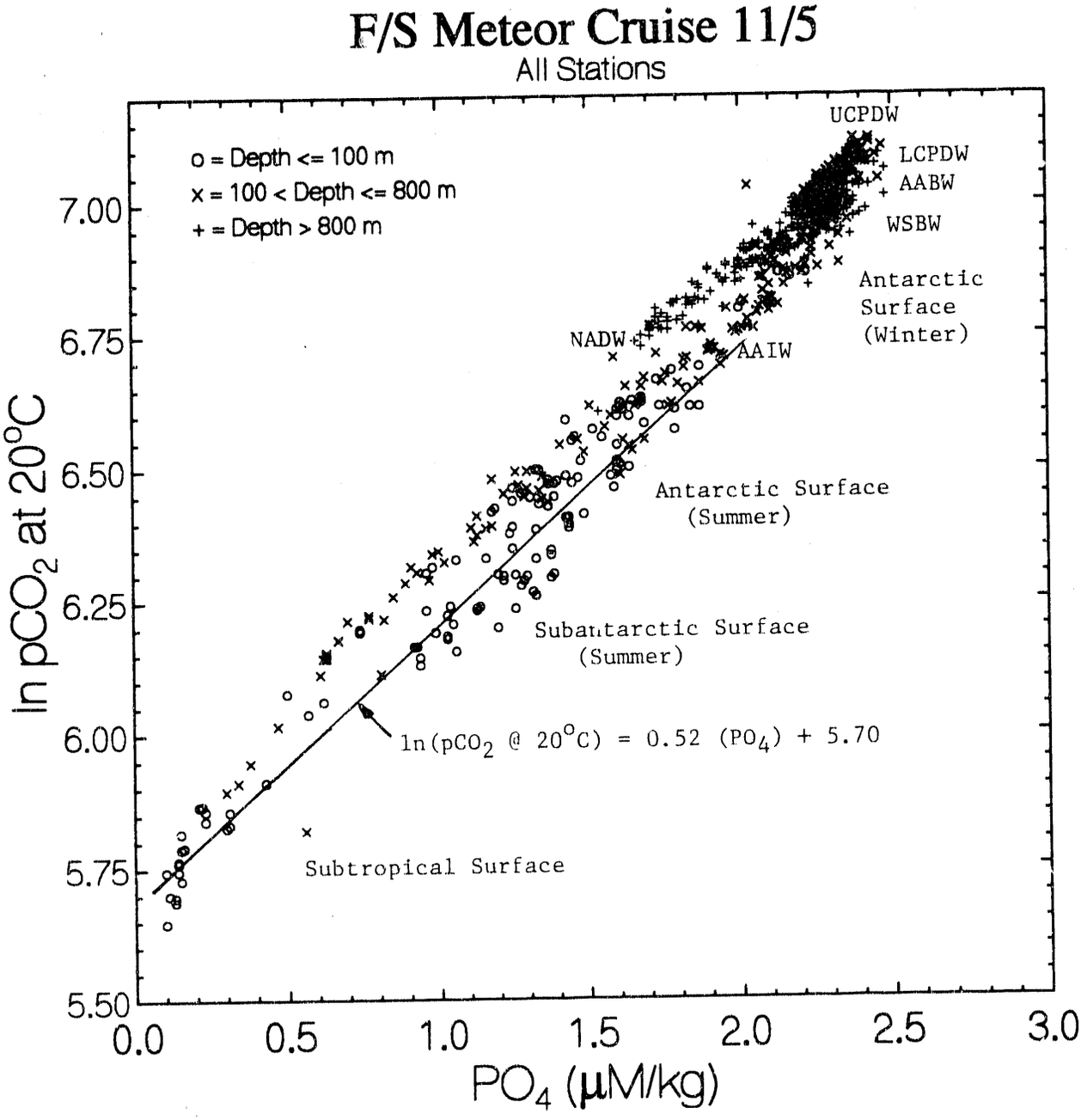

Fig. 09 - Relationships between the potential alkalinity and the total CO_2 concentration observed in the South Altantic Ocean and the northern Weddell Sea. Both quantities are normalized to a salinity of 35.00 o/oo. CBBW = Cabe Basin Bottom Water; LCPDW and UCPDW = Lower and Upper Circumpolar Deep Water; WSDW = Weddell Sea Deep Water; WSBW = Weddell Sea Bottom Water; NADW = North Atlantic Deep Water;

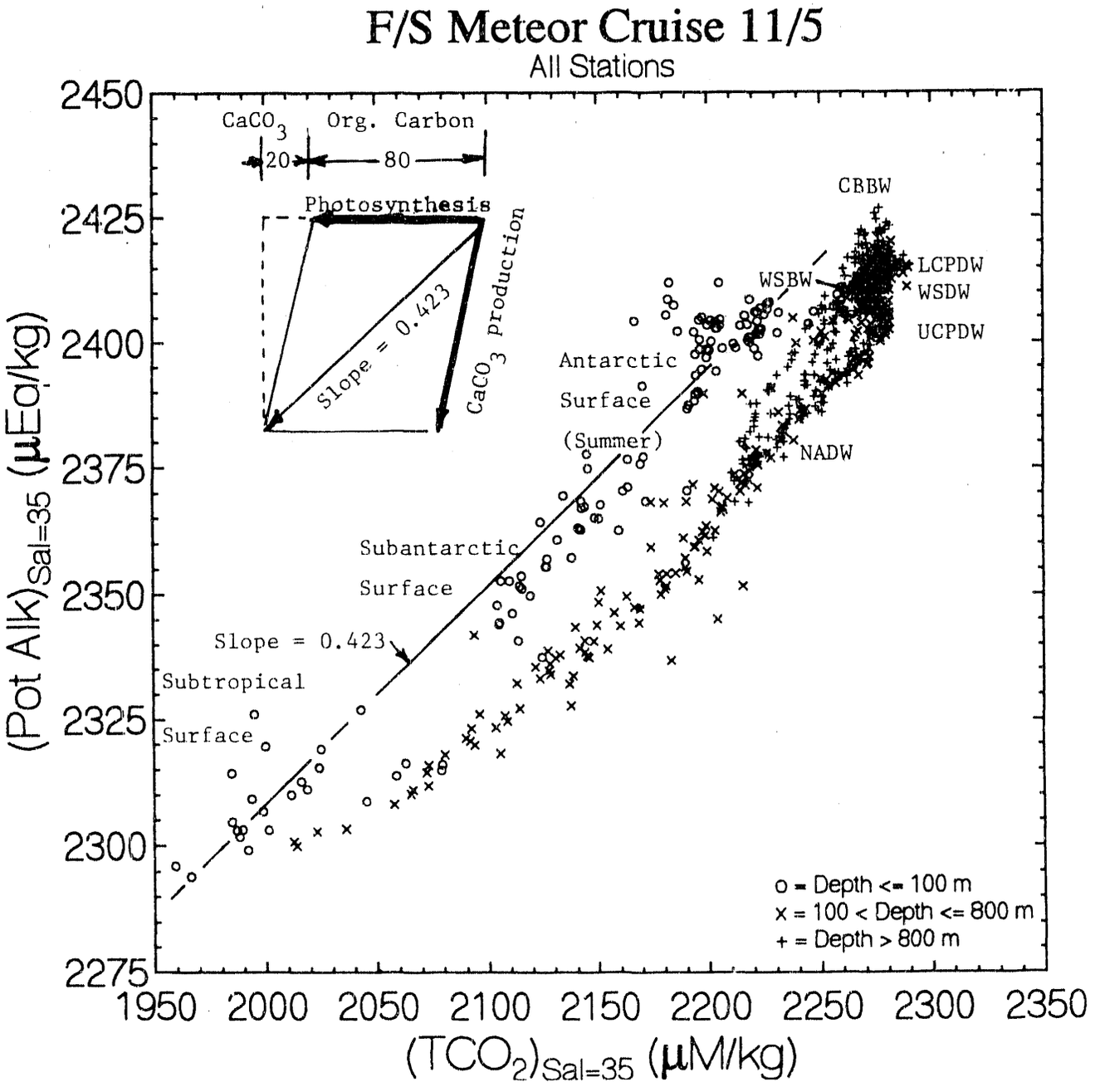

Fig. 70 - Relationships between the concentrations of nitrate and phosphate in seawater observed during the F/S Meteor Expedition, Jan.-March, 1990, in the South Atlantic Ocean and northern Weddell Sea. A linear least-squares fit to the data yields a mean Redfield N/P ratio of 15.5.

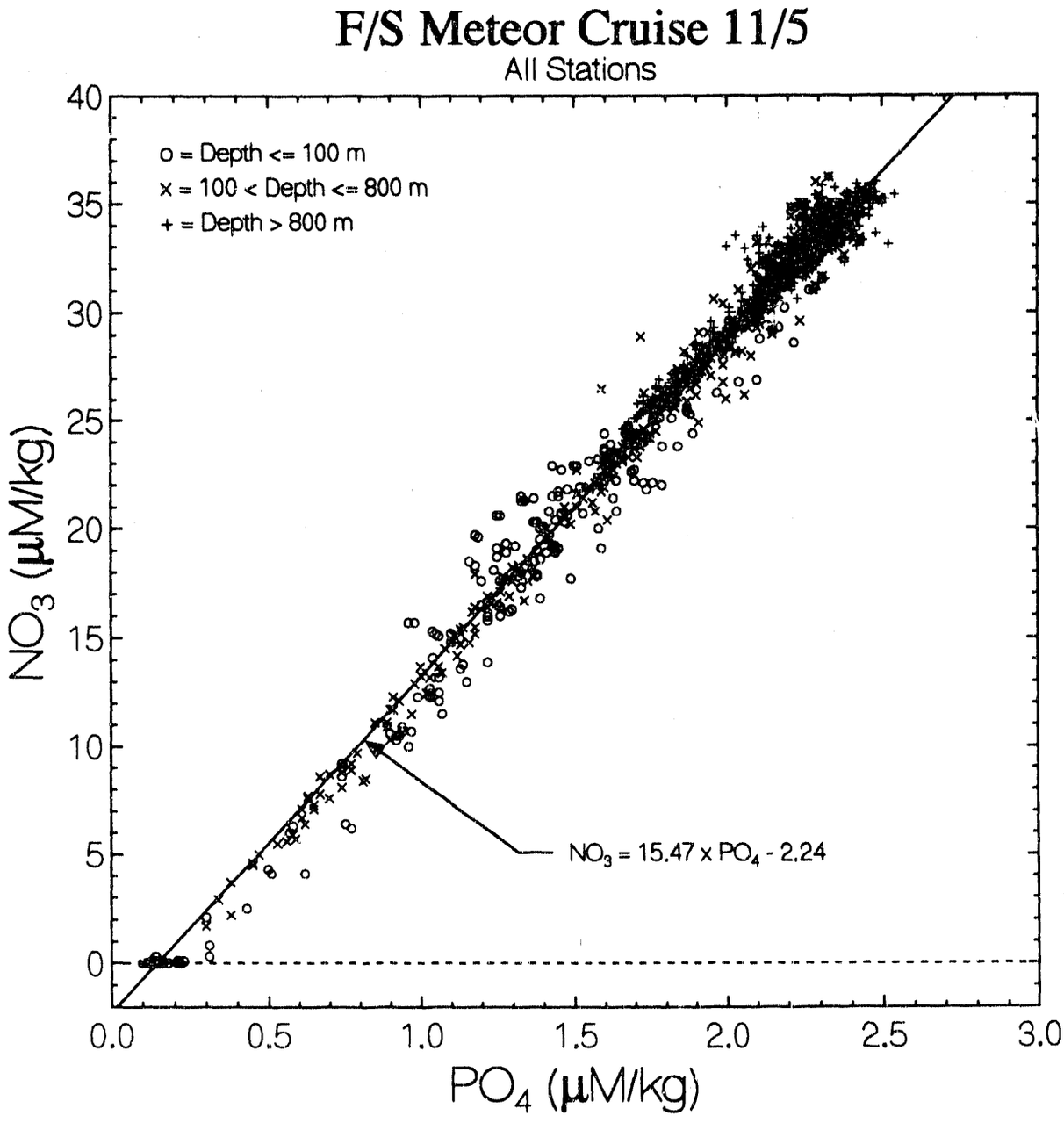

Figs. 71 and 72 show respectively the changes in the nitrate and phosphate concentrations with potential temperature. The surface water values (open circles) for the both quantities appear to decline linearly northward in the subantarctic regime (between the Antarctic polar front and the northern edge of the subtropical convergence) to near-zero values in waters warmer than about 18°C. On the other hand, in the areas south of the Antarctic front (less than 2°C), another trend is observed indicating a different biological regime in the Weddell and Antarctic waters.

The Upper Circumpolar Deep Water (UCPDW) has the highest nitrate and phosphate values observed during the expedition. The North Atlantic Deep Water (NADW) is clearly depicted by a minimum in nitrate and phosphate in the vicinity of 2°C.

Fig. 73 shows the relationships between the silica concentration and potential temperature. Unlike the concentrations of nitrate and phosphate shown in Figs. 71 and 72, the silica concentration in surface water is reduced to near-zero values north of the Antarctic polar front and remains low through the subantarctic and subtropical regions.

The highest silica concentrations are found in the Southeast Pacific Bottom Water (SPBW), which is present in the Drake Passage section. The Weddell Sea Deep Water (WSDW) has the second highest silica concentration exhibiting a maximum at about -0.5°C whereas the Weddell Sea Bottom Water (WSBW) is shown with a sharp silica minimum in the vicinity of -1.0°C.

Fig. 74 shows the relationships between the silica concentration and salinity. In this plot, the relationships between various deep water masses are well resolved. The Southeast Pacific Bottom Water (SPBW) and the Weddell Sea Deep Water (WSDW) are depicted by two high peaks up to 143 uM/kg and 136 uM/kg respectively. In contrast, the North Atlantic Deep Water (NADW) exhibits a sharp minimum at a salinity of about 38.0 o/oo. The Upper and Lower Circumpolar Deep Water (UCPDW and LCPDW), between which the NADW has been shown to intrude (see Figs. 41 through 48), are depicted as a kink point.

Fig. 75 shows the relationships between the nitrate and silica concentrations. The surface water data (open circles) indicate that the silica concentration is reduced to near-zero values while the waters still contain 15 to 20 uM/kg nitrate.

The Upper Circumpolar Deep Water (UCPDW) and Southeast Pacific Low Oxygen Water (SPLOW) exhibit the highest nitrate values, while the Southeast Pacific Deep and Bottom Waters (SPDW and SPBW) show the highest silica values.

Fig. 71 - Relationships between the nitrate concentration and potential temperature observed during the F/S Meteor Expedition, Jan.-March, 1990, in the South Atlantic Ocean and northern Weddell Sea. UCPDW and LCPDW = Upper and Lower Circumpolar Deep Water; WSDW = Weddell Sea Deep Water; AABW = Antarctic Bottom Water; WSBW = Weddell Sea Bottom Water; NADW = North Atlantic Deep Water; AASW = Antarctic Surface Water.

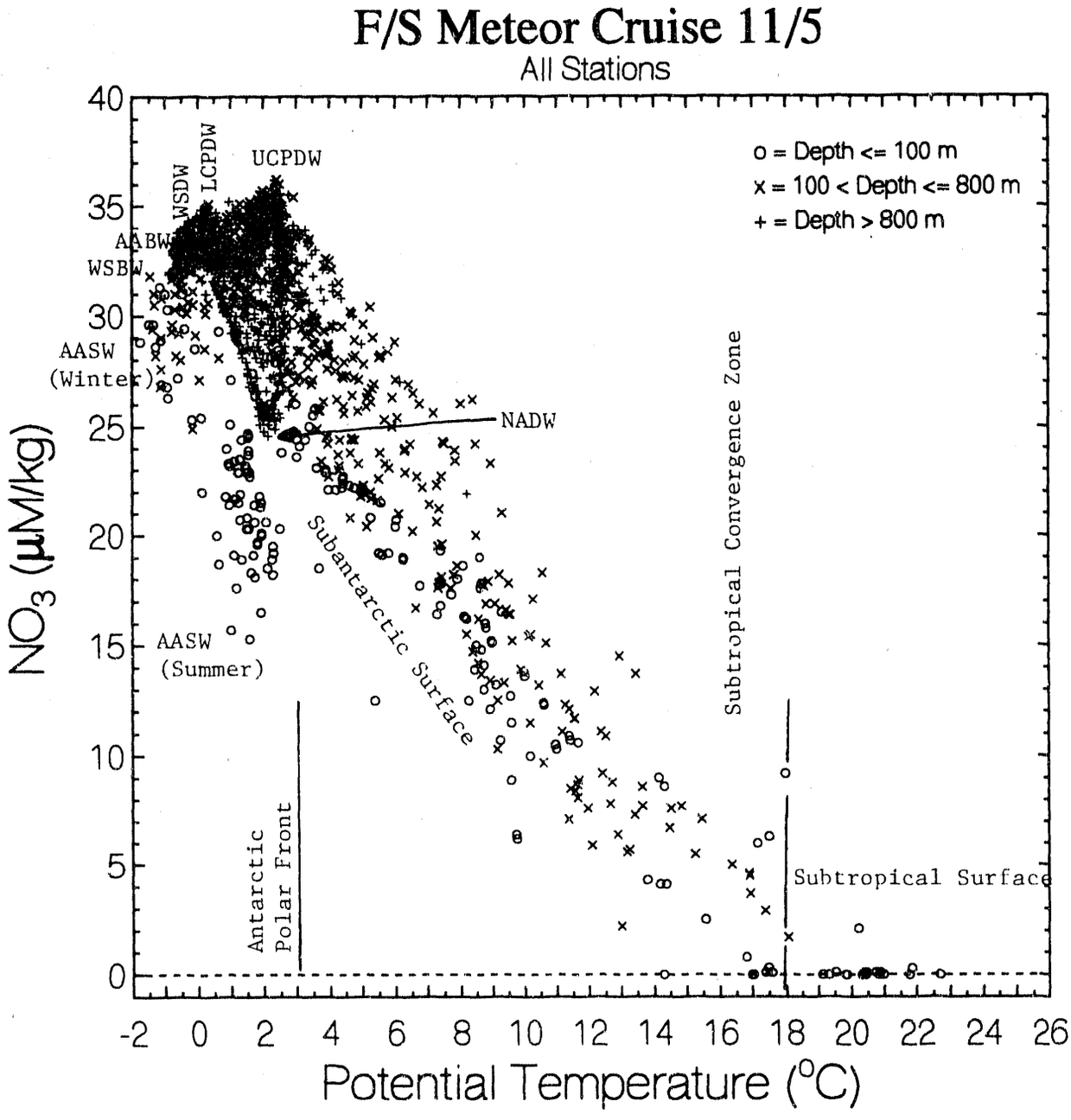

Fig. 72 - Relationships between the phosphate concentration and potential temperature observed during the F/S Meteor Expedition, Jan.-March, 1990, in the South Atlantic Ocean and northern Weddell Sea. UCPDW and LCPDW = Upper and Lower Circumpolar Deep Water; AABW = Antarctic Bottom Water; WSBW = Weddell Sea Bottom Water; NADW = North Atlantic Deep Water; AASW = Antarctic Surface Water.

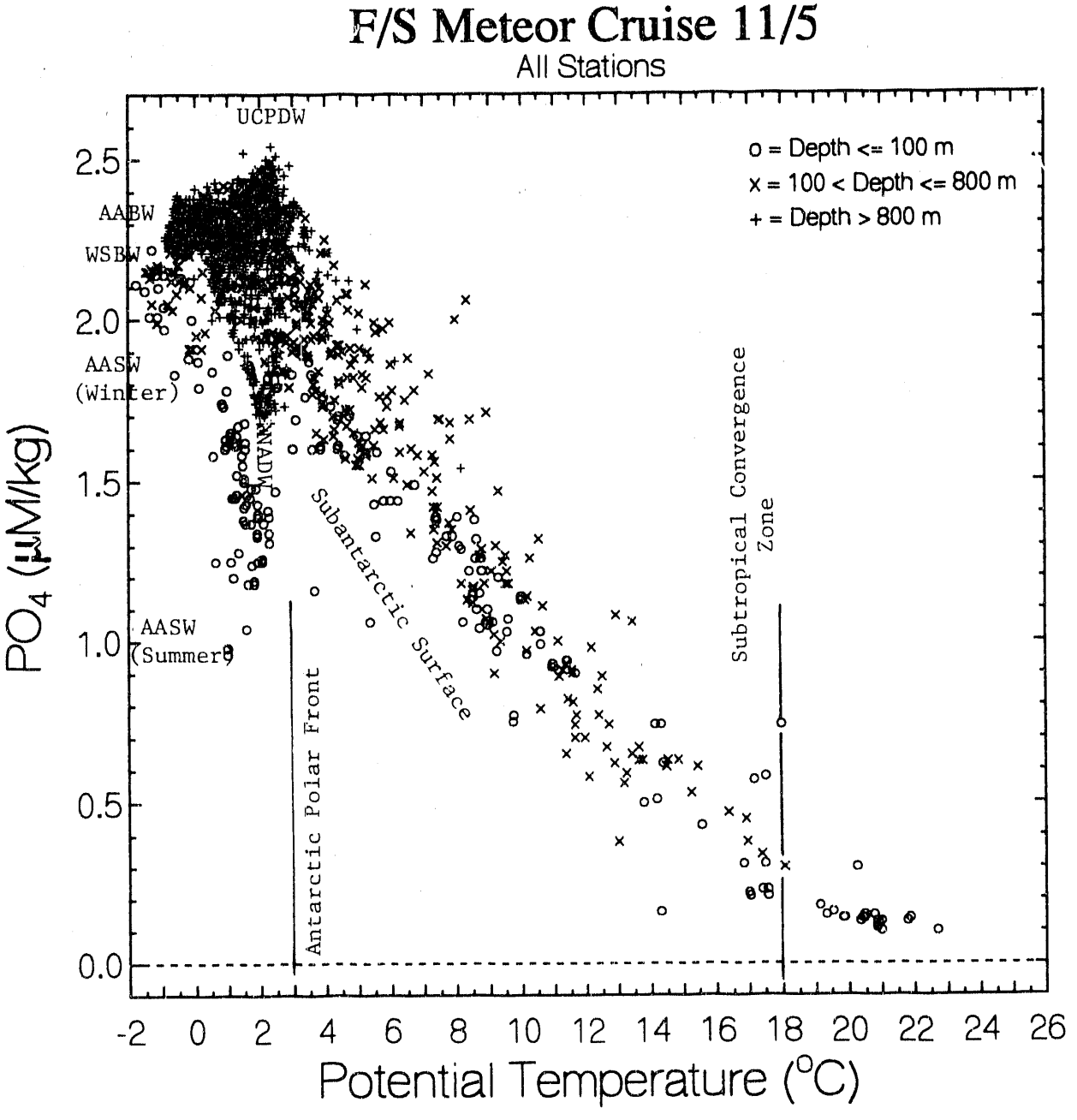

Fig. 73 - Relationships between the concentration of silica and potential temperature observed during the F/S Meteor Expedition, Jan.-March, 1990, in the South Atlantic Ocean and northern Weddell Sea. SPBW = Southeast Pacific Bottom Water; WSDW = Weddell Sea Deep Water; WSBW = Weddell Sea Bottom Water; AABW = Antarctic Bottom Water; NADW = North Atlantic Deep Water; AASW = Antarctic Surface Water; SbAASW = Subantarctic Surface Water.

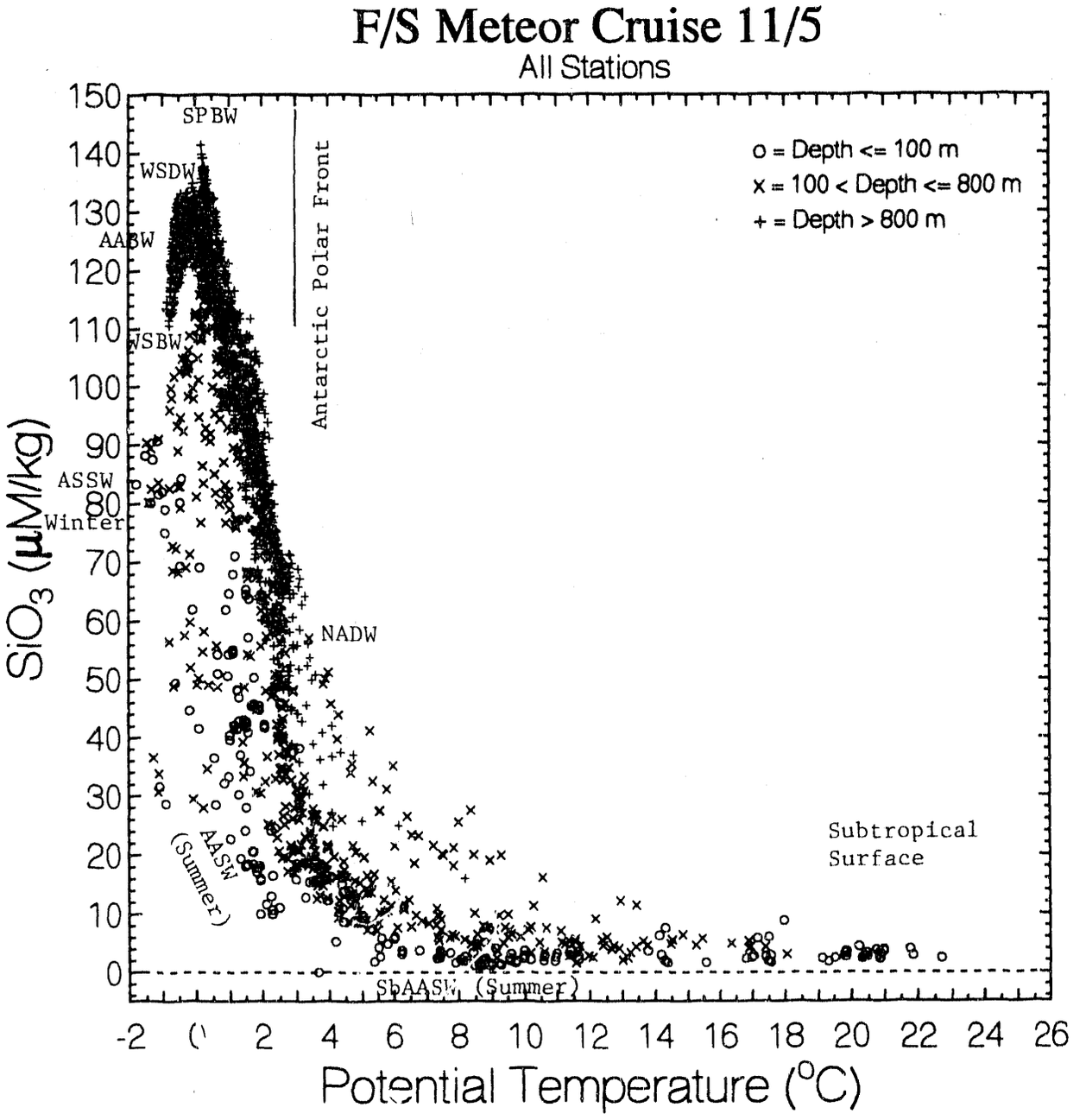

Fig. 74 - Relationships between the concentration of silica and salinity observed during the F/S Meteor Expedition, Jan.-March, 1990, in the South Atlantic Ocean and northern Weddell Sea. SPBW = Southeast Pacific Bottom Water; WSDW = Weddell Sea Bottom Water; WSDW = Weddell Sea Deep Water; AABW = Antarctic Bottom Water; LCPDW = Lower Circumpolar Deep Water; NADW = North Atlantic Deep Water; AAIW = Antarctic Intermediate Water; UCPDW = Upper Circumpolar Deep Water.

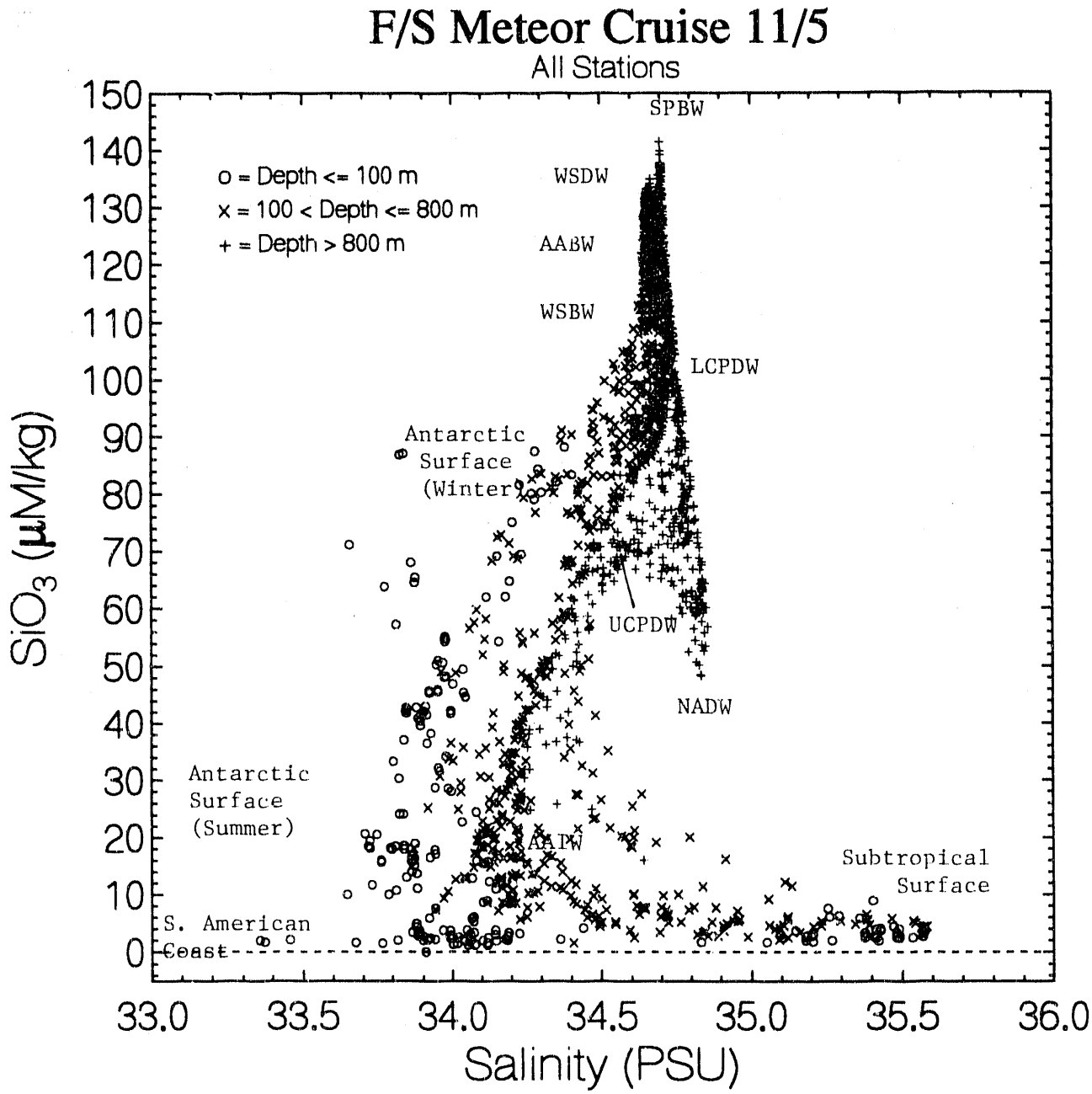

Fig. 75 - Nitrate and silicate relationships observed during the F/S Meteor 11/5 Expedition in the South Atlantic Ocean and northern Weddell Sea, January-March, 1990. UCPDW and LCPDW = Upper and lower Circumpolar Deep Water; SPLOW = South Pacific Low Oxygen Water; SPDW = Southeast Pacific Deep Water; SPBW = Southeast Pacific Bottom Water; NADW = North Atlantic Deep Water; AAIW = Antarctic Intermediate Water.

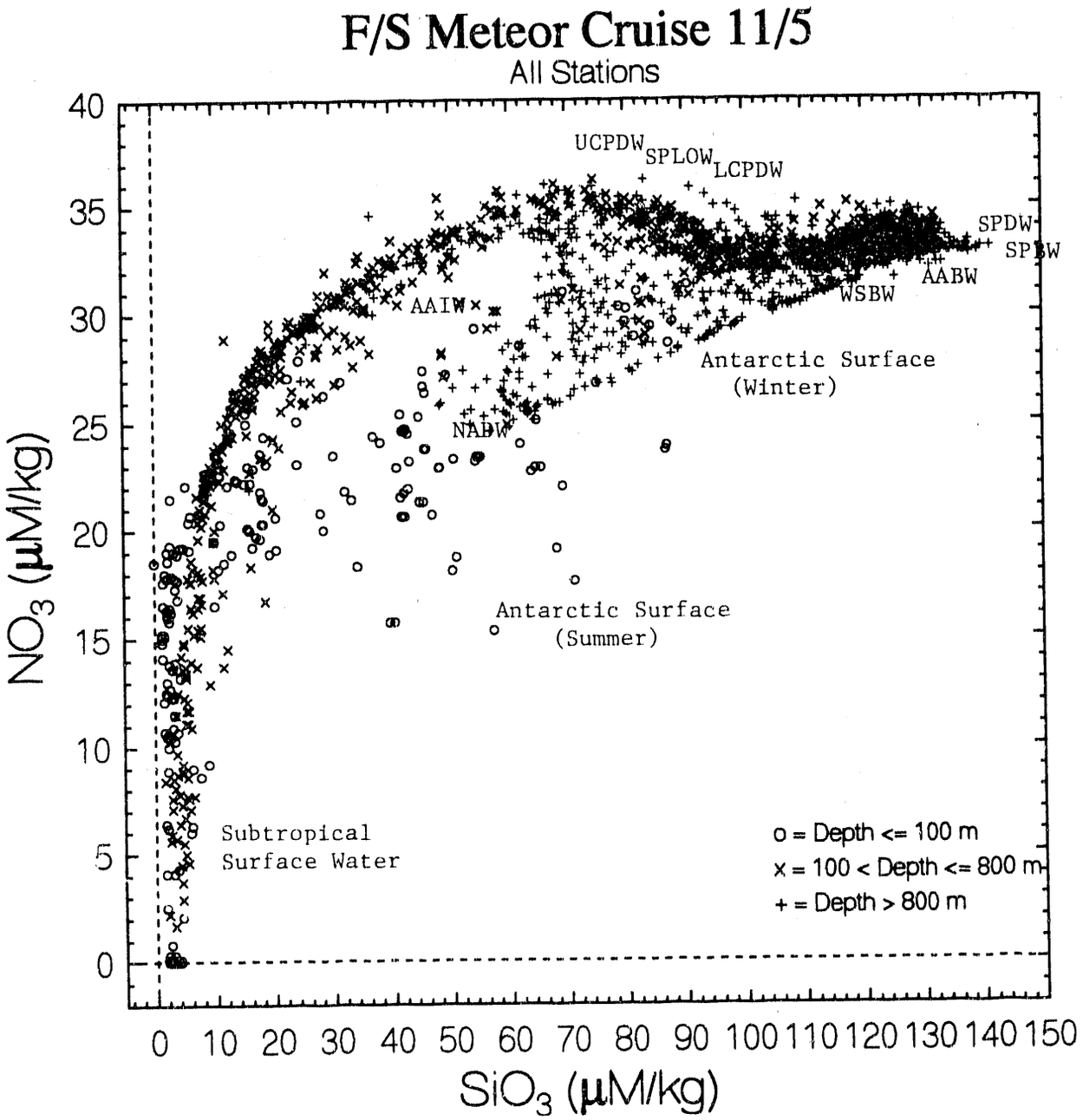

Fig. 76 shows the relationships between the potential alkalinity and salinity. The potential alkalinity has been computed by [(Total Alkalinity) + (Nitrate)] (Brewer and Goldman, 1977) and has been normalized to a salinity of 35.00 o/oo. The potential alkalinity values for the summer and winter Antarctic surface waters are nearly constant, whereas the total CO_2 (Fig. 67), nitrate (Fig. 71), phosphate (Figs. 67 and 72) and silica (Fig. 74) concentration indicate substantial reductions from winter to summer. This suggests that little production of $CaCO_3$ occurred during the year in the Antarctic and Weddell Sea surface waters. On the other hand, the potential alkalinity values decrease rapidly in the subantarctic and subtropical surface waters, suggesting production of calcareous shells.

As mentioned earlier, the Cape Basin Bottom Water (CBBW) has the highest potential alkalinity values, whereas the NADW is depicted as a sharp minimum in the vicinity of 34.8 o/oo salinity.

Fig. 77 shows the relationships between the potential alkalinity and the silica concentration. The potential alkalinity values are normalized to a salinity of 35.00 o/oo. In the Antarctic surface waters, it is observed that the potential alkalinity values are nearly constant with a slight decline to lower silica values during the summer and winter seasons and that these surface water values are only slightly smaller than the deep water values (see "x" and "+" signs). This indicates that only a small amount of $CaCO_3$ is removed from the Antarctic and Weddell Sea surface water, while the silica concentration in these waters is reduced to near-zero values by the growth of silica secreting organisms. The potential alkalinity is reduced only after silica concentrations reach near-zero values. This suggests that the production of biogenic $CaCO_3$ occurs mainly in the subantarctic and subtropical surface waters.

Fig. 76 - Relationships between the potential alkalinity and salinity observed during the F/S Meteor Expedition, Jan.-March, 1990, in the South Atlantic Ocean and northern Weddell Sea. Potential alkalinity is computed by (Total Alkalinity) + (Nitrate), and is normalized to a salinity of 35.00 o/oo. The highest potential alkalinity values were observed near the bottom of the Cape Basin, southeastern Atlantic.

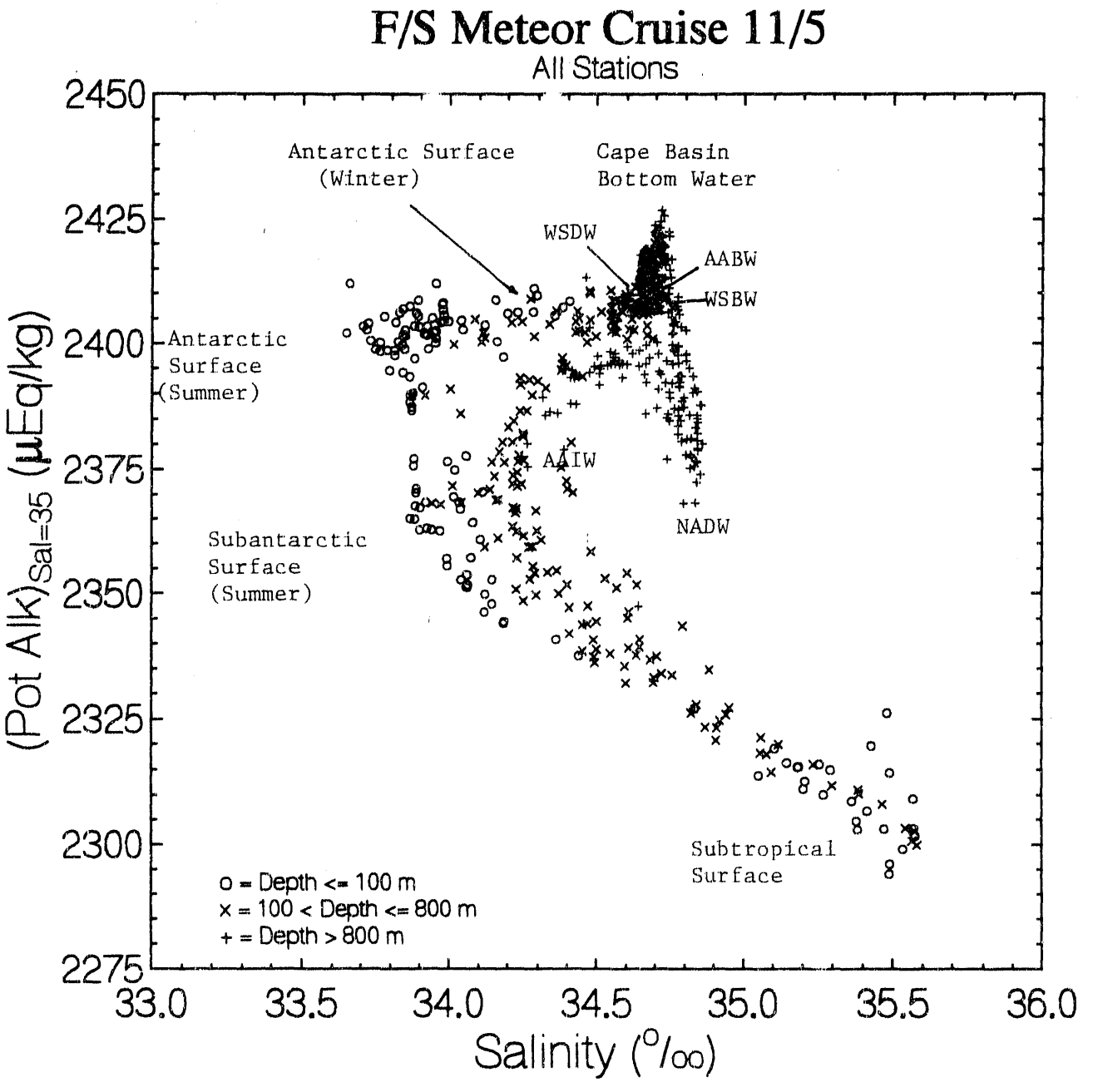

Fig. 77 - Relationships between the potential alkalinity and the concentration of silica in seawater. The former is normalized to a salinity of 35.00 o/oo. UCPDW = Upper Circumpolar Deep Water; SPBW = Southeast Pacific Bottom Water; WSDW and WSBW = Weddell Sea Deep and Bottom Waters; and NADW = North Atlantic Deep Water.

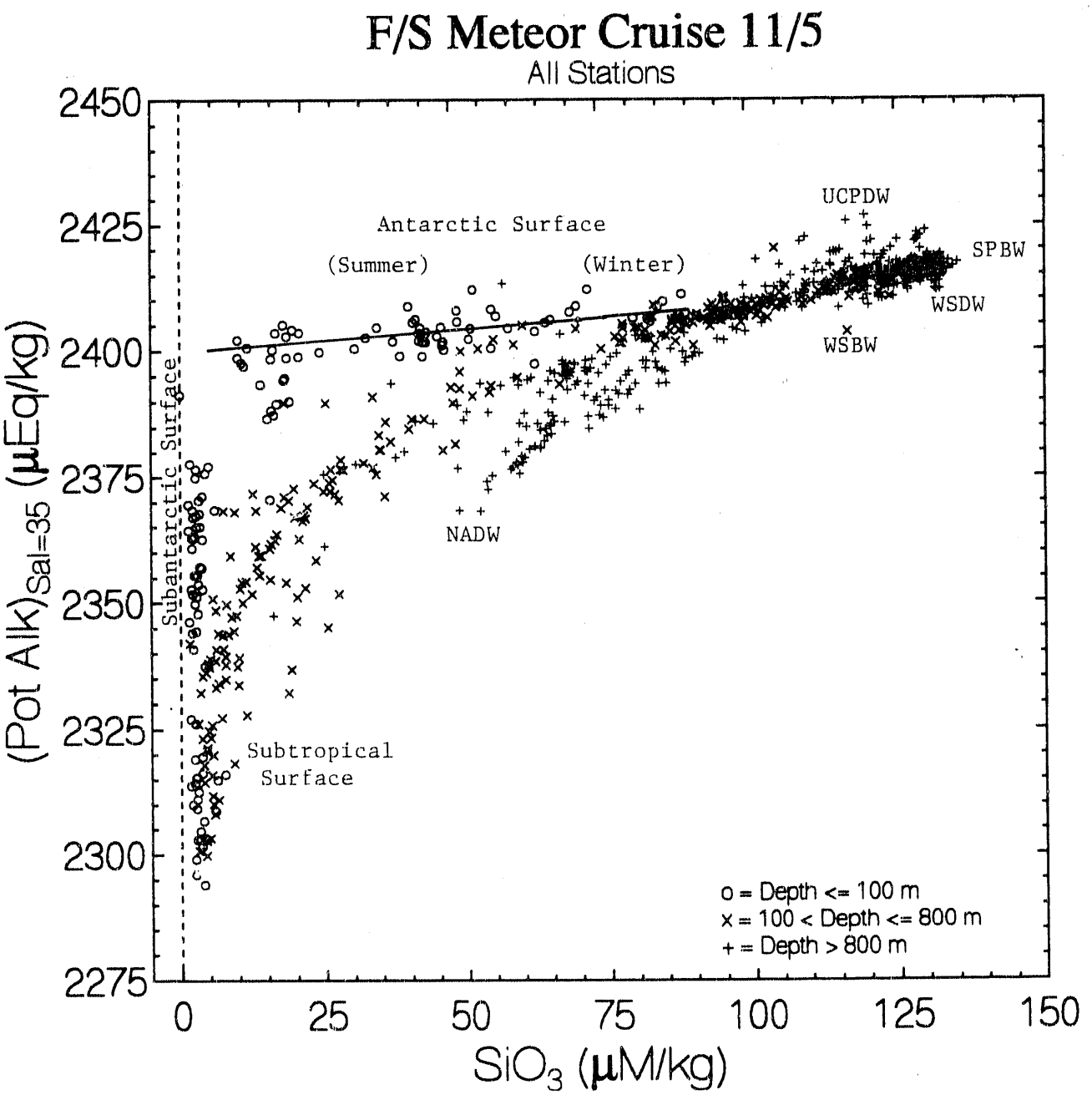

V. REFERENCES CITED

Brewer, P. G. and J. C. Goldman (1976). Alkalinity changes generated by phytoplankton growth. Lim. and Oceanogr., 21, 108-117.

Bryden, H. L. (1973), New polynomials for thermal expansion, adiabatic temperature gradient and potential temperature of seawater. Deep-Sea Res., 20, 401-408.

Carmack, E.. C. and T. D. Foster (1975). On the flow of deep water out of the Weddell Sea. Deep Sea Res., 22, 711-724.

Chipman, D. W. and J. Goddard (1991). Technical manual for gas chromatographic system for high precision measurements of carbon dioxide partial pressures in discrete ocean water and air samples. Final Technical Report for DOE Contract 19X-91319C, Lamont-Doherty Geol. Obs., Palisades, NY, pp.40.

Culberson, C. H. and R. M. Pytkowicz (1973). Ionization of water in seawater. Mar. Chem., 1, 403-417.

Fofonoff, N. P. (1980), Computation of potential temperature of seawater for an arbitrary reference pressure, Deep-Sea Res., 24, 489-491.

Gordon, A. L. (1971-a). Oceanography of Antarctic waters. in "Antarctic Oceanography I", J. L. Reid, editor, Antarctic Research Series, Vol. 15, Am. Geophys. Union, Washington, D. C., 169-203.

Gordon, A. L. (1971-b). Antarctic polar front zone. in "Antarctic Oceanography I", J. L. Reid, editor, Antarctic Research Series, Vol. 15, Am. Geophys. Union, Washington, D. C., 205-221.

Gordon, A. L. and E. J. Molinelli (1982). Thermohalince and chemical distributions and the atlas data set. in "Southern Ocean Atlas", Columbia University Press, New York, 248 plates and 33 pages.

Ingri, N. (1959). Equilibrium studies of polyanions, IV. Silicate ions in NaCl medium. Acta Chem Scand., 13, 758-775.

Johnson, K. M., A. E. King. and J. McN. Sieburth (1985). Coulometric TCO_2 analyses for marine studies: an introduction. Mar. Chem., 16, 61-82.

Jacobs, S. S., R. G. Fairbanks and Y. Horibe (1985). Origin and evolution of water masses near the Antarctic continental margin: evidence from $H_2{}^{18}O/H_2{}^{16}O$ ratios in seawater. in "Oceanology of the Antarctic Continental Shelf", S. S. Jacobs editor, Antarctic Research Series #43, Amer. Geophys Union, Washington, D. C., 59-85.

Kester, D. R. and R. M. Pytkowicz (1967). Determination of the apparent dissociation constants of phosphoric acid in seawater. Limnol. Oceanogr., 12, 243-252.

Kester, D. R. (1975), Dissolved gases other than CO_2. in "Chemical Oceanography", 2nd Edition, J. P. Riley, G. Skirrow editors, Vol. 1, 497-556, Academic Press, London.

Lyman, J. (1956). Buffer mechanism of sea water. Ph.D. Thesis, University of California, Los Angeles, Los Angeles, California, 196 pp.

Mehrbach, C., C. H. Culberson, J. E. Hawley, and R. M. Pytkowicz (1973). Measurement of the apparent dissociation constants of carbonic acid in seawater at atmospheric pressure. Limnol. and Oceanogr., 18, 897-907.

Millero, F. J., C.-T. Chen, A. Bradshaw and K. Schleicher (1980), A new high pressure equation of state for seawater. Deep-Sea Res., 27, 255-264.

Millero, F. J. (1979). The thermodynamics of the carbonate system in seawater. Geochim. et Cosmochim. Acta, 43, 1651-1661.

Murray, N. N. and J. P. Riley (1969) The solubility of gases in distilled water and sea water - II. Oxygen. Deep-Sea Res., 16, 311-320.

Peng, T.-H., T. Takahashi, W. S. Broecker, J. Olafsson (1987). Seasonal variability of carbon dioxide, nutrients and oxygen in the northern North Atlantic surface water: Observations and a model, Tellus, 39B, 439-458.

Reid, J. L., Nowlin, W. D. Jr., Patzert, W. C. (1977). On the characteristics and circulation of the southwestern Atlantic Ocean. Jour. Phys. Ocean., 7, 62-91.

Takahashi T., D. Chipman, N. Schechtman, J. Goddard and R. Wanninkof (1982). Measurements of the partial pressure of CO_2 in discrete water samples during the North Atlantic Expedition, the Transient Tracers of Oceans Project. Technical Report to NSF, Lamont-Doherty Geological Observatory, Palisades, NY, pp. 268.

Weiss, R. F. (1974). Carbon dioxide in water and seawater: The solubility of a non-ideal gas, Marine Chem., 2, 203-215.

Weiss, R. F. (1981). Determinations of CO_2 and methane by dual catalyst flame ionization chromatography and nitrous oxide by electron capture chromatography. Jour. of Chromatogr. Sci., 19, 611-616.

Whitworth, T. III and W. D. Nowlin (1987). Water masses and currents of the Southern Ocean at the Greenwich Meridian, Jour. Geophys. Res., 92, 6462-6476.

IV. DATA TABLES

Because of the agreements made by the participants of WOCE expeditions, the numerical data for the expedition will not be released to the public domain until two full years will be passed after the end of the expedition. Accordingly, the data will be released in the end of March, 1992. All the data obtained during the expedition have been submitted to the Carbon Dioxide Information and Analysis Center at the Oak Ridge National Laboratory for archiving and for the distribution to the public after March, 1992.

The data are presented in two sections. The first is to summarize the chemical data for surface waters as well as the atmospheric CO_2 concentration and the sea-air pCO_2 difference. The second is to list the total CO_2 concentration and pCO_2 data as well as the associated hydrographic data. The latter data set was obtained by the participating members of the Oceanographic Data Facilities of Scripps Institution of Oceanography, and the members of the University of Bremen and other German scientific institutions and the Argentine Hydrographic Office.

END

DATE FILMED

4/30/92